msp

Geometry & Topology 19 (2015) 2619–2689

1–efficient triangulations and the index of a cusped hyperbolic 3–manifold

STAVROS GAROUFALIDIS
CRAIG D HODGSON
J HYAM RUBINSTEIN
HENRY SEGERMAN

In this paper we will promote the 3D index of an ideal triangulation $\mathcal{T}$ of an oriented cusped 3–manifold M (a collection of q–series with integer coefficients, introduced by Dimofte, Gaiotto and Gukov) to a topological invariant of oriented cusped hyperbolic 3–manifolds. To achieve our goal we show that (a) $\mathcal{T}$ admits an index structure if and only if $\mathcal{T}$ is 1–efficient and (b) if M is hyperbolic, it has a canonical set of 1–efficient ideal triangulations related by 2–3 and 0–2 moves which preserve the 3D index. We illustrate our results with several examples.

57N10, 57M50; 57M25

1 Introduction

1.1 The 3D index of Dimofte, Gaiotto and Gukov

The goal of this paper is to convert the index of an ideal triangulation $\mathcal{T}$ (a remarkable collection of Laurent series in $q^{1/2}$ introduced by Dimofte, Gaiotto and Gukov [10; 11] and further studied in Garoufalidis [16]) to a topological invariant of oriented cusped hyperbolic 3–manifolds M. Our goal will be achieved in two steps.

The first step identifies the existence of an index structure of $\mathcal{T}$ (a necessary and sufficient condition for the existence of the index of $\mathcal{T}$; see [16]) with the nonexistence of sphere or non-vertex-linking torus *normal surfaces* of $\mathcal{T}$; see Theorem 1.2 below. Such ideal triangulations are called 1–efficient in Jaco and Rubinstein [25] and Kang and Rubinstein [28]. The unexpected connection between the index of an ideal triangulation (a recent quantum object) and the classical theory of normal surfaces places restrictions on the topology of M; see Remark 1.3 below.

The second step constructs a canonical collection $\mathcal{X}^{\mathrm{EP}}_M$ of triangulations of the Epstein–Penner ideal cell decomposition of a cusped hyperbolic 3–manifold M, such that the

Published: 20 October 2015 DOI: 10.2140/gt.2015.19.2619

index behaves well with respect to 2–3 and 0–2 moves that connect any two members of $\mathcal{X}^{\mathrm{EP}}_M$. The index of those triangulations then gives the desired topological invariant of M; see Theorem 1.8 below.

We should point out that normal surfaces were also used by Frohman and Bartoszynska [14] in an attempt to construct topological invariants of 3–manifolds, in the style of a Turaev–Viro TQFT. Strict angle structures (a stronger form of an index structure) play a role in quantum hyperbolic geometry studied by Baseilhac and Benedetti [3; 4]. In the recent work of Andersen and Kashaev [2], strict angle structures were used as sufficient conditions for convergence of analytic state-integral invariants of ideal triangulations. The latter invariants are expected to depend on the underlying cusped 3–manifold and to form a generalisation of the Kashaev invariant [29]. The q–series of Theorem 1.8 below are q–holonomic, of Nahm-type and, apart from a meromorphic singularity at $q=0$, admit analytic continuation in the punctured unit disc.

Before we get to the details, we should stress that the origin of the 3D index is the exciting work of Dimofte, Gaiotto and Gukov [10; 11] (see also Beem, Dimofte and Pasquetti [5]) who studied gauge theories with $N=2$ supersymmetry that are associated to an ideal triangulation $\mathcal{T}$ of an oriented 3–manifold M with at least one cusp. The low-energy limit of these gauge theories gives rise to a partially defined function, the so-called *3D index*

$$I : \{\text{ideal triangulations}\} \longrightarrow \mathbb{Z}((q^{1/2}))^{H_1(\partial M;\mathbb{Z})}, \quad \mathcal{T} \mapsto I_{\mathcal{T}}([\varpi]) \in \mathbb{Z}((q^{1/2})) \tag{1}$$

for $[\varpi] \in H_1(\partial M;\mathbb{Z})$.[1] The function I is only partially defined because the expression for the 3D index may not converge. The above gauge theories provide an analytic continuation of the coloured Jones polynomial and play an important role in Chern–Simons perturbation theory and in categorification. Although the gauge theory depends on the ideal triangulation $\mathcal{T}$, and the 3D index in general may not be defined, physics predicts that the gauge theory ought to be a topological invariant of the underlying 3–manifold M. Recall that any two ideal triangulations of a cusped 3–manifold are related by a sequence of 2–3 moves; see Matveev [37; 38] and Piergallini [42]. In Garoufalidis [16] the following was shown. For the definition of an index structure, see Section 2.

Theorem 1.1 (a) *$I_{\mathcal{T}}$ is well-defined if and only if $\mathcal{T}$ admits an* index structure.

(b) *If $\mathcal{T}$ and $\mathcal{T}'$ are related by a 2–3 move and both admit an index structure, then $I_{\mathcal{T}} = I_{\mathcal{T}'}$.*

[1] Here and below we will use the notation M for both a cusped hyperbolic 3–manifold and the corresponding compact manifold with boundary ∂M consisting of a disjoint union of tori; the intended meaning should be clear from the context.

1.2 Index structures and 1–efficiency

Theorem 1.2 *An ideal triangulation $\mathcal{T}$ of an oriented 3–manifold with cusps admits an index structure if and only if $\mathcal{T}$ is 1–efficient.*

The above theorem has some consequences for our sought topological invariants.

Remark 1.3 1–efficiency of $\mathcal{T}$ implies restrictions on the topology of M: it follows that M is irreducible and atoroidal. Note that here by *atoroidal*, we mean that any *embedded* torus is either compressible or boundary parallel. It follows by Thurston's hyperbolisation theorem in dimension 3 that M is hyperbolic or small Seifert-fibred.

Remark 1.4 If K is the connected sum of the 4_1 and 5_2 knots, or K' is the Whitehead double of the 4_1 knot and $\mathcal{T}$ is any ideal triangulation of the complement of K or K', then $\mathcal{T}$ is not 1–efficient, thus $I_{\mathcal{T}}$ never exists. On the other hand, the (coloured) Jones polynomial, the Kashaev invariant and the $\mathrm{PSL}(2,\mathbb{C})$–character variety of K and K' happily exist; see Jones [26], Kashaev [29] and Cooper, Culler, Gillet, Long and Shalen [7].

Theorem 1.5 *Let $\mathcal{T}$ be an ideal triangulation of an oriented atoroidal 3–manifold with at least one cusp. If $\mathcal{T}$ admits a semiangle structure then $\mathcal{T}$ is 1–efficient.*

Remark 1.6 Taut and strict angle structures are examples of semiangle structures, and for these cases this is proved in Kang and Rubinstein [28, Theorem 2.6]. In Section 3, we give a brief outline of the argument for a general semiangle structure.

Remark 1.7 In Corollary 3.4, we note that a construction of Lackenby produces triangulations with taut angle structures, which are therefore 1–efficient, on all irreducible cusped 3–manifolds containing no essential annulus. However, it is not clear that the triangulations produced by this construction are connected by the appropriate $2{-}3$ and $0{-}2$ moves, so we cannot prove that the 3D index is independent of the choice of taut triangulation for the manifold.

1.3 Regular ideal triangulations and topological invariance

In view of Remark 1.3, we restrict our attention to hyperbolic 3–manifolds M with at least one cusp. All we need is a canonical set $\mathcal{X}_M$ of 1–efficient ideal triangulations of M such that any two of these triangulations are related by moves that preserve $I_{\mathcal{T}}$. From Theorem 1.1, we know that we can use $2{-}3$ and $3{-}2$ moves for this purpose. Given the choice we will make for $\mathcal{X}_M$ below, it turns out that we will also need

to use 0–2 and 2–0 moves to connect together the triangulations of $\mathcal{X}_M$. Using the dual language of special spines, it is shown in Matveev [38, Lemma 2.1.11] and Piergallini [42] (see also Petronio [41, Proposition I.1.13]) that the 0–2 and 2–0 moves can be derived from the 2–3 and 3–2 moves, as long as the triangulation has at least two tetrahedra. However, the required sequence of 2–3 and 3–2 moves takes us out of our set $\mathcal{X}_M$, and it is not clear that the triangulations the sequence passes through are 1–efficient.

Every cusped hyperbolic 3–manifold M has a canonical *cell decomposition* by Epstein and Penner [13], where the cells are convex ideal polyhedra in $\mathbb{H}^3$. The cells can be triangulated into ideal tetrahedra, with layered flat tetrahedra inserted to form a bridge between two polyhedron faces that are supposed to be glued to each other but whose induced triangulations do not match. Unfortunately, it is not known whether any two triangulations of a 3–dimensional polyhedron are related by 2–3 and 3–2 moves; the corresponding result trivially holds in dimension 2 and nontrivially fails in dimension 5; see De Loera, Rambau and Santos [9] and Santos [44]. Nonetheless, it was shown by Gelfand, Kapranov and Zelevinsky that any two *regular* triangulations of a polytope in $\mathbb{R}^n$ are related by a sequence of geometric bistellar flips; Gelfand, Kapranov and Zelevinsky [21]. Using the Klein model of $\mathbb{H}^3$, we define the notion of a *regular ideal triangulation* of an ideal polyhedron and observe that every two regular ideal triangulations are related by a sequence of geometric 2–2, 2–3 and 3–2 moves. Our set $\mathcal{X}^{\mathrm{EP}}_M$ of ideal triangulations of a cusped hyperbolic manifold M consists of all possible choices of regular triangulation for each ideal polyhedron, together with all possible "bridge regions" of layered flat tetrahedra joining the induced triangulations of each identified pair of polyhedron faces. From the geometric structure of the cell decomposition, we obtain a natural semiangle structure on each triangulation of $\mathcal{X}^{\mathrm{EP}}_M$, which shows that they are all 1–efficient by Theorem 1.5, and so the 3D index is defined for each triangulation by Theorems 1.1(a) and 1.2. We show that any two of these triangulations are related to each other by a sequence of 2–3, 3–2, 0–2 and 2–0 moves through 1–efficient triangulations, the moves all preserving the 3D index, using Theorems 1.1(b), 1.2 and 5.1. (The intermediate triangulations are mostly also within $\mathcal{X}^{\mathrm{EP}}_M$, although we sometimes have to venture outside of the set briefly.) Therefore we obtain a topological invariant of cusped hyperbolic 3–manifolds M.

Theorem 1.8 *If M is a cusped hyperbolic 3–manifold, and $\mathcal{T} \in \mathcal{X}^{\mathrm{EP}}_M$ we have $I_M := I_{\mathcal{T}}$ is well-defined.*

The next theorem is of independent interest, and may be useful for the problem of constructing topological invariants of cusped hyperbolic 3–manifolds. For a definition

of the gluing equations of an ideal triangulation, see Neumann and Zagier [40] and Thurston [48] and also Section 4.3 below.

Theorem 1.9 *Fix a cusped hyperbolic 3–manifold M.*

(a) *For every $\mathcal{T} \in \mathcal{X}_M^{\mathrm{EP}}$, there exists a solution $Z_{\mathcal{T}}$ to the gluing equations of $\mathcal{T}$ which recovers the complete hyperbolic structure on M. Moreover, all shapes of $Z_{\mathcal{T}}$ have nonnegative imaginary part.*

(b) *If $\mathcal{T}, \mathcal{T}' \in \mathcal{X}_M^{\mathrm{EP}}$ are related by 2–3, 3–2, 0–2 or 2–0 moves, then so are $Z_{\mathcal{T}}$ and $Z_{\mathcal{T}'}$.*

(c) *For every $\mathcal{T}$, the arguments of $Z_{\mathcal{T}}$ give a semiangle structure on $\mathcal{T}$.*

Remark 1.10 In Hodgson, Rubinstein, and Segerman [24], it is shown that a cusped hyperbolic 3–manifold M admits an ideal triangulation with strict angle structure if $H_1(M, \partial M; \mathbb{Z}_2) = 0$. All link complements in the 3–sphere satisfy this condition. Such triangulations admit index structures but it is not known if they can be connected by 2–3 and 0–2 moves within the class of 1–efficient triangulations.

Remark 1.11 For a typical cusped hyperbolic manifold, one expects that the Epstein–Penner ideal cell decomposition consists of ideal tetrahedra, ie that $\mathcal{X}_M^{\mathrm{EP}}$ consists of one element. Many examples of such cusped hyperbolic manifolds appear in the SnapPy census [8] and also in Akiyoshi [1] and Guéritaud and Schleimer [22].

Remark 1.12 In a later paper we intend to extend this work in the following ways:

- Extend the domain of the 3D index $I_{\mathcal{T}}([\varpi])$ to $[\varpi] \in H_1(\partial M; \frac{1}{2}\mathbb{Z})$ such that $2[\varpi] \in \mathrm{Ker}(H_1(\partial M; \mathbb{Z}) \to H_1(M; \mathbb{Z}/2\mathbb{Z}))$.
- Give a definition of the 3D index using singular normal surfaces in M.

Remark 1.13 Theorem 1.8 constructs a family of q–series $I_M([\varpi])(q)$ (parametrised by $[\varpi] \in H_1(\partial M, \mathbb{Z})$) associated to a cusped hyperbolic manifold M. When $M = S^3 \setminus K$ is the complement of a knot K, we can choose $[\varpi] = \mu$ to be the homology class of the meridian and consider the series

$$I_K^{\mathrm{tot}}(q) = \sum_{e \in \mathbb{Z}} I_M(e\mu)(q). \tag{2}$$

Since the semiangle structures of Theorem 1.9 have zero holonomy at all peripheral curves, it can be shown that $I_K^{\mathrm{tot}}(q)$ is well-defined. It turns out that $I_K^{\mathrm{tot}}(q)$ is closely related to the state-integral invariants of Andersen and Kashaev [2] and Kashaev, Luo and Vartanov [30]. The relation between state-integrals of the quantum dilogarithm and q–series is explained in detail in Garoufalidis and Kashaev [17]. An empirical study of the asymptotics of the series $I_{4_1}^{\mathrm{tot}}(q)$ is given in Garoufalidis and Zagier [20].

1.4 Plan of the paper

In Section 2 we review the basic definitions of ideal triangulations, efficiency, angle structures and index structures.

In Section 3 we prove Theorem 1.2. So for an ideal triangulation, existence of an index structure is equivalent to being 1–efficient.

In Section 4 we review the basic properties of the tetrahedron index from Garoufalidis [16], and give a detailed discussion of the 3D index for an ideal triangulation of a cusped 3–manifold.

In Section 5 we study the behaviour of the 3D index under the $0-2$ and $2-0$ move.

In Section 6 we discuss the Epstein–Penner ideal cell decomposition and its subdivision into regular triangulations. At the end of Section 6.4 we prove Theorems 1.8 and 1.9.

In Section 7 we compute the first terms of the 3D index for some example manifolds.

Finally in the appendix, we give a detailed and self-contained proof of the invariance of the 3D index of 1–efficient triangulations under $2-3$ moves, following [16] and Dimofte, Gaiotto and Gukov [10].

2 Definitions

Definition 2.1 Let M be a topologically finite 3–manifold which is the interior of a compact 3–manifold with torus boundary components. An *ideal triangulation* $\mathcal{T}$ of M consists of a pairwise disjoint union of standard Euclidean 3–simplices $\widetilde{\Delta} = \bigcup_{k=1}^{n} \widetilde{\Delta}_k$ with vertex set $\widetilde{\Delta}^{(0)}$, together with a collection Φ of Euclidean isometries between the 2–simplices in $\widetilde{\Delta}$ called *face pairings*, such that the quotient space $(\widetilde{\Delta} \setminus \widetilde{\Delta}^{(0)})/\Phi$ is homeomorphic to M. The images of the simplices in $\mathcal{T}$ may be singular in M.

Definition 2.2 Let $\mathcal{T}$ be an ideal triangulation with at least 2 distinct tetrahedra. A $2-3$ *move* can be performed on any pair of distinct tetrahedra of $\mathcal{T}$ that share a triangular face t. We remove t and the two tetrahedra, and replace them with three tetrahedra arranged around a new edge, which has endpoints the two vertices not on t. See Figure 1(a). A $3-2$ *move* is the reverse of a $2-3$ move, and can be performed on any triangulation with a degree 3 edge, where the three tetrahedra incident to that edge are distinct.

Definition 2.3 Let $\mathcal{T}$ be an ideal triangulation. A $0-2$ *move* can be performed on any pair of distinct triangular faces of $\mathcal{T}$ that share an edge e.[2] Around the edge e, the

[2]Unlike for the $2-3$ move, it is possible to make sense of the $0-2$ move when the two triangles are not distinct. However, we will not make use of this variant in this paper.

tetrahedra of $\mathcal{T}$ are arranged in a cyclic sequence, which we call a *book of tetrahedra*. (Note that tetrahedra may appear more than once in the book.) The two triangles and e separate the book into two *half–books*. We unglue the tetrahedra that are identified across the two triangles, duplicating the triangles and also duplicating e. We glue into the resulting hole a pair of tetrahedra glued to each other in such a way that there is a degree-2 edge between them. See Figure 1(b). A 2–0 *move* is the reverse of a 0–2 move, and can be performed on any triangulation with a degree-2 edge, where the two tetrahedra incident to that edge are distinct, there are no face pairings between the four external faces of the two tetrahedra, and the two edges opposite the degree 2 edge are not identified.

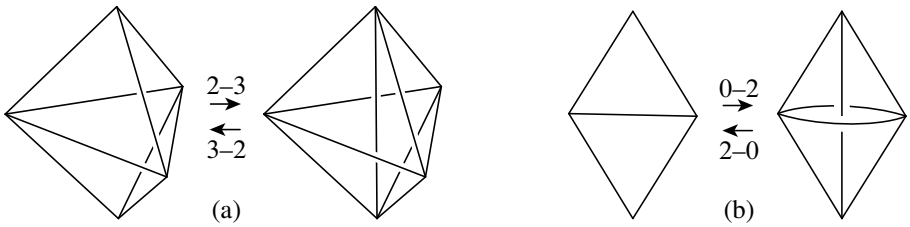

Figure 1: Moves on (topological) triangulations: (a) The 2–3 and 3–2 moves. (b) The 0–2 and 2–0 moves.

Remark 2.4 A 0–2 move is also called a *lune* move in the dual language of standard spines [37; 38; 42; 6]. In [37, Lemma 2.1.11] and [42] (see also [41, Proposition I.1.13]) it was shown that a 0–2 move follows from a combination of 2–3 moves as long as the initial triangulation has at least 2 ideal tetrahedra.

Definition 2.5 Let Δ^3 be the standard 3–simplex with a chosen orientation. Each pair of opposite edges corresponds to a normal isotopy class of quadrilateral discs in Δ^3 disjoint from the pair of edges. We call such an isotopy class a *normal quadrilateral type*. Each vertex of Δ^3 corresponds to a normal isotopy class of triangular discs in Δ^3 disjoint from the face of Δ^3 opposite the vertex. We call such an isotopy class a *normal triangle type*. Let $\mathcal{T}^{(k)}$ be the set of all k–simplices in $\mathcal{T}$. If $\sigma \in \mathcal{T}^{(3)}$ then there is an orientation preserving map $\Delta^3 \to \sigma$ taking the k–simplices in Δ^3 to elements of $\mathcal{T}^{(k)}$ and which is a bijection between the sets of normal quadrilateral and triangle types in Δ^3 and in σ. Let $\square$ and $\triangle$ denote the sets of all normal quadrilateral and triangle types in $\mathcal{T}$ respectively.

Definition 2.6 Given a 3–manifold M with an ideal triangulation $\mathcal{T}$, the *normal surface solution space* $C(M;\mathcal{T})$ is a vector subspace of $\mathbb{R}^{7n}$, where n is the number

of tetrahedra in $\mathcal{T}$, consisting of vectors satisfying the *compatibility equations* of normal surface theory. The coordinates of $x \in \mathbb{R}^{7n}$ represent weights of the four normal triangle types and the three normal quadrilateral types in each tetrahedron, and the compatibility equations state that normal triangles and quadrilaterals have to meet the 2–simplices of $\mathcal{T}$ with compatible weights.

A vector in $\mathbb{R}^{7n}$ is called *admissible* if at most one quadrilateral coordinate from each tetrahedron is nonzero and all coordinates are nonnegative. An integral admissible element of $C(M;\mathcal{T})$ corresponds to a unique embedded, closed *normal surface* in $(M,\mathcal{T})$ and vice versa.

Definition 2.7 [25; 28] An ideal triangulation $\mathcal{T}$ of an orientable 3–manifold is 0–*efficient* if there are no embedded normal 2–spheres or one-sided projective planes. An ideal triangulation $\mathcal{T}$ is 1–*efficient* if it is 0–efficient, the only embedded normal tori are vertex-linking and there are no embedded one-sided normal Klein bottles. An ideal triangulation $\mathcal{T}$ is *strongly* 1–*efficient* if there are no immersed normal 2–spheres, projective planes or Klein bottles and the only immersed normal tori are coverings of the vertex-linking tori.

Note that in some contexts, "atoroidal" is taken to mean that there is no immersed torus whose fundamental group injects into the fundamental group of the 3–manifold. In our context, we mean that there are no embedded incompressible tori or Klein bottles, other than tori isotopic to boundary components. In Corollary 3.4 and Remark 3.5 we highlight this distinction.

Note that if M is orientable, it is sufficient to consider only normal 2–spheres and tori, except in the special case that M is a twisted I–bundle over a Klein bottle. For any embedded normal projective plane or Klein bottle must be one-sided, so the boundary of a small regular neighbourhood is a normal 2–sphere or torus. However in the nonorientable case, one must consider two-sided projective planes and Klein bottles. In this paper we will consider only the orientable case.

Definition 2.8 If $e \in \mathcal{T}^{(1)}$ is any edge, then there is a sequence $(q_{n_1},\dots,q_{n_k})$ of normal quadrilateral types facing e which consists of all normal quadrilateral types dual to e listed in sequence as one travels around e Then k equals the degree of e and a normal quadrilateral type may appear at most twice in the sequence. This sequence is called the *normal quadrilateral type sequence* for e and is well-defined up to cyclic permutations and reversing the order.

Definition 2.9 A function $\alpha\colon \square \to \mathbb{R}$ is called a *generalised angle structure on* $(M, \mathcal{T})$ if it satisfies the following two properties:

(1) If $\sigma^3 \in \mathcal{T}^{(3)}$ and q, q', q'' are the three normal quadrilateral types supported by it, then
$$\alpha(q) + \alpha(q') + \alpha(q'') = \pi.$$

(2) If $e \in \mathcal{T}^{(1)}$ is any edge and $(q_{n_1}, \dots, q_{n_k})$ is its normal quadrilateral type sequence, then
$$\sum_{i=1}^{k} \alpha(q_{n_i}) = 2\pi.$$

Dually, one can regard α as assigning angles $\alpha(q)$ to the two edges opposite to q in the tetrahedron containing q. The triangulations we consider are of oriented manifolds, so we may assume that the triangulation is also oriented. We fix an ordering $q \to q' \to q'' \to q$ on these quad types, well defined up to cyclic permutation. See Figure 2.

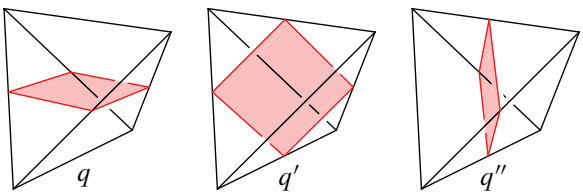

Figure 2: The three quad types within an oriented tetrahedron, arranged in our chosen cyclic order

Definition 2.10 If we restrict the angles of a generalised angle structure to be in

- $[0, \pi]$, then the generalised angle structure is a *semiangle structure*,
- $(0, \pi)$, then the generalised angle structure is a *strict angle structure*,
- $\{0, \pi\}$, then the generalised angle structure is a *taut angle structure*.

The set of generalised angle structures is denoted by $\mathrm{GA}(\mathcal{T})$ and is an affine subspace of $\mathbb{R}^{3N}$, where N is the number of tetrahedra in $\mathcal{T}$. The subset of semiangle structures is denoted by $\mathrm{SA}(\mathcal{T})$, and is a closed polytope in $\mathrm{GA}(\mathcal{T})$.

Remark 2.11 It is easy to see that a taut angle structure can only happen if every tetrahedron has a pair of opposite edges with angles π and the other four edges have angles 0.

Definition 2.12 For an ideal triangulation $\mathcal{T}$ with N tetrahedra, a *quad-choice* is an element $Q = (Q_1, \dots, Q_N) \in \square^N$ such that Q_n is a choice of one of the three quad types in the n^{th} tetrahedron. An *index structure* α on $\mathcal{T}$ consists of 3^N generalised angle structures, indexed by the quad-choices Q, with the property that $\alpha_Q(Q_n) > 0$ for $n = 1, \dots, N$, for each quad-choice Q.

Definition 2.13 The equations determining a generalised angle structure can be read off as three $N \times N$ integer-valued matrices $\overline{\mathbb{A}} = (\overline{a}_{ij})$, $\overline{\mathbb{B}} = (\overline{b}_{ij})$ and $\overline{\mathbb{C}} = (\overline{c}_{ij})$ whose rows are indexed by the N edges of $\mathcal{T}$ and whose columns are indexed by the $\alpha(q_j), \alpha(q'_j), \alpha(q''_j)$ variables respectively, where q_j, q'_j, q''_j are the quad types in the j^{th} tetrahedron. These are the so-called *Neumann–Zagier matrices* that encode the exponents of the *gluing equations* of $\mathcal{T}$, originally introduced by Thurston [40; 48]. In terms of these matrices, a generalised angle structure is a triple of vectors $Z, Z', Z'' \in \mathbb{R}^N$ that satisfy the equations

$$\overline{\mathbb{A}}Z + \overline{\mathbb{B}}Z' + \overline{\mathbb{C}}Z'' = 2\pi(1, \dots, 1)^T, \quad Z + Z' + Z'' = \pi(1, \dots, 1)^T. \tag{3}$$

Note that the matrix entries $\overline{a}_{ij}, \overline{b}_{ij}, \overline{c}_{ij}$ give the coefficients of Z_j, Z'_j, Z''_j in the i^{th} edge equation corresponding to the edges of tetrahedron j facing quad types q_j, q'_j, q''_j respectively.

We can combine these into a single matrix equation

$$\begin{pmatrix} \overline{\mathbb{A}} & \overline{\mathbb{B}} & \overline{\mathbb{C}} \\ \mathbb{I}_N & \mathbb{I}_N & \mathbb{I}_N \end{pmatrix} \begin{pmatrix} Z \\ Z' \\ Z'' \end{pmatrix} = \begin{pmatrix} 2\pi(1, \dots, 1)^T \\ \pi(1, \dots, 1)^T \end{pmatrix}, \tag{4}$$

where $\mathbb{I}_N$ is the $N \times N$ identity matrix. We call this matrix equation *the matrix form of the generalised angle structure equations*.

3 Index structures and 1–efficiency

We first give a sketch proof of Theorem 1.5, showing that a semiangle structure implies 1–efficiency. We follow [28] and indicate the required small modification. Suppose that M is oriented with cusps and has an ideal triangulation $\mathcal{T}$ with a semiangle structure. Assume that there is an embedded normal torus or Klein bottle or sphere or projective plane, where the normal torus is not a peripheral torus. Firstly, exactly as in [32] the latter two cases are excluded by a simple Euler characteristic argument. Similarly, if there is a cube with knotted hole bounded by an embedded normal torus, then a barrier argument as in [25] establishes that there is a normal 2–sphere bounding a ball containing this normal torus, which is a contradiction. Embedded Klein bottles

are excluded, so we are reduced to the cases of an embedded essential nonperipheral normal torus or a normal torus bounding a solid torus.

In both cases, there is a sweep-out between the normal torus and a peripheral normal torus (for essential tori) or to a core circle of the solid torus. By a minimax argument (see [43; 47]), there is an almost normal[3] torus associated with this sweep-out. This is either obtained by attaching a tube parallel to an edge to a normal 2–sphere or has a single properly embedded octagonal disc in a tetrahedron and a collection of normal triangular and quadrilateral discs. The first case is excluded, since we have ruled out such normal 2–spheres.

The semiangle structure now implies that a standard combinatorial Gauss–Bonnet argument can be applied. Each polygonal disc in our torus has curvature given by $\sum_i \alpha_i - (n-2)\pi$, where n is the number of edges of the disc and α_i are the interior angles at the vertices of the disc. Gauss–Bonnet then says that the sum of the curvatures of all the discs is zero, since the Euler characteristic of the torus is zero. Every normal triangular disc contributes zero and each normal quadrilateral is nonpositive in the curvature sum. On the other hand, any embedding of an octagon into an ideal tetrahedron with a semiangle structure gives a strictly negative contribution. See Figure 3. Hence the Euler characteristic of such a surface cannot be zero and there could not have been an embedded normal torus to begin with. This completes the sketch proof. □

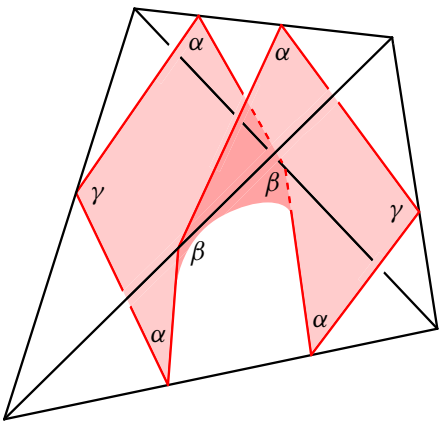

Figure 3: A normal octagon in a tetrahedron with a semiangle structure with angles $\alpha, \beta, \gamma \in [0, \pi]$. The curvature of this octagon is $4\alpha + 2\beta + 2\gamma - (8-2)\pi = 2\alpha + 2\pi - 6\pi = 2\alpha - 4\pi < 0$.

[3] A closed properly embedded surface is *almost normal* if it is a union of normal discs together with precisely one exceptional piece (lying inside one tetrahedron), which is an octagon or an annulus consisting of two disjoint normal discs joined by a tube.

Remark 3.1 Lackenby gives a result similar to Theorem 1.5 in [33, Theorem 2.1].

A useful observation (see [28]) following from Theorem 1.5 is the following;

Corollary 3.2 *Suppose that $\mathcal{T}$ is an ideal triangulation of an oriented 3–manifold M with cusps. If M is an-annular and $\mathcal{T}$ admits a semiangle structure then M is strongly 1–efficient.*

Proof The key observation is that the semiangle structure on $\mathcal{T}$ lifts to a semiangle structure on the lifted triangulation $\widetilde{\mathcal{T}}$, for any covering space $\widetilde{M}$ of M. Assume that there is an immersed normal torus T in M which is not a covering of the peripheral torus. If $\widetilde{M}$ is chosen as the covering space whose fundamental group corresponds to the image of $\pi_1(T)$, then T lifts to a normal torus $\widetilde{T}$ so that the inclusion map induces an onto map $\pi_1(\widetilde{T}) \to \pi_1(\widetilde{M})$.

We can now use $\widetilde{T}$ as a barrier (see [25]) to produce an embedded normal nonperipheral torus T^*, which is either essential and isotopic into a boundary cusp, or bounds a solid torus or cube with knotted hole. (Here the an-annular assumption is used to show that the covering space $\widetilde{M}$ is atoroidal). The rest of the argument is exactly the same as in Theorem 1.5. □

Proof of Theorem 1.2 We closely follow Luo and Tillmann [35]. We use the following version of Farkas' lemma, which is given in [35, Lemma 10(3)]:

Lemma 3.3 *Let A be a real $K \times L$ matrix, $b \in \mathbb{R}^K$, and $\cdot$ denote the usual Euclidean inner product on $\mathbb{R}^K$. Then $\{x \in \mathbb{R}^L \mid Ax = b, x > 0\} \neq \varnothing$ if and only if for all $y \in \mathbb{R}^K$ such that $A^T y \neq 0$ and $A^T y \leq 0$ one has $y \cdot b < 0$.*

For our purposes, $Ax = b$ is the matrix form (4) of the generalised angle structure equations, so $b = (2\pi, \dots, 2\pi, \pi, \dots, \pi)^T$. Consider a particular quad-choice Q, as in Definition 2.12. If there is to be an index structure, then we must be able to find the appropriate generalised angle structure x. That is, $x_l > 0$ if l corresponds to one of the Q_n, and x_l can have any real value if not. We refer to the former as *restricted* variables, and the latter as *unrestricted* variables.

The problem with applying Farkas' lemma directly is that it applies to the set of solutions $\{Ax = b \mid x > 0\}$. That is, *all* variables are strictly positive. However, we use a standard trick: For each unrestricted variable x_l, introduce a new variable x'_l. The new variable acts precisely like $-x_l$ so the old x_l can be written in the new coordinates as $x_l - x'_l$. This allows both new variables $x_l, x'_l > 0$, making them restricted variables, so that Farkas' lemma can be applied.

The effect that this has on the matrix A is as follows: We get a new column after each unrestricted x_l for x_l', and the values in the new column are the negatives of the values in the column for x_l.

Now we apply Farkas' lemma. We get a solution to our system if and only if for all $y \in \mathbb{R}^K$ such that $A^T y \neq 0$ and $A^T y \leq 0$ we have $y \cdot b < 0$ The transposed matrix A^T has dual variables $(z_1, \dots, z_n, w_1, \dots, w_t)$, where the w_i correspond to the tetrahedra and the z_j correspond to the edges. The dual system $A^T(z,w)^T \leq 0$ is given by inequalities

$$w_i + z_j + z_k \leq 0$$

whenever the i^{th} tetrahedron contains a quad that faces the edges j and k (which may not be distinct). This holds for all the rows corresponding to the x_l, and we get the following for the x_l':

$$-(w_i + z_j + z_k) \leq 0.$$

The two of these together imply that $w_i + z_j + z_k = 0$ for the quads corresponding to unrestricted angles, while $w_i + z_j + z_k \leq 0$ for restricted angles. The rest of the argument is the same as in [35], as follows.

Kang and Rubinstein [27] give a basis of the normal surface solution space $C(M;\mathcal{T})$ which consists of one element for each edge and one element for each tetrahedron of $\mathcal{T}$. For the edge e, the corresponding basis element has each of the quad types in the normal quadrilateral type sequence for e with coefficient -1 (or -2 if that quad appears twice), and each of the triangle disc types that intersect e with coefficient $+1$. For each tetrahedron σ, the corresponding basis element has each of the quad types in σ with coefficient -1, and each of the triangle disc types in σ with coefficient $+1$.

If we have a solution to the dual system, then we can form a normal surface solution class $W_{w,z}$ as a sum of tetrahedral and edge basis elements with coefficients given by the w_i and z_j corresponding to their tetrahedra and edges respectively. There is a linear functional χ^* on $\mathbb{R}^{7n}$ called the *generalised Euler characteristic*, which agrees with the Euler characteristic in the case of an embedded normal surface represented by an element of $C(M;\mathcal{T})$. It is shown in [35] that the generalised Euler characteristic $\chi^*(W_{w,z})$ is equal to $y \cdot b$, and that the normal quad coordinates of $W_{w,z}$ are given by $-(w_i + z_j + z_k)$. From the above inequalities, we find that the obstruction classes are solutions to the normal surface matching equations with zero quad coordinates for unrestricted angles, nonnegative quad coordinates for restricted angles (ie the quads specified by the quad-choice Q), at least one quad coordinate strictly positive, and generalised Euler characteristic $\chi^*(W_{w,z}) \geq 0$.

If there are any negative triangle coordinates, we can add vertex linking copies of the boundary tori to the solution until all normal disc coordinates are nonnegative. Now, since at most one quad coordinate in each tetrahedron is nonzero, we can in fact realise the normal surface solution class as an embedded normal surface, and so the generalised Euler characteristic is equal to the Euler characteristic. Therefore, an obstruction class to this quad-choice having an associated generalised angle structure is an embedded normal sphere, projective plane, Klein bottle or torus, with the only quads appearing being of the quad types given by the quad-choice. Thus, if the triangulation is 1–efficient, then there can be no such obstruction.

The above argument shows that a 1–efficient triangulation admits an index structure. For the converse, note that if a triangulation is not 1–efficient, then there is an embedded normal sphere, projective plane, Klein bottle or nonvertex linking torus. This must then have at least one nonzero quad coordinate, and since it is embedded, there can be only one nonzero quad coordinate in each tetrahedron. Choosing these quad types in the tetrahedra containing the surface, and arbitrarily choosing quad types in any other tetrahedra, we construct a quad-choice that by the above argument cannot have a suitable generalised angle structure, and so there is no index structure. This completes the proof of Theorem 1.2. □

Corollary 3.4 *Suppose that M is a compact oriented irreducible 3–manifold with incompressible tori boundary components and no immersed incompressible tori or Klein bottles, except those which are homotopic into the boundary tori. Then M admits an ideal triangulation $\mathcal{T}$ having an index structure. Moreover if M has no essential annuli (ie M is an-annular) then for any finite sheeted covering space $\widetilde{M}$, the lifted triangulation also admits an index structure.*

Proof To construct 1–efficient triangulations, we can use a construction of Lackenby [31]. He proves that if M is a compact oriented irreducible 3–manifold with incompressible tori boundary components and M has no immersed essential annuli, except those homotopic into the boundary tori, then M admits a taut ideal triangulation $\mathcal{T}$. Then by Corollary 3.2 such triangulations are strongly 1–efficient. Note that the lift of such a triangulation to any finite sheeted covering space is also 1–efficient.

The case of small Seifert fibred spaces remains, for these are precisely the oriented 3–manifolds with tori boundary components which admit essential annuli, but no embedded incompressible tori which are not homotopic into the boundary components.

Such examples have base orbifold either a disc with two cone points or an annulus with one cone point or Möbius band with no cone points. The cone points are the images of the exceptional fibres in the Seifert structure. These manifolds have immersed

incompressible tori, but do not have embedded incompressible tori or Klein bottles, except in the case where the base orbifold has orbifold Euler characteristic zero: a disc with two cone points corresponding to exceptional fibres of multiplicity two or orbit surface a Möbius band with no cone points. This represents two different Seifert fibrations of the same manifold. We exclude this latter case.

Now to construct a suitable ideal triangulation, note that these Seifert fibred spaces M are bundles over a circle with a punctured surface of negative Euler characteristic as the fibre. To see this, note that M is Seifert fibred over an orientable base orbifold B with $\chi^{\text{orb}}(B) < 0$. Then M admits a connected horizontal surface F which is orientable with $\chi(F) < 0$ since F is an orbifold covering of B. (A surface is *horizontal* if it is everywhere transverse to the Seifert fibration.) Since M is orientable it follows that F nonseparating, so M fibres over the circle with F as fibre (see for example [23, Sections 1.2 and 2.1]).

After [31, Lemma 6], it is shown that, starting with any ideal triangulation of the punctured surface F, a bundle can be formed as a layered triangulation. This is done by realising a sequence of diagonal flips on the surface triangulation needed to achieve any given monodromy map. Such a triangulation then gives an ideal triangulation with a taut structure. So by Theorem 1.5 these are 1–efficient triangulations and hence admit index structures. □

Remark 3.5 The small Seifert fibred spaces from the proof of Corollary 3.4 have finite sheeted coverings with embedded incompressible tori so that the lifted triangulations do not all admit index structures, in contrast with the hyperbolic case.

Example 3.6 The trefoil knot complement has an ideal layered triangulation with two tetrahedra and two edges, one of degree 2 and one of degree 10. See Figure 4. The complement of the trefoil knot can be seen as a punctured torus bundle with monodromy given by RL^{-1}, where

$$L = \left(\begin{smallmatrix} 1 & 0 \\ 1 & 1 \end{smallmatrix}\right) \qquad R = \left(\begin{smallmatrix} 1 & 1 \\ 0 & 1 \end{smallmatrix}\right).$$

Following the caption of Figure 4, we obtain a triangulation of the complement of the trefoil consisting of two tetrahedra. The matrix form of the generalised angle structure equations for this triangulation is

$$\begin{pmatrix} 1 & 1 & 0 & 0 & 0 & 0 \\ 1 & 1 & 2 & 2 & 2 & 2 \\ 1 & 0 & 1 & 0 & 1 & 0 \\ 0 & 1 & 0 & 1 & 0 & 1 \end{pmatrix} \begin{pmatrix} Z_1 \\ Z_2 \\ Z_1' \\ Z_2' \\ Z_1'' \\ Z_2'' \end{pmatrix} = \begin{pmatrix} 2\pi \\ 2\pi \\ \pi \\ \pi \end{pmatrix}.$$

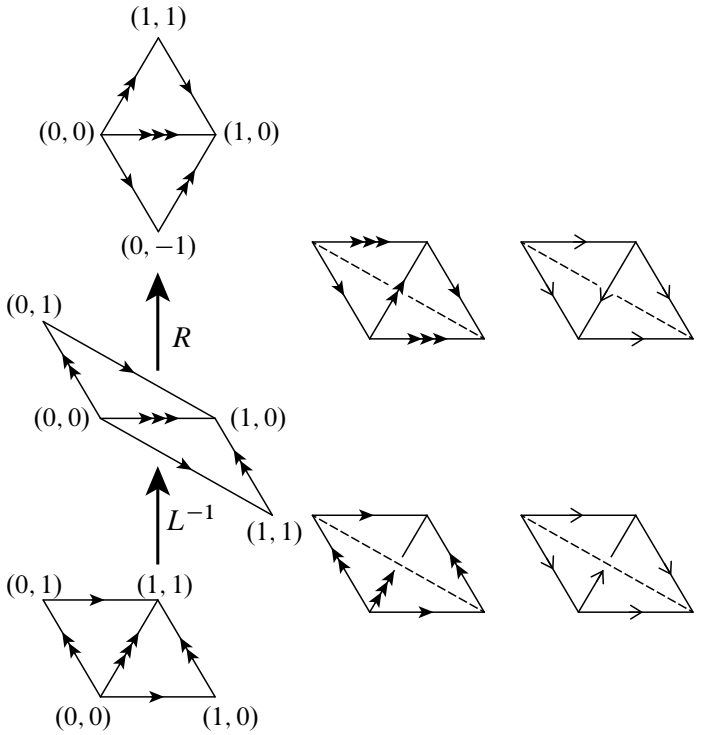

Figure 4: A layered triangulation of the complement of the trefoil knot, seen as a punctured torus bundle. On the left, the monodromy is decomposed into generators which act on the punctured torus. The diagrams are shown sheared to highlight the fact that the monodromy has the effect of rotation by $-\pi/3$. The arrows show where edges of a triangulation of the punctured torus map to under the generators. In the middle, we realise each change in the triangulation by layering on a flat tetrahedron. The arrows are shown on the bottom and top of the stack of two tetrahedra to show the gluing. On the right, we see the edges after the identifications induced by gluing the top to the bottom. There are two tetrahedra and two edges in the triangulation, one of degree two (shown with a dashed line) and the other of degree ten.

There is a taut structure given by choosing angles $(\pi, \pi, 0, 0, 0, 0)^T$. This assigns the angle π to the quad types facing the degree 2 edge and 0 to all other angles. This taut structure is compatible with the layering construction. By Theorem 1.5, this triangulation is 1–efficient.

It is easy to see that there are no other semiangle structures for this particular triangulation, because of the degree 2 edge. However, consistent with Theorem 1.2, it admits an index structure. To see this, we have to produce a generalised angle structure for

each of the $3^2 = 9$ possible quad-choices. However, by symmetry of the matrix we can reduce this number to three, represented by the following three pairs of conditions that must be satisfied by three generalised angle structures:

$$(Z_1 > 0, Z_2 > 0), \quad (Z_1 > 0, Z_2' > 0), \quad (Z_1' > 0, Z_2' > 0).$$

These three representatives are all satisfied by, for example, $(\pi, \pi, x, x, -x, -x)^T$ for any $x > 0$.

Note that there is a well-known 6–fold cyclic covering by the bundle which is a product of a once punctured torus and a circle. This covering is toroidal so we see that there is an index structure on the trefoil knot space but not on this covering space.

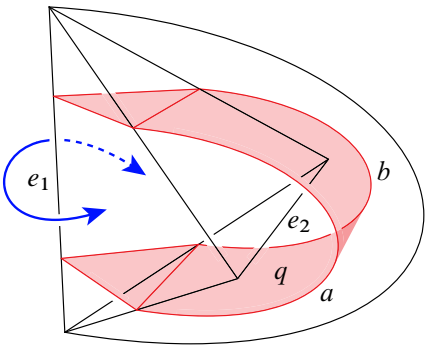

Figure 5: Part of a triangulation that does not admit an index structure, and part of the corresponding surface. The edge e_1 is degree 1, so the two faces incident to it are identified (indicated by the arrows).

Example 3.7 We give an example of a subset of a triangulation consisting of two tetrahedra identified in a particular way. Namely, we have a tetrahedron σ_1 with opposite edges e_1 of degree 1 and e_2 of degree 2, and another tetrahedron σ_2 which is the second tetrahedron incident to e_2. See Figure 5. If these tetrahedra are part of any ideal triangulation with torus boundary components then that triangulation will not have an index structure, and will have a normal torus that is not vertex-linking, so it is not 1–efficient.

First we show that there is no index structure. Since e_1 is degree 1, for any generalised angle structure the angle of σ_1 at the quad type facing e_1 must be 2π. This quad type also faces e_2. The angle of the quad type in σ_2 facing e_2 must add to 2π to give 2π, and so it must be zero. Therefore this angle can never be strictly positive, and so there is no index structure.

Next, we find the corresponding embedded normal torus. It has a single quadrilateral in σ_2, labelled q in Figure 5. Two of its triangles are in σ_1, also shown. When the two identified faces of σ_1 are glued to each other, the boundary of the shown surface consists of the two arcs labelled a and b, on two of the boundary faces of σ_2. Now consider the vertex–linking normal torus T, given by the link of the vertex at which the endpoints of e_2 meet. We complete our surface into an embedded normal torus by deleting from T the normal triangles in σ_1 and σ_2 at the endpoints of e_2, and gluing the resulting boundary arcs to a and b. The resulting surface is boundary parallel and so is a torus, but is obviously not vertex–linking since it contains a quadrilateral.

4 A review of the index of an ideal triangulation

4.1 The tetrahedron index and its properties

In this section we review the definition and the identities satisfied by the tetrahedron index of [10]. For a detailed discussion, see [16].

The building block of the index $I_{\mathcal{T}}$ of an ideal triangulation $\mathcal{T}$ is the *tetrahedron index* $I_\Delta(m,e)(q) \in \mathbb{Z}[\![q^{1/2}]\!]$ defined by

$$I_\Delta(m,e) = \sum_{n=(-e)_+}^{\infty} (-1)^n \frac{q^{n(n+1)/2-(n+e/2)m}}{(q)_n (q)_{n+e}}, \tag{5}$$

where

$$e_+ = \max\{0, e\}$$

and $(q)_n = \prod_{i=1}^{n}(1-q^i)$. If we wish, we can sum in the above equation over the integers, with the understanding that $1/(q)_n = 0$ for $n < 0$.

The tetrahedron index satisfies the *linear* recursion relations

$$q^{e/2} I_\Delta(m+1,e) + q^{-m/2} I_\Delta(m,e+1) - I_\Delta(m,e) = 0, \tag{6a}$$

$$q^{e/2} I_\Delta(m-1,e) + q^{-m/2} I_\Delta(m,e-1) - I_\Delta(m,e) = 0 \tag{6b}$$

and

$$I_\Delta(m,e+1) + (q^{e+m/2} - q^{-m/2} - q^{m/2}) I_\Delta(m,e) + I_\Delta(m,e-1) = 0, \tag{7a}$$

$$I_\Delta(m+1,e) + (q^{-e/2-m} - q^{-e/2} - q^{e/2}) I_\Delta(m,e) + I_\Delta(m-1,e) = 0 \tag{7b}$$

and the *duality* identity

$$I_\Delta(m,e)(q) = I_\Delta(-e,-m)(q) \tag{8}$$

and the *triality* identity

$$I_\Delta(m,e)(q) = (-q^{1/2})^{-e} I_\Delta(e,-e-m)(q) = (-q^{1/2})^{m} I_\Delta(-e-m,m)(q) \tag{9}$$

and the *pentagon* identity

$$\begin{aligned} I_\Delta(m_1-e_2,e_1)I_\Delta(m_2-e_1,e_2) \\ = \sum_{e_3\in\mathbb{Z}} q^{e_3} I_\Delta(m_1,e_1+e_3)I_\Delta(m_2,e_2+e_3)I_\Delta(m_1+m_2,e_3), \end{aligned} \tag{10}$$

and the *quadratic* identity

$$\sum_{e\in\mathbb{Z}} I_\Delta(m,e)I_\Delta(m,e+c)q^e = \delta_{c,0} = \begin{cases} 1 & \text{if } c=0, \\ 0 & \text{if } c\neq 0. \end{cases} \tag{11}$$

The above relations are valid for all integers m, e, m_i, e_i, c.

4.2 The degree of the tetrahedron index

The (minimum) degree $\delta(m,e)$ with respect to q of $I_\Delta(m,e)$ is given by

$$\delta(m,e) = \tfrac{1}{2}(m_+(m+e)_+ + (-m)_+e_+ + (-e)_+(-e-m)_+ + \max\{0,m,-e\}). \tag{12}$$

It follows that $\delta(m,e)$ is a piecewise quadratic polynomial as shown in Figure 6.

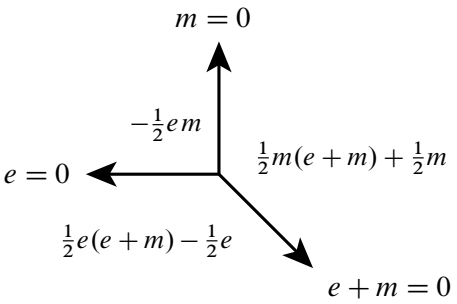

Figure 6: The degree of the tetrahedron index $I_\Delta(m,e)$. Here the positive m axis is to the right and the positive e axis is upwards.

The regions of polynomiality of $\delta(m,e)$ give a fan in $\mathbb{R}^2$ with rays spanned by the vectors $(0,1)$, $(-1,0)$ and $(1,-1)$. An important feature of δ is that it is a convex function on rays.

4.3 Angle structure equations

Recall the equations for a generalised angle structure from Definition 2.13. In this section, we will refer to the angle variables within the i^{th} tetrahedron, $\alpha(q_i), \alpha(q_i'), \alpha(q_i'')$, as Z_i, Z_i', Z_i'' respectively.

We can view a quad-choice Q for $\mathcal{T}$ (as in Definition 2.12) as a choice of pair of opposite edges at each tetrahedron Δ_i for $i = 1, \dots, N$. The quad-choice Q can be used to eliminate one of the three variables Z_i, Z_i', Z_i'' at each tetrahedron using the relation $Z_i + Z_i' + Z_i'' = \pi$. Doing so, equations (3) take the form

$$\mathbb{A}Z + \mathbb{B}Z'' = \pi\boldsymbol{\nu},$$

where $\boldsymbol{\nu} \in \mathbb{Z}^N$. (For example, if we eliminate the variables Z_i' then $\mathbb{A} = \overline{\mathbb{A}} - \overline{\mathbb{B}}$, $\mathbb{B} = \overline{\mathbb{C}} - \overline{\mathbb{B}}$ and $\boldsymbol{\nu} = 2(1, \dots, 1)^T - \overline{\mathbb{B}}(1, \dots, 1)^T$.)

The matrices $(\mathbb{A} \mid \mathbb{B})$ have some key *symplectic properties*, discovered by Neumann and Zagier when M is a hyperbolic 3–manifold (and $\mathcal{T}$ is well-adapted to the hyperbolic structure) [40], and later generalised to the case of arbitrary 3–manifolds in [39]. Neumann and Zagier show that the rank of $(\mathbb{A} \mid \mathbb{B})$ is $N - r$, where r is the number of boundary components of M; all assumed to be tori.

4.4 Peripheral equations

Assume first, for simplicity, that ∂M consists of a single torus, and let ϖ be an oriented simple closed curve in ∂M that is in *normal position* with respect to the induced triangulation $\mathcal{T}_\partial$ of ∂M. Let

$$(\overline{a}_\varpi \mid \overline{b}_\varpi \mid \overline{c}_\varpi) = (\overline{a}_{\varpi,1} \dots, \overline{a}_{\varpi,N} \mid \overline{b}_{\varpi,1}, \dots, \overline{b}_{\varpi,N} \mid \overline{c}_{\varpi,1}, \dots, \overline{c}_{\varpi,N}) \tag{13}$$

denote the vector in $\mathbb{Z}^{3N}$ computed as follows. See Figure 7.

The term $\overline{a}^l_\varpi$ counts the signed number of normal arcs of ϖ that turn anticlockwise around the corner of the truncated tetrahedron associated to the variable Z, at vertex number l of this tetrahedron. The entry in the vector $\overline{a}_\varpi$ for this tetrahedron is $\sum_{l=0}^{3} \overline{a}^l_\varpi$, and similarly for the $\overline{b}_\varpi$ and $\overline{c}_\varpi$ terms. We suppress the vertex number superscripts from now on, since this data is implied by the location of the labels in the figures.

If we eliminate Z_j' using $Z_j + Z_j' + Z_j'' = \pi$, then we obtain the vector in $\mathbb{Z}^{2N}$

$$(a_\varpi \mid b_\varpi) = (\overline{a}_\varpi - \overline{b}_\varpi \mid \overline{c}_\varpi - \overline{b}_\varpi) \tag{14}$$

as well as the scalar

$$\nu_{\varpi} = -\sum_{j=1}^{N} \overline{b}_{\varpi,j}. \tag{15}$$

Similarly, we can define "turning number" vectors $(\overline{a}_{\varpi} \mid \overline{b}_{\varpi} \mid \overline{c}_{\varpi}) \in \mathbb{Z}^{3N}$ and $(a_{\varpi} \mid b_{\varpi}) \in \mathbb{Z}^{2N}$ for any oriented multicurve ϖ on ∂M (ie a disjoint union of oriented simple closed normal curves on ∂M).

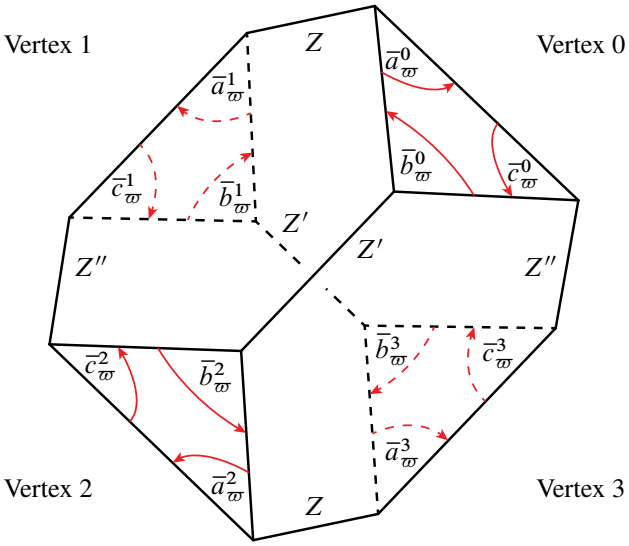

Figure 7: Each term of the "turning number" vector $(\overline{a}_{\varpi} \mid \overline{b}_{\varpi} \mid \overline{c}_{\varpi})$ is calculated as a sum of the signed number of times the curve ϖ turns anticlockwise around the corners of the triangular ends of the truncated tetrahedra. Edges and arcs on the back side of the tetrahedron are drawn with dashed lines.

More generally, suppose that M is a 3–manifold whose boundary ∂M consists of $r \geq 1$ tori $T_1, \dots, T_r$. Let $\varpi = (\varpi_1, \dots, \varpi_r)$, where ϖ_h is an oriented multicurve on T_h for each $h = 1, \dots, r$. Then we will use the notation

$$\begin{aligned} (\overline{a}_{\varpi} \mid \overline{b}_{\varpi} \mid \overline{c}_{\varpi}) &= \sum_{h=1}^{r} (\overline{a}_{\varpi_h} \mid \overline{b}_{\varpi_h} \mid \overline{c}_{\varpi_h}), \\ (a_{\varpi} \mid b_{\varpi}) &= \sum_{h=1}^{r} (a_{\varpi_h} \mid b_{\varpi_h}), \\ \nu_{\varpi} &= \sum_{h=1}^{r} \nu_{\varpi_h}. \end{aligned} \tag{16}$$

Remark 4.1 Suppose that $\varpi = C_i$ is a small linking circle on ∂M around one of the two vertices at the ends of the i^{th} edge, with C_i oriented anticlockwise as viewed from a cusp of M. Then

$$(\overline{a}_\varpi \mid \overline{b}_\varpi \mid \overline{c}_\varpi) = (\overline{a}_{i1} \ldots, \overline{a}_{iN} \mid \overline{b}_{i1}, \ldots, \overline{b}_{iN} \mid \overline{c}_{i1}, \ldots, \overline{c}_{iN})$$

gives the coefficients of the i^{th} edge equation as a special case of this construction.

4.5 The index of an ideal triangulation

Suppose that M is a 3–manifold whose boundary ∂M consists of $r \geq 1$ tori $T_1, \ldots, T_r$, and let $\mathcal{T}$ be an ideal triangulation of M. Let $\varpi = (\varpi_1, \ldots, \varpi_r)$ be a collection of oriented peripheral curves as above. By Theorem 4.3, proved below, we can order the edges of $\mathcal{T}$ so that the first $N-r$ rows of the Neumann–Zagier matrix $(\mathbb{A} \mid \mathbb{B})$ form an *integer basis* for its integer row space (ie the $\mathbb{Z}$–module of all linear combinations of its rows with integer coefficients). Then we define

$$I_{\mathcal{T}}(\varpi)(q) = \sum_{\boldsymbol{k} \in \mathbb{Z}^{N-r} \subset \mathbb{Z}^N} (-q^{1/2})^{\boldsymbol{k}\cdot\boldsymbol{\nu}+\nu_\varpi} \prod_{j=1}^{N} I_\Delta(-b_{\varpi,j} - \boldsymbol{k}\cdot\boldsymbol{b}_j, a_{\varpi,j} + \boldsymbol{k}\cdot\boldsymbol{a}_j), \tag{17}$$

where $\boldsymbol{a}_j$ and $\boldsymbol{b}_j$ for $j = 1, \ldots, N$ denote the columns of $\mathbb{A}$ and $\mathbb{B}$, and

$$\mathbb{Z}^{N-r} = \big\{(k_1, \ldots, k_N) \in \mathbb{Z}^N \;\big|\; k_j = 0 \text{ for } j > N-r\big\}.$$

It can be checked that this definition is independent of the quad choice involved in forming $(\mathbb{A} \mid \mathbb{B})$; see (25). It is also independent of the choice of $N-r$ edges used to produce an integer basis for the integer row space of the Neumann–Zagier matrix, by Remark 4.6. In the case of a 1–cusped manifold M, any $N-1$ edges can be used; in other words we could replace the domain of summation $\mathbb{Z}^{N-1}$ by any of the coordinate hyperplanes $\{(k_1, \ldots, k_N) \in \mathbb{Z}^N \mid k_s = 0\}$ with $s \in \{1, \ldots, N\}$. In general, we choose a set $\mathcal{B}$ of $N-r$ *basic edges* whose corresponding rows we sum over, for example by using Theorem 4.3. Equivalently, we choose the complementary set $\mathcal{X}$ of *excluded edges*.

Theorem 4.7 below shows that the index is unchanged by an isotopy of ϖ so only depends on the homology class

$$[\varpi] = \Big[\sum \varpi_i\Big] \in H_1(\partial M; \mathbb{Z}) = \bigoplus_{i=1}^{N} H_1(T_i; \mathbb{Z}).$$

So the index gives a well-defined function

$$I_{\mathcal{T}} \colon H_1(\partial M; \mathbb{Z}) \longrightarrow \mathbb{Z}((q^{1/2})), \qquad \text{where } I_{\mathcal{T}}([\varpi]) = I_{\mathcal{T}}(\varpi).$$

If M is a 1–cusped manifold M, and μ and λ in $H_1(\partial M;\mathbb{Z})$ are a fixed oriented meridian and longitude on ∂M (a canonical choice exists when M is the complement of an oriented knot in S^3). Then we can write

$$[\varpi] = -\tfrac{1}{2}m\lambda + e\mu \tag{18}$$

for integers e, m. The naming of the integers e and m (electric and magnetic charge) and the above choice of signs was chosen to make our index compatible with the definition of [10] and [16].

4.6 Choice of edges in the summation for index

Let M be an orientable 3–manifold with $r \geq 1$ torus cusps and let $\mathcal{T}$ be an ideal triangulation of M with N tetrahedra and, hence, N edges which we denote $e_1, \dots, e_N$. Let G be the 1–skeleton $\mathcal{T}^{(1)}$ of $\mathcal{T}$ together with one (ideal) vertex for each cusp of M. Note that G has r vertices and N edges, and may contain loops (ie edges with both ends at a single vertex) or multiple edges between the same two vertices. The incidence matrix $C = (c_{hi})$ for G is an $r \times N$ matrix whose (h,i) entry gives the number of ends of edge i on cusp h. Note that each $c_{hi} \in \{0,1,2\}$ and the sum of entries is 2 in each column of C. Let $E(e_i) = E_i \subset \mathbb{Z}^{2N}$ be the edge equation coefficients corresponding to edge e_i in $\mathcal{T}$, and let

$$\Lambda = \left\{ \sum_{\boldsymbol{k} \in \mathbb{Z}^N} k_i E_i \right\} \subset \mathbb{Z}^{2N} \tag{19}$$

be the lattice of all integer linear combinations of these. In other words, E_i is the i^{th} row of the Neumann–Zagier matrix $(\mathbb{A} \mid \mathbb{B})$, and Λ is the integer row space of this matrix.

From the work of Neumann and Zagier (see [40] and [39, Theorem 4.1]), the lattice Λ has rank $N - r$ and the matrix C gives the linear relations between the edge equation coefficients $E_i \in \mathbb{Z}^{2N}$. More precisely,

$$\sum_i c_{hi} E_i = 0 \quad \text{for all } h = 1, \dots, r \tag{20}$$

and any other linear relation between the E_i arises from a real linear combination of the rows of C.

Definition 4.2 A subset of the edges of a graph Γ is a *maximal tree with* 1– *or* 3–*cycle* in Γ if (together with the vertices) it consists of any maximal tree T together with one additional edge that either (1) is a loop at one vertex, or (2) forms a 3–cycle together with two edges in T.

Theorem 4.3 *There exists an integer basis for Λ consisting of $N-r$ of the edge equation coefficients $E_1,\dots,E_N$. In fact, we can choose such a basis by omitting r edge equations corresponding to a maximal tree with 1– or 3–cycle in G.*

Remark 4.4 In other words, we can choose any maximal tree with 1– or 3– cycle for our set $\mathcal{X}$ of excluded edges, and hence choose the remaining edges as our set $\mathcal{B}$ of basic edges.

This result and its proof were inspired by Jeff Weeks' argument in [49, pages 35–36].

Proof First we show that we can find a maximal tree with 1– or 3–cycle. If there exists a loop in G we use this loop together with any maximal tree. If not, any face of the triangulation has its ideal vertices on 3 distinct cusps. Pick two edges of this face and extend these to a maximal tree $T\subset G$. Adding the third edge of the face gives the desired subgraph.

Now let S be a maximal tree with 1– or 3–cycle. Next we show that the $N-r$ equations $E(e)$ corresponding to the edges $e\notin S$ give an integer basis for Λ. We show that for each $s\in S$ the equation $E(s)$ can be written as an integer linear combination of the equations $E(e)$ with $e\notin S$. Given this, the $N-r$ equations $E(e)$ with $e\notin S$ form an integer spanning set for Λ. The work of Neumann and Zagier ([40] and [39, Theorem 4.1]), implies that these equations are also linearly independent, hence form an integer basis for Λ, and we are done.

So, we have to show that every $E(s)$ can be written as an integer linear combination of the $E(e)$ for $e\notin S$. To organise the construction, we use the following sequence of *decorated graphs*. At each step we have a graph G_k whose edges are labelled by names of edges of G. We decorate each end of each edge of G_k with a sign. Each vertex v of G_k is then incident to a set of ends of edges with signs. We list the names of the edges, together with the sign associated to this end: $\{(e_{i_v(1)},\epsilon_v(1)),(e_{i_v(2)},\epsilon_v(2)),\dots,(e_{i_v(d)},\epsilon_v(d))\}$. Here d is the degree of the vertex v. To this vertex we associate the equation

$$R_k(v)=\sum_{l=1}^{d}\epsilon_v(l)E(e_{i_v(l)})=0.$$

For each G_k we have a subset S_k of the edges of G_k which is a maximal tree with 1– or 3–cycle in G_k. We set $G_0=G$ and $S_0=S$, with all signs set to $+$. Note that the equations associated to the vertices of G_0 are then the same as those given by (20).

We obtain the graph and edge subset (G_{k+1},S_{k+1}) from (G_k,S_k) as follows. We arbitrarily choose a vertex v of G_k that has only one end of one edge s of S_k incident.

If there are no such vertices then the sequence ends at (G_k, S_k). Let w be the other end of s, which by assumption is distinct from v. The graph G_{k+1} is the result of collapsing the edge s of G_k; the two ends of s, v and w, are identified in G_{k+1}. We label the edges of G_{k+1} with the same names as in G_k and set $S_{k+1} = S_k \setminus \{s\}$ All of the signs decorating G_{k+1} are the same as in G_k, except that the ends of edges that were incident to v have their signs flipped. See Figure 8.

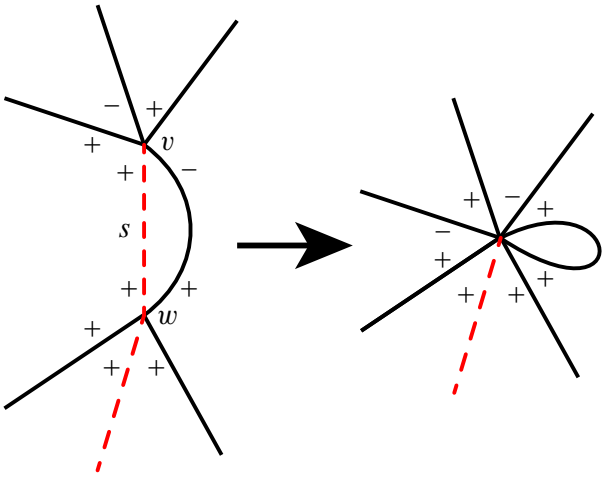

Figure 8: Collapsing the edge s flips the signs on the ends of the edges incident to v. Edges in S are drawn dashed.

Note that at each step of the sequence, both ends of each element of S_k have a $+$ sign, since they do in G_0 and we never collapse an edge from a vertex with more than one incident edge end in S. Consider the equations associated to the vertices of G_k and G_{k+1}. We have

$$R_k(v) = +E(s) + \sum_{l, e_{i_v(l)} \neq s} \epsilon_v(l) E(e_{i_v(l)}) = 0,$$

$$R_k(w) = +E(s) + \sum_{m, e_{i_w(m)} \neq s} \epsilon_w(m) E(e_{i_w(m)}) = 0.$$

If we use $R_k(v)$ to solve for $E(s)$ we get

$$E(s) = \sum_{l, e_{i_v(l)} \neq s} -\epsilon_v(l) E(e_{i_v(l)}).$$

Substituting this into $R_k(w)$ gives

$$\sum_{l, e_{i_v(l)} \neq s} -\epsilon_v(l) E(e_{i_v(l)}) + \sum_{m, e_{i_w(m)} \neq s} \epsilon_w(m) E(e_{i_w(m)}) = 0.$$

This is the equation associated to the vertex of G_{k+1} formed by the identification of v with w. Thus, the sequence of graphs gives an expression for $E(s)$ for each edge $s \in S$ which is removed.

This expression is an integer linear combination of the $E(e)$ for $e \notin S$. The sequence ends, at G_K say. By construction G_K has no vertices for which only one end of an edge of S is incident. If we are in case (1) of Definition 4.2 then G_K has one vertex, S_K has one edge and G_K looks like Figure 9 (left). If we are in case (2) then G_K has three vertices, S_K has three edges, and G_K looks like Figure 9 (right).

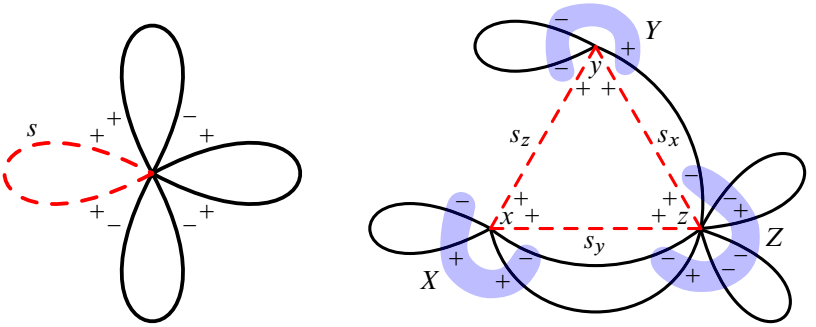

(a) (b)

Figure 9: The last graph in the sequence has one of these two forms: (a) The last graph when S has a 1–cycle. (b) The last graph when S has a 3–cycle.

In the first case, the equation from the last vertex is of the form

$$2E(s) + \sum_{l, e_i(l) \neq s} \epsilon(l) E(e_{i(l)}) = 0.$$

Notice that since all edges are now loops, each $E(e_i)$ appears with total coefficient either $-2, 0$ or 2. So we can divide the entire equation by 2, and get $E(s)$ as an integer linear combination of the $E(e_i)$.

The second case is slightly more complicated. We have three vertices x, y, z, with three edges $s_x, s_y, s_z \in S$ connecting the vertices into a triangle. The three vertices give equations of the form

$$E(s_y) + E(s_z) + X = 0, \quad E(s_z) + E(s_x) + Y = 0, \quad E(s_x) + E(s_y) + Z = 0,$$

where X, Y, Z are terms coming from the edges not in S. We can solve these equations for $E(s_z)$ as

$$2E(s_z) = -X - Y + Z$$

and the other two expressions similarly. We just have to show that $-X-Y+Z$ has even coefficients, and then we will be done. As before, any loops contribute a coefficient in $\{-2,0,2\}$ to one of X, Y or Z. For edges with the same endpoints as one of s_x, s_y or s_z, their coefficients are 1 or -1 at two of X, Y and Z and 0 at the third. Thus their contribution to $-X-Y+Z$ is also in $\{-2,0,2\}$, and so $-X-Y+Z$ has even coefficients, as required. □

Example 4.5 The following example shows that the edges omitted must be chosen carefully in the multicusped case. Let M be the Whitehead link complement (with the triangulation given by m129 in SnapPy notation). Then the matrix of edge equations is

$$(\mathbb{A} \mid \mathbb{B}) = \left(\begin{array}{cccc|cccc} 2 & -1 & 1 & 1 & 1 & -2 & 0 & 0 \\ -1 & 0 & 0 & 0 & -1 & 1 & 1 & 1 \\ 0 & 1 & -1 & -1 & 1 & 0 & -2 & -2 \\ -1 & 0 & 0 & 0 & -1 & 1 & 1 & 1 \end{array}\right).$$

The cusp incidence matrix is

$$C = \begin{pmatrix} 1 & 2 & 1 & 0 \\ 1 & 0 & 1 & 2 \end{pmatrix}$$

and the corresponding graph G is shown in Figure 10.

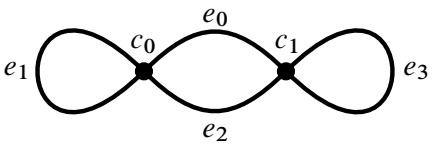

Figure 10: The graph of edges and cusps for the Whitehead link

The rows E_0, E_1, E_2, E_3 of $(\mathbb{A} \mid \mathbb{B})$ satisfy the relations

$$E_0 + 2E_1 + E_2 = 0 \text{ (from cusp 0)}$$

and

$$E_0 + E_2 + 2E_3 = 0 \text{ (from cusp 1)}$$

which imply that $E_1 = E_3$.

It follows that E_0, E_1 are linearly independent and form an integer basis for the $\mathbb{Z}$–span of $\{E_0, E_1, E_2, E_3\}$. (This basis corresponds to removing the edge e_2 in a maximal tree and an additional loop e_3.)

On the other hand, E_0, E_2 are also linearly independent and $2E_1$ is in the $\mathbb{Z}$–span of $\{E_0, E_2\}$ but E_1 is not in $\mathbb{Z}$–span of $\{E_0, E_2\}$. So $\mathbb{Z}$–span$\{E_0, E_2\}$ is an index-2 subgroup in $\mathbb{Z}$–span$\{E_0, E_1\}$. Thus, a summation using E_0, E_2 will most likely give a different result for the index than using E_0, E_1.

4.7 A reformulation of the definition of the index

It is sometimes convenient to work with a slight variation on the tetrahedral index function (5). Whenever $a-b, b-c \in \mathbb{Z}$ we define

$$J_\Delta(a,b,c) = (-q^{1/2})^{-b} I_\Delta(b-c, a-b) \\ = (-q^{1/2})^{-c} I_\Delta(c-a, b-c) = (-q^{1/2})^{-a} I_\Delta(a-b, c-a). \tag{21}$$

Note that the above expressions are equal by the triality identity (9) for I_Δ, and by using the duality identity (8), it follows that J_Δ is invariant under *all permutations* of its arguments. Further, we have

$$J_\Delta(a+s, b+s, c+s) = (-q^{1/2})^{-s} J_\Delta(a,b,c) \quad \text{for all } s \in \mathbb{R}. \tag{22}$$

We also note that the quadratic identity (11) can be rewritten in the form

$$\sum_{a\in\mathbb{Z}} J_\Delta(a,b,c) J_\Delta(a+x,b,c) q^a = \delta_{x,0}. \tag{23}$$

This follows since

$$\begin{aligned} \text{LHS} &= \sum_{a\in\mathbb{Z}} (-q^{1/2})^{-b} I_\Delta(b-c, a-b)(-q^{1/2})^{-b} I_\Delta(b-c, a-b+x) q^a \\ &= \sum_{e\in\mathbb{Z}} I_\Delta(m,e) I_\Delta(m, e+x) q^e = \delta_{x,0} \end{aligned}$$

by (11) with $m = b-c$ and $e = a-b$.

Now suppose that M is a 3–manifold whose boundary ∂M consists of $r \geq 1$ tori. Let $\overline{\mathbb{A}}$, $\overline{\mathbb{B}}$ and $\overline{\mathbb{C}}$ be the matrices of angle structure equation coefficients as in Definition 2.13, and let $\overline{\boldsymbol{a}}_j, \overline{\boldsymbol{b}}_j, \overline{\boldsymbol{c}}_j$ for $j = 1, \dots N$ denote the columns of $\overline{\mathbb{A}}$, $\overline{\mathbb{B}}$ and $\overline{\mathbb{C}}$ respectively. For each $\boldsymbol{k} \in \mathbb{Z}^N$ and oriented multicurve ϖ in ∂M representing a homology class $[\varpi] \in H_1(\partial M, \mathbb{Z})$, let

$$\overline{a}_j(\boldsymbol{k}, \varpi) = \boldsymbol{k} \cdot \overline{\boldsymbol{a}}_j + \overline{a}_{\varpi,j}, \quad \overline{b}_j(\boldsymbol{k}, \varpi) = \boldsymbol{k} \cdot \overline{\boldsymbol{b}}_j + \overline{b}_{\varpi,j}, \quad \overline{c}_j(\boldsymbol{k}, \varpi) = \boldsymbol{k} \cdot \overline{\boldsymbol{c}}_j + \overline{c}_{\varpi,j}$$

and

$$a_j(\boldsymbol{k}, \varpi) = \overline{a}_j(\boldsymbol{k}, \varpi) - \overline{b}_j(\boldsymbol{k}, \varpi), \quad b_j(\boldsymbol{k}, \varpi) = \overline{c}_j(\boldsymbol{k}, \varpi) - \overline{b}_j(\boldsymbol{k}, \varpi).$$

Then the definition (17) of the index of the triangulation $\mathcal{T}$ of a manifold M can be written

$$I_{\mathcal{T}}(\varpi)(q) = \sum_{\boldsymbol{k}\in\mathbb{Z}^{N-r}\subset\mathbb{Z}^N} (-q^{1/2})^{\boldsymbol{k}\cdot\boldsymbol{\nu}+\nu_\varpi} \prod_{j=1}^{N} I_\Delta(-b_j(\boldsymbol{k}, \varpi), a_j(\boldsymbol{k}, \varpi)), \tag{24}$$

where the sum is over $\boldsymbol{k}$ in any coordinate plane $\mathbb{Z}^{N-r} \subset \mathbb{Z}^N$ corresponding to a set $\mathcal{B}$ of $N-r$ basic edges as given by Theorem 4.3.

Let $\boldsymbol{k} = (k_1, \dots, k_N)$, $\boldsymbol{v} = (v_1, \dots, v_N)$ and let $\overline{b}_{ij}$ be the (i, j) entry of $\overline{\mathbb{B}}$. Then we have

$$\boldsymbol{k} \cdot \boldsymbol{v} = \sum_i k_i v_i = \sum_i 2k_i - \sum_{i,j} k_i \overline{b}_{ij} = \sum_i 2k_i - \sum_j \boldsymbol{k} \cdot \overline{\boldsymbol{b}}_j$$

and $v_\varpi = -\sum \overline{b}_{\varpi,j}$, so

$$\boldsymbol{k} \cdot \boldsymbol{v} + v_\varpi = \sum_i 2k_i - \sum_j \overline{b}_j(k, \varpi).$$

Hence, grouping together the contributions from tetrahedron j, we have

$$\begin{aligned} I_{\mathcal{T}}(\varpi)(q) &= \sum_{\boldsymbol{k} \in \mathbb{Z}^{N-r}} q^{\sum_i k_i} \prod_j (-q^{1/2})^{-\overline{b}_j(k,\varpi)} \\ &\qquad \times I_\Delta(\overline{b}_j(\boldsymbol{k}, \varpi) - \overline{c}_j(\boldsymbol{k}, \varpi), \overline{a}_j(\boldsymbol{k}, \varpi) - \overline{b}_j(\boldsymbol{k}, \varpi)) \\ &= \sum_{\boldsymbol{k} \in \mathbb{Z}^{N-r}} q^{\sum_i k_i} \prod_j J_\Delta(\overline{a}_j(\boldsymbol{k}, \varpi), \overline{b}_j(\boldsymbol{k}, \varpi), \overline{c}_j(\boldsymbol{k}, \varpi)), \end{aligned} \tag{25}$$

where $\mathbb{Z}^{N-r} \subset \mathbb{Z}^N$ corresponds to a set $\mathcal{B}$ of $N-r$ basic edges as given by Theorem 4.3.

In particular, this expression shows that the index does not depend on the quad-choice used in the original definition.

Remark 4.6 Next we show that the definition of index in (17) does not depend on the choice of integer basis for the integer row space $\Lambda \subset \mathbb{R}^{2N}$ of the Neumann–Zagier matrix $(\mathbb{A} \mid \mathbb{B})$.

Each $x \in \Lambda$ can be written in the form

$$x = \sum_i k_i E_i, \tag{26}$$

where E_i is the i^{th} row of $(\mathbb{A} \mid \mathbb{B})$ and $\boldsymbol{k} = (k_1, \dots, k_N) \in \mathbb{Z}^N$. We claim that the expression

$$J(x, \varpi) = q^{\sum_i k_i} \prod_j J_\Delta(\overline{a}_j(\boldsymbol{k}, \varpi), \overline{b}_j(\boldsymbol{k}, \varpi), \overline{c}_j(\boldsymbol{k}, \varpi)) \tag{27}$$

is well-defined, depending only on $x \in \Lambda$ and not on the choice of $\boldsymbol{k}$ in (26).

To see this, consider the linear map $\psi : \mathbb{R}^N \to \mathbb{R}^{2N}$ defined by $\psi(k_1, \dots, k_N) = \sum_i k_i E_i$ and let $\langle C \rangle \subset \mathbb{R}^N$ be the real subspace generated by the cusp relation vectors

$(c_{h1}, \dots, c_{hN})$, where the cusp index h varies over $\{1, \dots, r\}$. Then $\psi(\langle C \rangle) = 0$ by the cusp relations (20), and the work of Neumann and Zagier [40; 39] also shows that $\dim \operatorname{Im} \psi = N - r$ and $\dim \langle C \rangle = r$, where r is the number of cusps. Hence $\langle C \rangle = \ker \psi$.

So if $x = \sum_i k_i E_i = \sum_i k'_i E_i$, where $\boldsymbol{k}' = (k'_1, \dots, k'_N) \in \mathbb{R}^N$ then $\boldsymbol{k}' = \boldsymbol{k} + \boldsymbol{c}$, where $\boldsymbol{c} \in \langle C \rangle$. We claim that replacing $\boldsymbol{k}$ by $\boldsymbol{k}'$ does not change the expression (27). To see this, suppose we replace $\boldsymbol{k}$ by $\boldsymbol{k}'$, where $k'_i = k_i + s c_{hi}$ for $i = 1, \dots, N$ and $s \in \mathbb{R}$. Then the term $q^{\sum_i k_i}$ in (27) is multiplied by $q^{s n_h}$, where n_h is the number of vertices in the triangulation of cusp h, while $\overline{a}_j(\boldsymbol{k}, \varpi), \overline{b}_j(\boldsymbol{k}, \varpi), \overline{c}_j(\boldsymbol{k}, \varpi)$ are increased by s for each triangle of tetrahedron j lying in the cusp h. By (22), this changes $\prod_j J_\Delta(\overline{a}_j(\boldsymbol{k}, \varpi), \overline{b}_j(\boldsymbol{k}, \varpi), \overline{c}_j(\boldsymbol{k}, \varpi))$ by a factor $(-q^{1/2})^{-2 s n_h}$ since there are $2n_h$ triangles on cusp h. Hence the right-hand side of (27) does not change.

We conclude that the expression for index in (25) can be rewritten in the form

$$I_{\mathcal{T}}(\varpi) = \sum_{x \in \Lambda} J(x, \varpi) \tag{28}$$

and so does not depend on a choice of basis for Λ. Further, we can evaluate $I_{\mathcal{T}}(\varpi)$ by choosing an integer basis for Λ corresponding to a set of basic edges as given by Theorem 4.3, and we recover the definition of index in (17).

It also follows that we can write the index in the form

$$I_{\mathcal{T}}(\varpi) = \sum_{\boldsymbol{k} \in S} q^{\sum_i k_i} \prod_j J_\Delta(\overline{a}_j(\boldsymbol{k}, \varpi), \overline{b}_j(\boldsymbol{k}, \varpi), \overline{c}_j(\boldsymbol{k}, \varpi)), \tag{29}$$

where $S \subset \mathbb{Z}^N$ is any complete set of coset representatives for $(\mathbb{Z}^N + \langle C \rangle)/\langle C \rangle \subset \mathbb{R}^N/\langle C \rangle$.

4.8 Invariance of index under isotopy of peripheral curve

Theorem 4.7 *Let ϖ be an oriented simple closed curve ϖ in ∂M which is a normal curve relative to the triangulation $\mathcal{T}_\partial$ of ∂M. Then the index $I_{\mathcal{T}}(\varpi)$ is invariant under isotopy of the curve ϖ in ∂M.*

Proof Suppose we have two isotopic oriented normal curves ϖ_1, ϖ_2. Then we can convert one into the other via a sequence of moves (and their inverses) of the form shown in Figure 11. That is, we choose a point p on the curve ϖ and an arc α, disjoint from ϖ other than at p, and which joins p to either a vertex or a point in the interior of an edge of $\mathcal{T}_\partial$. We then push the curve along and in a regular neighbourhood of α over the vertex or edge.

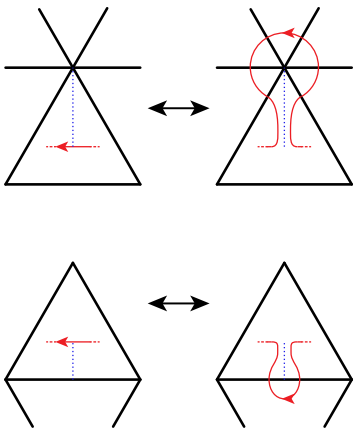

Figure 11: The two kinds of isotopy moves on a curve relative to the triangulation of ∂M

We will show that $I_{\mathcal{T}}(\varpi)$ is invariant under these moves. Note that the result of these isotopies will not in general be normal curves, so we need to extend the definition of the index to deal with these cases as well. The class of curves we work in consists of oriented simple closed curves, transverse to $\mathcal{T}_\partial^{(1)}$ and disjoint from $\mathcal{T}_\partial^{(0)}$. For our purposes we will deal only with curves that are nontrivial in $H_1(\partial M)$, and so none of our curves is disjoint from $\mathcal{T}_\partial^{(1)}$. Given such a curve, it enters a triangle somewhere on one edge, and can exit out either of the two other edges, or the same edge that it entered, either to the left or the right of its entry point. Thus there are four ways in which a component of a curve intersects a given triangle. These contribute to the index in the following way. See Figure 12.

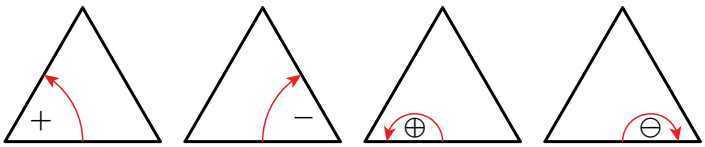

Figure 12: The four ways in which a curve can travel through a triangle. We call the last two possibilities a *positive backtrack* and *negative backtrack* respectively.

If the curve turns either left or right around a corner of the triangle then it contributes to the index in exactly the same way as for a normal curve: we add $+1$ to the entry in the vector $(\overline{a}_\varpi \mid \overline{b}_\varpi \mid \overline{c}_\varpi)$ corresponding to the angle at the edge of the tetrahedron we are turning around if we are going anticlockwise around the corner, and add -1 if we are going clockwise. Compare with Figure 7.

Here we define the effect of backtracks on the index calculation: (This is, of course, chosen in such a way as to be consistent with the index calculated with curves without backtracks.) We do not change the vector $(\overline{a}_\varpi \mid \overline{b}_\varpi \mid \overline{c}_\varpi)$. These backtracks only alter the power of $(-q^{1/2})$, either multiplying the expression by $(-q^{1/2})$ for a positive backtrack (turning to the left), or by $(-q^{1/2})^{-1}$ for a negative backtrack (turning to the right). We indicate these using the symbols $\oplus$ and $\ominus$.

Note that by (22), a positive backtrack has the same effect on the index as anticlockwise turns around each of the three corners of a triangle. Note also that by (25), an anticlockwise loop around a vertex of the triangulation produces a power of $(-q^{1/2})^2$. This follows since adding an anticlockwise loop around an end of the i^{th} edge has the effect of shifting the sum by one in the k_i component. The terms are unchanged after shifting other than the term $q^{\sum_i k_i}$, and the effect is to multiply the index by q.

Thus an anticlockwise loop around a vertex is cancelled by two negative backtracks, and anticlockwise turns around each of the three corners of a triangle are cancelled by one negative backtrack.

Now all we need to do is to show that each version of the moves from Figure 11 preserves the index, using the above rules. There are different versions of the isotopy moves depending on where the curve we are acting on enters or exits the triangle. We show the possibilities in Figure 13. Here the $+, -, \oplus$ and $\ominus$ signs show the *difference* in the index calculation under the isotopy as we change from one curve to the other in the direction following the double head arrow. Note that reversing the arrow on the curve flips all of the signs, as does reflecting the picture. With combinations of these symmetries applied to the ten cases shown we obtain all possible ways in which the isotopy can be made relative to the position of the curve. Considering each case in turn, we can see that the signs cancel out and so the index is unchanged by these moves.

For example, consider the second diagram in the top row of Figure 13. We start with a curve that enters the right side of the triangle and exits the bottom. We isotope this curve by pushing it over the top vertex of the triangle. This has the following effects:

- Remove an anticlockwise turn around the lower right corner of the triangle, this changes the coefficient at that angle by -1.
- Add a negative backtrack to the right edge of the triangle.
- Add an anticlockwise turn around each of the angles at the top vertex of the triangle other than the top corner of the triangle itself.
- Add a clockwise turn around the lower left corner of the triangle.

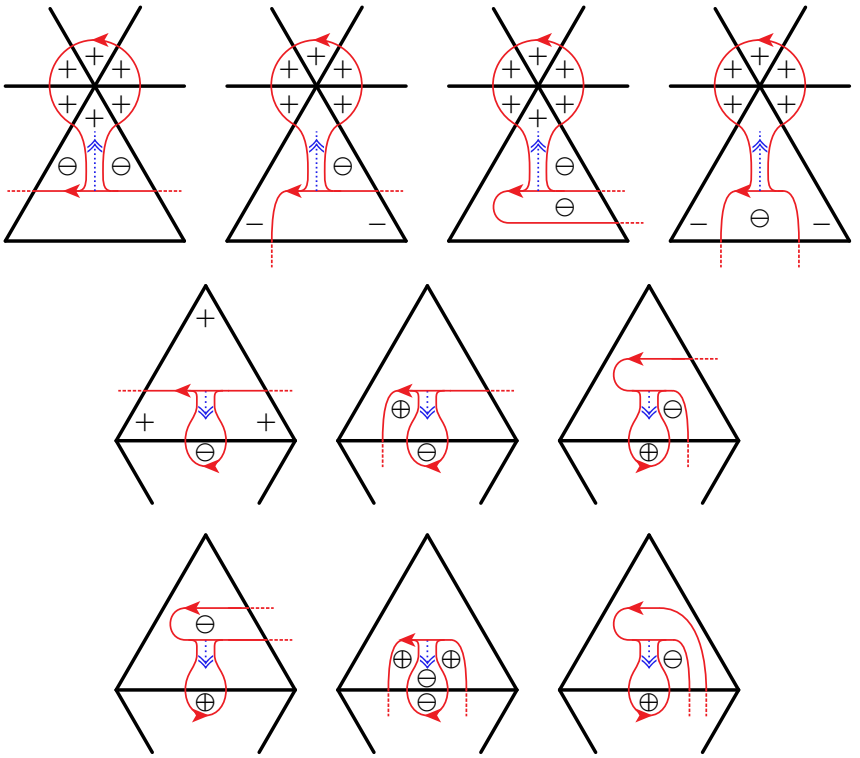

Figure 13: Four cases of isotopy across a vertex and six cases of isotopy across an edge. All other cases are symmetries of these.

We view the top corner of the triangle as having both a $+$ and a $-$, so that the total change in the index calculation consists of one anticlockwise turn around a vertex, one negative backtrack and clockwise turns around each of the three corners of the triangle. By our above rules, these cancel out and so the index is unchanged. □

Remark 4.8 These calculations are exactly analogous to those for calculating the holonomy of a peripheral curve given shapes of ideal hyperbolic tetrahedra satisfying Thurston's gluing equations. Thus this argument can easily be adapted to reprove the well-known fact that the holonomy is independent of the choice of simple closed curve representing an element of $H_1(\partial M;\mathbb{Z})$

5 Invariance of index under the 0–2 move

Let M be a cusped 3–manifold and consider the 0–2 move on a pair $\mathcal{T}$ and $\widetilde{\mathcal{T}}$ of ideal triangulations of M with N and $N+2$ tetrahedra, as shown in Figure 14.

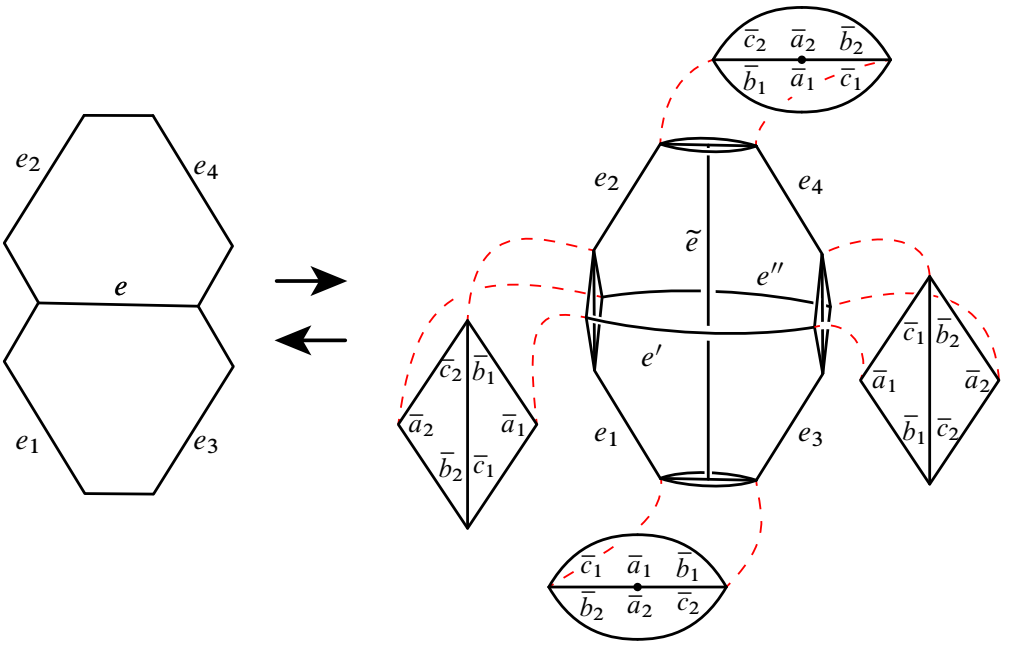

Figure 14: The 0–2 move shown with truncated tetrahedra. The four triangulated ends of the new pair of tetrahedra are shown. All of the "zoomed in" pictures are as seen from viewpoints outside of the pair of tetrahedra. The labels at the corners of the triangles in the "zoomed in" pictures are explained in Section 4.4.

Theorem 5.1 *Suppose that $\mathcal{T}$ and $\widetilde{\mathcal{T}}$ are ideal triangulations related by a 0–2 move and both admit an index structure. Then, for any $[\varpi] \in H_1(\partial M; \mathbb{Z})$, $I_{\mathcal{T}}([\varpi]) = I_{\widetilde{\mathcal{T}}}([\varpi])$.*

Proof Our assumptions imply that both $I_{\mathcal{T}}$ and $I_{\widetilde{\mathcal{T}}}$ exist. We now compare these indices using the alternative definition (25) and quadratic identity (23).

We use the labelling of the two bigons and triangles on $\widetilde{\mathcal{T}}$ shown in Figure 14. Let T_i for $i = 3, \dots, N+2$ denote the tetrahedra in $\mathcal{T}$, and let T_1, T_2 be the additional tetrahedra added in $\widetilde{\mathcal{T}}$. Note that the edge e in $\mathcal{T}$ splits into two edges e', e'' in $\widetilde{\mathcal{T}}$, and there is another new edge $\tilde{e}$ in $\widetilde{\mathcal{T}}$. We abuse notation by identifying the symbols for the corresponding remaining edges in $\mathcal{T}$ and $\widetilde{\mathcal{T}}$. We denote these as $e_1, \dots, e_{N-1}$.

Let $\widetilde{\boldsymbol{k}} \in \mathbb{Z}^{N+2}$ be a weight function on the edges of $\widetilde{\mathcal{T}}$ and write

$$\widetilde{\boldsymbol{k}} = (k', k'', \tilde{k}, k_1, \dots, k_{N-1}),$$

where $k', k'', \widetilde{k}, k_i$ are the values of $\widetilde{\boldsymbol{k}}$ on $e', e'', \widetilde{e}$ and e_i respectively. Similarly, let $\boldsymbol{k} = (k, k_1, \dots, k_{N-1}) \in \mathbb{Z}^N$ be a corresponding weight function on $\mathcal{T}$. We choose label $\overline{a}_j$ on the edge $\widetilde{e}$ on tetrahedron T_j for $j = 1, 2$; then the location of labels $\overline{b}_j, \overline{c}_j$ are determined using the orientation on M.

Let ϖ be an oriented multicurve which is normal with respect to the triangulation $\mathcal{T}_\partial$ of ∂M induced by $\mathcal{T}$, and let $\widetilde{\varpi}$ an oriented multicurve which is normal with respect to $\widetilde{\mathcal{T}}_\partial$ and represents the same homology class $[\varpi] \in H_1(\partial M; \mathbb{Z})$. Let $J(T_j, \boldsymbol{k}, \varpi) = J_\Delta(\overline{a}_j(\boldsymbol{k}, \varpi), \overline{b}_j(\boldsymbol{k}, \varpi), \overline{c}_j(\boldsymbol{k}, \varpi))$ denote the contribution of tetrahedron T_j to the index with weight function $\boldsymbol{k}$ on its edges and peripheral curve ϖ on its truncated ends, and similarly let $J(T_j, \widetilde{\boldsymbol{k}}, \widetilde{\varpi})$ be contribution with weight function $\widetilde{\boldsymbol{k}}$ and peripheral curve $\widetilde{\varpi}$.

To compute $I_{\mathcal{T}}$ we use Theorem 4.3 to choose an excluded set $\mathcal{X}$ of r edges in a maximal tree with 1– or 3–cycle in $\mathcal{T}$ to be omitted from the summation in (25).

Case 1 If $e \notin \mathcal{X}$ we can order the edges of $\mathcal{T}$ so that $\mathcal{X} = \{e_{N-r}, \dots, e_{N-2}, e_{N-1}\}$. Then we can compute $I_{\widetilde{\mathcal{T}}}$ by omitting the same edge set $\widetilde{\mathcal{X}} = \mathcal{X}$.

Case 2 If $e \in \mathcal{X}$ we can order the edges so $\mathcal{X} = \{e, e_{N-r+1}, \dots, e_{N-2}, e_{N-1}\}$. Then we can compute $I_{\widetilde{\mathcal{T}}}$ by omitting the edge set $\widetilde{\mathcal{X}} = \{e'', e_{N-r+1}, \dots, e_{N-2}, e_{N-1}\}$.

Then

$$I_{\widetilde{\mathcal{T}}}(\widetilde{\varpi}) = \sum_{\widetilde{\boldsymbol{k}} \in \widetilde{S}} q^{k'+k''+\widetilde{k}+\sum_{i=1}^{N-1} k_i} J(T_1, \widetilde{\boldsymbol{k}}, \widetilde{\varpi}) J(T_2, \widetilde{\boldsymbol{k}}, \widetilde{\varpi}) \prod_{j=3}^{N+2} J(T_j, \widetilde{\boldsymbol{k}}, \widetilde{\varpi}), \tag{30}$$

where

$$\widetilde{S} = \left\{ \widetilde{\boldsymbol{k}} = (k', k'', \widetilde{k}, k_1, \dots, k_{N-1}) \in \mathbb{Z}^{N+2} \;\middle|\; k_{N-i} = 0 \text{ for } i = 1, \dots, r \right\}$$

in Case 1 and

$$\widetilde{S} = \left\{ \widetilde{\boldsymbol{k}} = (k', k'', \widetilde{k}, k_1, \dots, k_{N-1}) \in \mathbb{Z}^{N+2} \;\middle|\; k'' = 0, k_{N-i} = 0 \text{ for } i = 1, \dots, r-1 \right\}$$

in Case 2. Note that in both cases, the new edge $\widetilde{e}$ is *included* in the set of basic edges so $\widetilde{k}$ varies over $\mathbb{Z}$ in the sum.

Now we look at the contribution to $I_{\widetilde{\mathcal{T}}}$ coming from the tetrahedra T_1, T_2 and summed over the weight $\widetilde{k}$ on $\widetilde{e}$, namely

$$\sum_{\widetilde{k} \in \mathbb{Z}} q^{\widetilde{k}} J(T_1; \widetilde{\boldsymbol{k}}, \widetilde{\varpi}) J(T_2; \widetilde{\boldsymbol{k}}, \widetilde{\varpi}), \tag{31}$$

where

$$\begin{aligned} J(T_1; \widetilde{\boldsymbol{k}}, \widetilde{\varpi}) &= J_\Delta(k' + \widetilde{k} + \overline{a}_{\widetilde{\varpi},1}, k_2 + k_3 + \overline{b}_{\widetilde{\varpi},1}, k_1 + k_4 + \overline{c}_{\widetilde{\varpi},1}), \\ J(T_2; \widetilde{\boldsymbol{k}}, \widetilde{\varpi}) &= J_\Delta(k'' + \widetilde{k} + \overline{a}_{\widetilde{\varpi},2}, k_1 + k_4 + \overline{b}_{\widetilde{\varpi},2}, k_2 + k_3 + \overline{c}_{\widetilde{\varpi},2}). \end{aligned}$$

Recall that ϖ is an oriented multicurve which is normal with respect to the triangulation $\mathcal{T}_\partial$ of ∂M induced by $\mathcal{T}$. Since the index only depends on the homology class of a peripheral curve, we can calculate $I_{\widetilde{\mathcal{T}}}([\varpi])$ by using for $\widetilde{\varpi}$ a corresponding curve on ∂M which is normal with respect to $\widetilde{\mathcal{T}}_\partial$ and goes "straight through" each pair of added triangles on ∂M. See Figure 15.

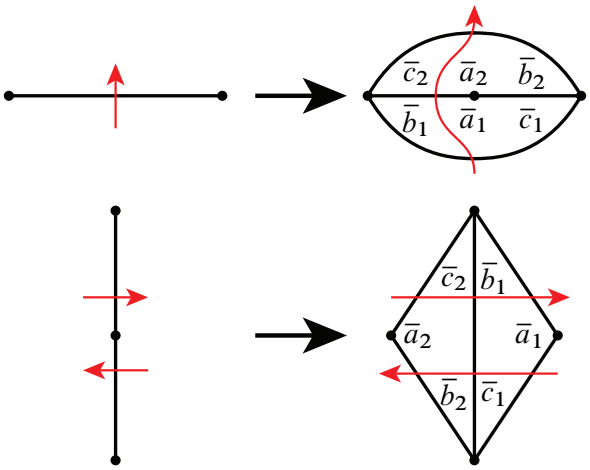

Figure 15: Changes in peripheral curve from ϖ in $\mathcal{T}_\partial$ to $\widetilde{\varpi}$ in $\widetilde{\mathcal{T}}_\partial$. Note that the curve in the top diagram could go either way around the new vertex.

Then we have

$$\overline{a}_{\widetilde{\varpi},1} = \overline{a}_{\widetilde{\varpi},2} = 0, \quad \overline{b}_{\widetilde{\varpi},1} = \overline{c}_{\widetilde{\varpi},2} = x, \quad \overline{b}_{\widetilde{\varpi},2} = \overline{c}_{\widetilde{\varpi},1} = y,$$

for some $x, y \in \mathbb{Z}$, and

$$\overline{a}_{\widetilde{\varpi},j} = \overline{a}_{\varpi,j}, \quad \overline{b}_{\widetilde{\varpi},j} = \overline{b}_{\varpi,j}, \quad \overline{c}_{\widetilde{\varpi},j} = \overline{c}_{\varpi,j} \quad \text{for } j = 3, \dots, N+2.$$

Using the invariance of J_Δ under all permutations of its arguments and the quadratic identity (23), the sum (31) becomes

$$\sum_{\widetilde{k}\in\mathbb{Z}} q^{\widetilde{k}} J_\Delta(k' + \widetilde{k}, k_2 + k_3 + x, k_1 + k_4 + y) J_\Delta(k'' + \widetilde{k}, k_1 + k_4 + y, k_2 + k_3 + x) = q^{-k'} \delta_{k',k''}.$$

This means that in the sum (30) we can remove the summation over $\widetilde{\boldsymbol{k}}$ and put $k' = k'' = k$. Hence $J(T_j, \widetilde{\boldsymbol{k}}, \widetilde{\varpi}) = J(T_j, \boldsymbol{k}, \varpi)$ for $j = 3, \dots, N+2$, and

$$I_{\widetilde{\mathcal{T}}}(\widetilde{\varpi}) = \sum_{\boldsymbol{k}\in S} q^{k + \sum_{i=1}^{N-1} k_i} \prod_{j=3}^{N+2} J(T_j, \boldsymbol{k}, \varpi) = I_{\mathcal{T}}(\varpi),$$

where

$$S = \{\boldsymbol{k} = (k, k_1, \dots, k_{N-1}) \in \mathbb{Z}^N \mid k_{N-i} = 0 \text{ for } i = 1, \dots, r\}$$

in Case 1 and

$$S = \{\boldsymbol{k} = (k, k_1, \dots, k_{N-1}) \in \mathbb{Z}^N \mid k = 0, k_{N-i} = 0 \text{ for } i = 1, \dots, r-1\}$$

in Case 2. This completes the proof of invariance of the index under the 0–2 move. □

6 The $\mathcal{X}_M^{\mathrm{EP}}$ class of triangulations

6.1 Subdivisions of the Epstein–Penner decomposition

For a once-cusped hyperbolic 3–manifold M, the Epstein–Penner decomposition (see [13]) divides M into a finite number of ideal hyperbolic polyhedra. This subdivision is canonical, depending only on the topology of the manifold, if M has a single cusp. If M has $r \geq 1$ cusps, then the Epstein–Penner cell decomposition is canonical up to the choice of a scale vector $(t_1, \dots, t_r)$ with $t_1, t_2, \dots, t_r > 0$ giving the relative size of the cusps. The scale vector is well-defined up to multiplication by a positive real number. For the purposes of defining our canonical set, we can choose all t_i to be the same.

Very often, the cells of the decomposition are all ideal tetrahedra, but other polyhedra can occur. For many applications, including the use in this paper, we need a subdivision of M into ideal tetrahedra only. It is well known that every cusped 3–manifold has a decomposition into ideal tetrahedra, but one often needs more than a purely topological structure on the tetrahedra. The Epstein–Penner decomposition, coming as it does with a geometric structure, provides all of the nice geometric properties one could want. So, in the cases when the cells of the decomposition are not themselves tetrahedra, we would like to further subdivide the polyhedra into tetrahedra. However, there is no canonical way to subdivide, and it is not even clear if one can subdivide the various polyhedra in a consistent way, so that the triangulations induced on the faces of the polyhedra match when the polyhedra are glued to each other. In particular, it is still unknown whether every cusped hyperbolic 3–manifold admits a *geometric triangulation* (that is, a subdivision into positive volume ideal hyperbolic tetrahedra), either constructed by further subdividing the Epstein–Penner decomposition or otherwise.

However, one can use the Epstein–Penner decomposition to produce an ideal triangulation by subdividing the ideal polyhedra, if we also allow flat tetrahedra inserted between faces of the polyhedra to bridge between incompatible triangulations of those

faces. Such an ideal triangulation has a *natural semiangle structure* (see Remark 6.6), and so by Theorem 1.5 all of these triangulations are 1–efficient.

To describe our triangulations more precisely, we use the same notation as in [24].

Definition 6.1 In this paper, the term *polyhedron* will mean a combinatorial object obtained by removing all of the vertices from a 3–cell with a given combinatorial cell decomposition of its boundary. We further require that this can be realised as a positive volume convex ideal polyhedron in hyperbolic 3–space $\mathbb{H}^3$.

Definition 6.2 An (ideal) *polygonal pillow* or *n–gonal pillow* is a combinatorial object obtained by removing all of the vertices from a 3–cell with a combinatorial cell decomposition of its boundary that has precisely two faces. The two faces are copies of an n–gon identified along corresponding edges.

Definition 6.3 Suppose that $\mathcal{P}$ is a cellulation of a 3–manifold consisting of polyhedra and polygonal pillows with the property that polyhedra are glued to either polyhedra or polygonal pillows, but polygonal pillows are only glued to polyhedra. Then we call $\mathcal{P}$ a *polyhedron and polygonal pillow cellulation*, or for short, a *PPP–cellulation*.

Definition 6.4 Let t be a triangulation of a polygon. A *diagonal flip* move changes t as follows. First we remove an internal edge of t, producing a four sided polygon, one of whose diagonals is the removed edge. Second, we add in the other diagonal, cutting the polygon into two triangles and giving a new triangulation of the polygon.

Definition 6.5 Let Q be a polygonal pillow, with triangulations t_- and t_+ given on its two polygonal faces Q_- and Q_+. By a *layered triangulation of Q, bridging between t_- and t_+*, we mean a triangulation produced as follows. We are given a sequence of diagonal flips which convert t_- into t_+. This gives a sequence of triangulations $t_- = L_1, L_2, \dots, L_k = t_+$, where consecutive triangulations are related by a diagonal flip. Starting from Q_- with the triangulation $t_- = L_1$, we glue a tetrahedron onto the triangulation L_1 so that two of its faces cover the faces of L_1 involved in the first diagonal flip. The other two faces together with the rest of L_1 produce the triangulation L_2. We continue in this fashion, adding one tetrahedron for each diagonal flip until we reach $L_k = t_+$, which we identify with Q_+.

Our class of triangulations $\mathcal{X}^{\mathrm{EP}}_M$ of M consists of triangulations that are subdivisions of PPP–cellulations. Our PPP–cellulation will have polyhedra being the polyhedra of the Epstein–Penner decomposition. It also has a polygonal pillow inserted between all pairs of identified faces that have at least 4 sides. We will form our triangulations by

first subdividing the ideal hyperbolic polyhedra into positive volume ideal hyperbolic tetrahedra. Secondly, for each polygonal pillow, we insert any layered triangulation that bridges between the induced triangulations of the two boundary polygons of the polyhedra to each side.

Remark 6.6 Any triangulation produced in the way described above has a *natural semiangle structure*. This comes from the shapes of the tetrahedra as ideal hyperbolic tetrahedra. The dihedral angles of the positive volume ideal hyperbolic tetrahedra, together with 0 and π angles for the flat tetrahedra in the layered triangulations in the polygonal pillows satisfy all of the rules for a generalised angle structure, and all angles are in $[0, \pi]$.

The natural semiangle structure together with Theorem 1.5 show that each triangulation in our class is 1–efficient. However, we also need to show that our class is connected under 2–3, 3–2, 0–2 and 2–0 moves, and for this we will need some extra machinery. The main tool we will use is the theory of regular triangulations of point configurations, following [9].

6.2 Regular triangulations

The concept of a regular triangulation comes from the study of triangulations of convex polytopes in $\mathbb{R}^n$. Here we are not dealing with topological triangulations, where tetrahedra may have self-identifications or two vertices may have multiple edges connecting them. Rather, the vertices are concrete points in $\mathbb{R}^n$, the edges are straight line segments in $\mathbb{R}^n$ and so on. In this context, a triangulation of a convex polytope is a subdivision of the polytope into concrete Euclidean simplices. Roughly speaking, a triangulation of a polytope in $\mathbb{R}^n$ is *regular* if it is isomorphic to the lower faces of a convex polytope in $\mathbb{R}^{n+1}$. The following series of definitions make this idea precise.

Definition 6.7 An *affine combination* of a set of points $(\boldsymbol{p}_j)_{j\in C}$ in $\mathbb{R}^n$ is a sum $\sum_{j\in C} \lambda_j \boldsymbol{p}_j$, where $\sum_{j\in C} \lambda_j = 1$ A set of points is *affinely independent* if none of them is an affine combination of the others. A *k–simplex* is the convex hull of an affinely independent set of $k+1$ points.

Definition 6.8 A *point configuration* is a finite set of labelled points in $\mathbb{R}^n$. Let $\boldsymbol{A} = (\boldsymbol{p}_j)_{j\in J}$ be a point configuration with label set J. For $C \subset J$, the *affine span of C in $\boldsymbol{A}$* is the set of affine combinations of the set of points labelled by C. The *dimension of C* is the dimension of the affine span of C. The *convex hull of C in $\boldsymbol{A}$*

is the convex hull in $\mathbb{R}^n$ of the set of points labelled by C:

$$\mathrm{conv}_{\boldsymbol{A}}(C) := \left\{ \sum_{j\in C} \lambda_j \boldsymbol{p}_j \;\middle|\; \lambda_j \geq 0 \text{ for all } j \in C, \text{ and } \sum_{j\in C} \lambda_j = 1 \right\}.$$

The *relative interior of C in $\boldsymbol{A}$* is the interior of the convex hull in its affine span:

$$\mathrm{relint}_{\boldsymbol{A}}(C) := \left\{ \sum_{j\in C} \lambda_j \boldsymbol{p}_j \;\middle|\; \lambda_j > 0 \text{ for all } j \in C, \text{ and } \sum_{j\in C} \lambda_j = 1 \right\}.$$

Definition 6.9 With the above notation, if $\psi \in (\mathbb{R}^n)^*$ is a linear functional, then the *face of C in direction ψ* is the subset of C given by

$$\mathrm{face}_{\boldsymbol{A}}(C,\psi) := \left\{ j \in C \;\middle|\; \psi(\boldsymbol{p}_j) = \max_{b\in C}(\psi(\boldsymbol{p}_b)) \right\}.$$

If F is a face of C, we write $F \leq_{\boldsymbol{A}} C$ and if in addition $F \neq C$ we write $F <_{\boldsymbol{A}} C$.

Definition 6.10 With the above notation, a collection $\mathcal{S}$ of subsets of J is a *polyhedral subdivision of $\boldsymbol{A}$* if it satisfies the following conditions. (The elements of $\mathcal{S}$ are called *cells*.)

(1) If $C \in \mathcal{S}$ and $F \leq C$ then $F \in \mathcal{S}$.

(2) $\bigcup_{C\in\mathcal{S}} \mathrm{conv}_{\boldsymbol{A}}(C) \supset \mathrm{conv}_{\boldsymbol{A}}(J)$.

(3) If $C \neq C'$ are two cells in $\mathcal{S}$ then $\mathrm{relint}_{\boldsymbol{A}}(C) \cap \mathrm{relint}_{\boldsymbol{A}}(C') = \varnothing$.

Remark 6.11 The first condition says that if some cell is in our subdivision then all faces of it are also. The second condition says that it is a subdivision of the whole convex hull of the points in $\boldsymbol{A}$. The third condition says that the cells can only overlap with each other on their faces, not their interiors.

Definition 6.12 With the above notation, a *triangulation of $\boldsymbol{A}$* is a polyhedral subdivision of $\boldsymbol{A}$ such that every cell is a simplex.

Definition 6.13 Let $\boldsymbol{A} = (\boldsymbol{p}_j)_{j\in J}$ be a point configuration with label set J. Suppose that $\omega\colon \boldsymbol{A} \to \mathbb{R}$ is any map. The *lifted point configuration* in $\mathbb{R}^{n+1}$ is the point configuration

$$\boldsymbol{A}^{\omega} = (\boldsymbol{p}_j^{\omega})_{j\in J} := (\boldsymbol{p}_j, \omega(\boldsymbol{p}_j))_{j\in J}$$

(again with label set J) given by adjoining to each vector an $(n+1)^{\text{st}}$ coordinate given by the value of ω at that point. Consider the set of faces of $\mathrm{conv}_{\boldsymbol{A}^{\omega}}(J)$. A *lower face* of this convex hull is a face that is "visible from below". That is, $\mathrm{face}_{\boldsymbol{A}^{\omega}}(J,\psi)$ is a lower face if ψ is negative on the last coordinate.

Definition 6.14 The *regular polyhedral subdivision of $\boldsymbol{A}$ produced by ω*, denoted $\mathcal{S}(\boldsymbol{A}, \omega)$, is the set of lower faces of the point configuration $\boldsymbol{A}^{\omega}$.

Note that a face in these definitions is a set of labels for the point configuration. So the set of faces making up the polyhedral subdivision of $\boldsymbol{A}$ is defined in terms of $\boldsymbol{A}^{\omega}$, but this works because the same set of labels is used for the two point configurations. [9, Lemma 2.3.11] shows that $\mathcal{S}(\boldsymbol{A}, \omega)$ is indeed a polyhedral subdivision of $\boldsymbol{A}$, for every ω.

Definition 6.15 A *regular triangulation of $\boldsymbol{A}$* is a regular polyhedral subdivision of $\boldsymbol{A}$ that is a triangulation of $\boldsymbol{A}$.

[9, Proposition 2.2.4] shows that every point configuration has a regular triangulation. The connection between regular triangulations of point configurations and our situation can be made via the Klein model of $\mathbb{H}^3$. In this model, geodesics are represented as straight lines in Euclidean space $\mathbb{E}^3$. A convex ideal hyperbolic polyhedron is represented as a convex Euclidean polyhedron whose vertices lie on a sphere. Such a Euclidean polyhedron can be seen as a point configuration, with the points consisting of the vertices of the polyhedron. Note that this is a more restrictive situation than the full generality discussed in [9]; since all the vertices lie on a sphere, there can be no internal points, and no three points can lie on a line. These observations imply that the set of subdivisions of a convex ideal hyperbolic polyhedron into (strictly positive) volume ideal hyperbolic tetrahedra is in one-to-one correspondence with the set of triangulations of the convex Euclidean polyhedron, in the sense of Definition 6.12. The bijective map between the two sets preserves the combinatorial structure of the triangulations.

Definition 6.16 Given the above discussion, we define a *regular ideal triangulation* of a convex ideal hyperbolic polyhedron to be an ideal triangulation of the polyhedron whose corresponding Euclidean triangulation of the corresponding convex Euclidean polyhedron is regular.[4]

We are now in a position to be able to define our class of triangulations $\mathcal{X}_M^{\mathrm{EP}}$.

Definition 6.17 Let M be a cusped hyperbolic 3–manifold. Let $\mathcal{P}$ be the PPP–cellulation of M derived from the Epstein–Penner decomposition of M (choosing equal volumes for the cusps if there is more than one) by inserting polygonal pillows between any two nontriangular faces of the decomposition. The class of triangulations $\mathcal{X}_M^{\mathrm{EP}}$ consists of all triangulations constructed via the following method:

[4]Note that this definition has no relation to the definition of a regular ideal hyperbolic tetrahedron, in the sense of a tetrahedron with all dihedral angles being $\pi/3$.

(1) Insert a regular ideal triangulation of each polyhedron P of $\mathcal{P}$ into P.

(2) Each polygonal pillow Q has two (not necessarily distinct) polyhedra P_- and P_+ glued to it. The regular ideal triangulations of P_- and P_+ induce triangulations t_- and t_+ of the two polygonal faces of Q. Insert into Q a layered triangulation of Q, bridging between t_- and t_+.

Note that although there are only finitely many regular ideal triangulations of a given convex ideal polyhedron, there may be infinitely many triangulations in $\mathcal{X}^{\mathrm{EP}}_{\boldsymbol{M}}$, since the layered triangulations can be arbitrarily long.

Remark 6.18 From the geometric construction, every triangulation of $\mathcal{X}^{\mathrm{EP}}_{\boldsymbol{M}}$ has a natural semiangle structure, as in Remark 6.6, so they are all 1–efficient by Theorem 1.5.

Definition 6.19 The *corank* of a d–dimensional point configuration with n points is the number $n-d-1$.

A point configuration has corank *zero* if and only if it is affinely independent. A point configuration has corank *one* if and only if it has a unique affine dependence relation. This means that there is a unique solution to

$$\sum_{j\in J}\lambda_j \boldsymbol{p}_j = 0 \quad \text{with} \quad \sum_{j\in J}\lambda_j = 0, \qquad \text{where at least one } \lambda_j \neq 0.$$

Uniqueness is up to scaling all λ by the same factor. The affine dependence divides J into three subsets:

$$J_+ := \{j \in J \mid \lambda_j > 0\}, \quad J_0 := \{j \in J \mid \lambda_j = 0\}, \quad J_- := \{j \in J \mid \lambda_j < 0\}.$$

(Which is which of J_+ and J_- is not well defined since we can multiply all of the coefficients by -1 to swap them.) Then $\operatorname{relint}_{\boldsymbol{A}}(J_+) \cap \operatorname{relint}_{\boldsymbol{A}}(J_-)$ is a single point, given by

$$\sum_{j\in J_+}\lambda_j \boldsymbol{p}_j = \sum_{j\in J_-} -\lambda_j \boldsymbol{p}_j,$$

where we have normalised the λ so that

$$\sum_{j\in J_+}\lambda_j = \sum_{j\in J_-} -\lambda_j = 1.$$

Definition 6.20 Let $\boldsymbol{A} = (\boldsymbol{p}_j)_{j\in J}$ be a point configuration with label set J. A subset of J is called a *circuit*, Z, if it is a minimal affinely dependent set (ie it is dependent, but every proper subset is independent).

In the above discussion, $Z = J_+ \cup J_-$, and Z is partitioned into the two sets, $Z_+ = J_+$ and $Z_- = J_-$ since if $\lambda_j = 0$ in the affine dependence then it could be removed from Z, contradicting minimality.

In $\mathbb{R}^3$, five points in general position are a circuit, but there may be circuits with fewer points. Four points are a circuit if they lie in a plane, three if they lie on a line, and two if they are coincident. However, for our purposes the points are the vertices of a convex Euclidean polyhedron, so we may assume that there are no repeated points. Moreover, the points lie on a sphere, so no three lie on a line. Therefore, the only two possibilities are five points in general position, or four points that lie on a plane, as shown in Figure 16.

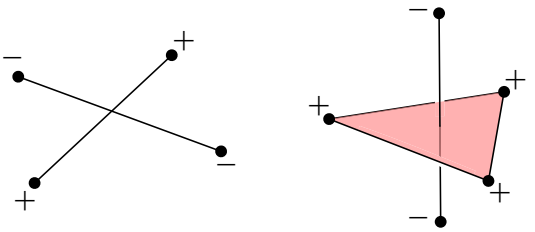

Figure 16: Circuits with 4 and 5 elements

Remark 6.21 For us then, the only possible corank one configurations are:

(1) Five points in general position.

(2) Four points in a plane.

(3) Four points in a plane plus one point not in that plane.

Definition 6.22 Let $\mathcal{S}$ be a polyhedral subdivision that is not a triangulation. Then $\mathcal{S}$ is an *almost–triangulation* if:

(1) All of the cells of $\mathcal{S}$ have corank at most one.

(2) All of the cells of $\mathcal{S}$ of corank one contain the same circuit.

Lemma 6.23 *In our case, the 3–cells of an almost–triangulation are all simplices apart from one or two 3–cells. These 3–cells can have the following forms:*

(1) *The convex hull of five points on a sphere, in general position, as in the upper diagram of Figure 17.*

(2) *A 4–sided pyramid, with the base of the pyramid on a boundary face of the polyhedron, as in the upper diagram of Figure 18.*

(3) *Two 4–sided pyramids whose bases are coincident, as in the upper diagram of Figure 18.*

Proof This follows immediately from Definition 6.22 and Remark 6.21. □

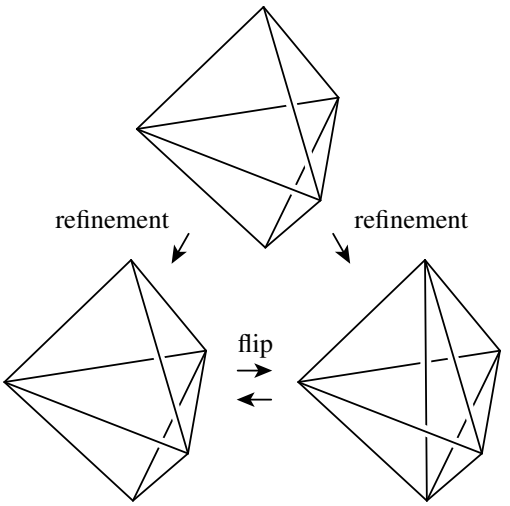

Figure 17: The almost–triangulation in case (1) of Lemma 6.23, and its two refinements to triangulations. Note that although the top and lower left pictures are identical, the top is to be interpreted as a single 3–cell, while the lower left shows two tetrahedra meeting in a triangle. The associated flip between the two triangulations is a 2–3 flip.

Definition 6.24 Let $\mathcal{S}$ and $\mathcal{S}'$ be two polyhedral subdivisions of a point configuration $\boldsymbol{A}$. Then $\mathcal{S}$ *is a refinement of* $\mathcal{S}'$ if for each $C \in \mathcal{S}$, there is a $C' \in \mathcal{S}'$ with $C \subset C'$.

Lemma 6.25 [9, Corollary 2.4.6] *Every almost–triangulation has exactly two proper refinements, which are both triangulations.*

Definition 6.26 Two triangulations of the same point configuration are *connected by a flip supported on the almost–triangulation* $\mathcal{S}$ if they are the only two triangulations refining $\mathcal{S}$.

Definition 6.27 We call the flips associated to the three possible almost–triangulation types listed in Lemma 6.23 the 2–3 *flip*, *external* 2–2 *flip*, and *internal* 2–2 *flip* respectively. See Figures 17 and 18.

Remark 6.28 The internal 2–2 flip acts on the triangulation by a move sometimes called the 4–4 *move*, as it removes four tetrahedra and replaces them with four others. However, here we stick with the notation derived from the bistellar flip terminology.

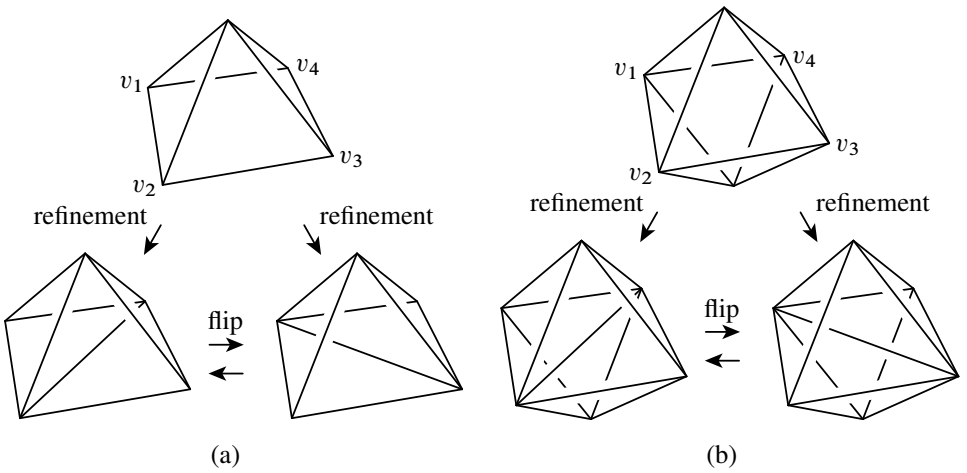

Figure 18: Almost–triangulations in cases (2) and (3) of Lemma 6.23, and the associated 2–2 flips. In all diagrams, vertices v_1 through v_4 are coplanar. (a) The almost–triangulation in case (2) of Lemma 6.23, and its two refinements to triangulations. (b) The almost–triangulation in case (3) of Lemma 6.23, and its two refinements to triangulations.

Definition 6.29 The *flip graph* of the point configuration $\boldsymbol{A}$ is the graph whose vertices are the triangulations of $\boldsymbol{A}$ and whose edges are triangulations connected by flips.

We use the following result, due to Gelfand, Kapranov and Zelevinsky, and given in [9, Corollary 5.3.14].

Theorem 6.30 (Gelfand, Kapranov and Zelevinsky [21]) *Let $\boldsymbol{A}$ be a point configuration. The subgraph of the flip graph induced by all regular triangulations of $\boldsymbol{A}$ that use the same vertices is connected.*

In our case, since the vertices lie on a sphere, all vertices are used in every triangulation, so this says that we can get from any regular triangulation of the polyhedron to any other by performing flips.

Remark 6.31 Our strategy for connecting two triangulations $\mathcal{T}_1, \mathcal{T}_2 \in \mathcal{X}_M^{\mathrm{EP}}$ is as follows. Both triangulations consist of regular triangulations of the polyhedra of the PPP–cellulation, together with layered triangulations in the polygonal pillows between them.

(1) Use Theorem 6.30 on each polyhedron, to change the triangulation of each polyhedron in $\mathcal{T}_1$ into the corresponding triangulation of the polyhedron in $\mathcal{T}_2$. This step may alter the triangulations of the polygonal pillows as well.

(2) Change the triangulation in each polygonal pillow of the resulting triangulation so that it matches with the corresponding triangulation in $\mathcal{T}_2$. This step does not alter the triangulations of the polyhedra.

6.3 Interpreting flip moves using 2–3 moves

In order to carry out step (1) of our plan in Remark 6.31, we will interpret the flip moves in terms of the 2–3 and 3–2 moves allowed in Theorem 1.1.

(1) First, consider a 2–3 flip in one polyhedron. This is simply a 2–3 move. Since the triangulations on either side of the move are in $\mathcal{X}^{\mathrm{EP}}_M$, they are both 1–efficient by Remark 6.18. Therefore the triangulations have the same index by Theorem 1.1.

(2) Second, consider an external 2–2 flip. See Figure 19. The base of the pyramid is on a face of the polyhedron that is glued to a polygonal pillow. The two triangles on the base of the pyramid are glued to either a single tetrahedron in the pillow, or two tetrahedra in either the polygonal pillow or the polyhedron on the other side of the polygonal pillow.
   - If the two triangles are glued to a single tetrahedron then we are in the situation shown in the top diagram of Figure 19, and we can perform a 3–2 move, which performs the flip to the polyhedron, and removes the single tetrahedron from the layered triangulation of the polygonal pillow.
   - Otherwise, we perform a 2–3 move, which performs the flip to the polyhedron, and adds a flat tetrahedron to the layered triangulation of the polygonal pillow. (Note that we could use only this move, even in the previous case; the difference between the two options is a 0–2 move.)

   Once again, the triangulations on either side of the move are in $\mathcal{X}^{\mathrm{EP}}_M$, so they are both 1–efficient and the triangulations have the same index.

(3) Lastly, consider an internal 2–2 flip. See Figure 19. We can perform a 2–3 move followed by a 3–2 move, which together perform the flip. Since the four vertices in the circuit are coplanar, at the intermediate step we introduce a flat tetrahedron. The intermediate triangulation is not in $\mathcal{X}^{\mathrm{EP}}_M$, since it includes a flat tetrahedron in a polyhedron, and so the polyhedron does not have a regular triangulation. However, the intermediate triangulation still has a natural semiangle structure in the obvious way, and so it is 1–efficient, and again the three triangulations involved all have the same index.

The arguments so far show that we can achieve step (1) of Remark 6.31. Now we need to deal with step (2).

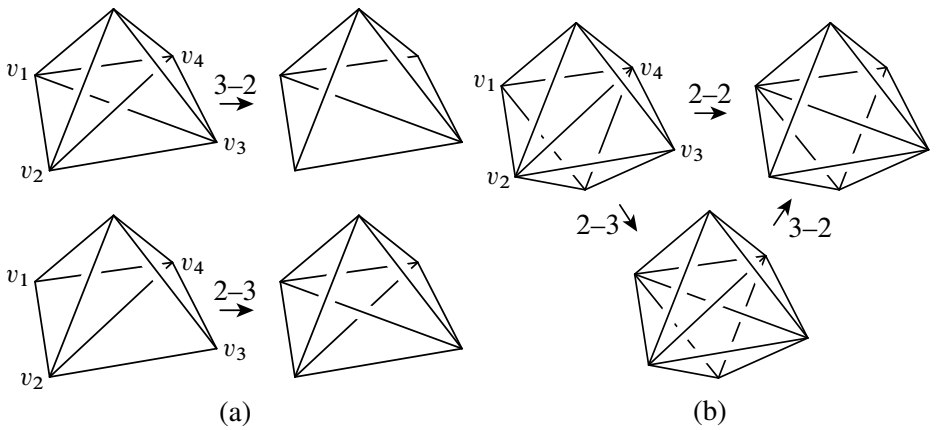

Figure 19: The possible 2–2 moves on a triangulation of a point configuration, realised using 2–3 and 3–2 moves. Again in each case, vertices v_1 through v_4 are coplanar. (a) Two possible ways to perform an external 2–2 move, depending on whether or not there is a suitable flat tetrahedron in the polygonal pillow that the base of the pyramid is glued to. (b) An internal 2–2 flip, obtained by performing a 2–3 move followed by a 3–2 move. At the intermediate step we get a flat tetrahedron with vertices v_1 through v_4.

6.4 Moving paths in the 1–skeleton of the associahedron using 2–3 and 0–2 moves

In order to carry out step (2) of our plan in Remark 6.31, we need to modify the layered triangulations in the polygonal pillows. We will do this using the 2–3, 3–2, 0–2 and 2–0 moves allowed in Theorems 1.1 and 5.1.

Having completed step (1), we have two triangulations, $\mathcal{T}_1$ and $\mathcal{T}_2$, which agree on the polyhedra but may differ in the polygonal pillows. Let Q be a polygonal pillow. Since $\mathcal{T}_1$ and $\mathcal{T}_2$ agree on the polyhedra glued to either side of Q, they agree on the triangulations of the polygonal faces Q_+ and Q_-. Call these triangulations t_+ and t_-.

The next well-known theorem concerns the identification of the set of triangulations of an n–gon with the vertices of the *associahedron* K_{n-2}, and the set of geometric bistellar flips with the edges of K_{n-2}. The associahedron K_{n-2} was introduced by Stasheff [45]. An identification of K_{n-2} with a convex polytope in Euclidean space was given in the appendix to [46]. The cellular decomposition of the polytope K_{n-2} (and in particular, its 2–skeleton) is discussed at length in the above references and also in [34]. The fact that the 2–dimensional faces of the associahedron are squares and pentagons also follows from MacLane's coherence theorem [36]. A vast generalisation of regular triangulations of point configurations was studied by Gelfand, Kapranov

and Zelevinsky, and in [21, Section 7.3] it is explained how to identify the secondary polytope of 2–dimensional configurations with the associahedron.

Theorem 6.32 *The set of triangulations of an n–gon and the set of diagonal flips connecting them correspond to the vertices and edges of a convex polytope called the* associahedron. *The set of 2–cells of the associahedron consists of squares and pentagons. Each square corresponds to two commuting diagonal flips (as in Definition 6.4) on two 4–gons whose interiors are disjoint. Each pentagon corresponds to a* pentagon relation *between the five triangulations of a pentagon. See Figure 20.*

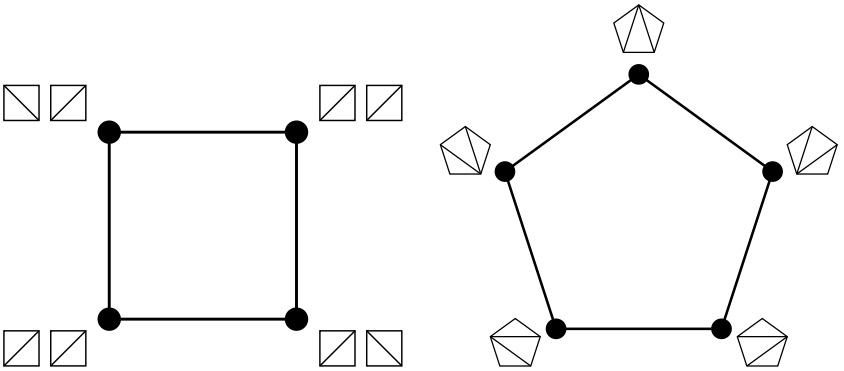

Figure 20: The 2–cells of the associahedron: (a) A square 2–cell of the associahedron. (b) A pentagon 2–cell of the associahedron.

Our two layered triangulations of the polygonal pillow Q can be represented as two paths p_1 and p_2 in the 1–skeleton of the associahedron that both start at the vertex corresponding to t_- and end at the vertex corresponding to t_+. Since the fundamental group of the 2–skeleton $X^{(2)}$ of a CW complex X satisfies $\pi_1(X^{(2)}) = \pi_1(X)$, it follows that the 2–skeleton of a convex polytope is simply connected, and every loop along the 1–skeleton can be trivialised by moving pieces of it across the 2–cells. It follows that the 2–skeleton of the associahedron is simply connected, and so we can homotope p_1 to p_2, fixing endpoints, by moving the path across some finite sequence of the 2–cells. To be precise, we can homotope p_1 to p_2 with a combination of the following moves and their inverses.

(1) Remove a *backtracking*, that is, replace a segment of a path of the form

$$\dots, t_1, t_2, t_1, \dots \quad \text{with} \quad \dots, t_1, \dots,$$

where t_1 and t_2 are related by a diagonal flip.

(2) Move a path that follows two consecutive sides of a square 2–cell to follow the other two sides.

(3) Move a path that follows three consecutive sides of a square 2–cell to follow the other side.

(4) Delete a part of a path that goes around all four sides of a square 2–cell.

(5) Move a path that follows three consecutive sides of a pentagon 2–cell to follow the other two sides.

(6) Move a path that follows four consecutive sides of a pentagon 2–cell to follow the other side.

(7) Delete a part of a path that goes around all five sides of a pentagonal 2–cell.

These moves can be achieved as follows.

- Move (1) corresponds to performing a 2–0 move on the triangulation. Since the two triangulations are both in $\mathcal{X}_M^{\mathrm{EP}}$, they are both 1–efficient by Remark 6.18. Therefore the two triangulations have the same index by Theorem 5.1.
- Move (2) does not change the layered triangulation at all, it only swaps the order in which we add two nonoverlapping flat tetrahedra to the layering.
- Move (3) can be made by applying move (2) followed by move (1).
- Move (4) can be made by applying move (2) followed by move (1) twice.
- Move (5) corresponds to performing a 3–2 move on the triangulation. As before, since the two triangulations are both in $\mathcal{X}_M^{\mathrm{EP}}$, they are both 1–efficient by Remark 6.18. Therefore the two triangulations have the same index by Theorem 1.1(b).
- Move (6) can be made by applying move (5) followed by move (1).
- Move (7) can be made by applying move (5) followed by move (1) twice.

Proof of Theorem 1.8 We have shown in this section that given any two triangulations in $\mathcal{X}_M^{\mathrm{EP}}$, the steps in Remark 6.31 can be made using 2–3, 3–2, 0–2 and 2–0 moves which preserve the index. Thus the entire class of triangulations has the same index. Since $\mathcal{X}_M^{\mathrm{EP}}$ depends only on the topology of M, we can take the index of any of these triangulations for the value of the index for the manifold, and this depends only on the topology of M. □

Proof of Theorem 1.9 Fix a cusped hyperbolic manifold M and $\mathcal{T} \in \mathcal{X}_M^{\mathrm{EP}}$. $\mathcal{T}$ consists of two types of tetrahedra: the ones that subdivide the ideal hyperbolic cells of the Epstein–Penner cell decomposition of M, and the ones that are parts of the pillows.

The former have geometric shapes (ie shapes that are in the upper half-plane), and the latter have real nondegenerate shapes. By construction, the shapes $Z_{\mathcal{T}}$ satisfy the gluing equations of $\mathcal{T}$, proving part (a). Their arguments also satisfy the gluing equations, proving part (c).

Also by construction, the shapes $Z_{\mathcal{T}}$ and $Z_{\mathcal{T}'}$ are related by 2–3, 3–2, 0–2 and 2–0 moves if the corresponding triangulations $\mathcal{T}$ and $\mathcal{T}'$ are related by the same moves. □

7 Computations

7.1 How to compute the coefficients of a q–series

In this section we will explain a general method to compute the coefficients of a q–series which is given by a multidimensional sum of some basic q–series. The idea is simple, but the effective aspects of it are tricky and were explained to the first author by D Zagier. The method is applied in [19] which computes the coefficients of the stabilisation of the coloured Jones polynomial of an alternating knot [18].

Fix a 1–efficient ideal triangulation $\mathcal{T}$ with n tetrahedra of a 1–cusped hyperbolic manifold M and an oriented multicurve ϖ on ∂M. The index $I_{\mathcal{T}}(\varpi)(q) \in \mathbb{Z}((q^{1/2}))$ is given by a convergent $(n-1)$–dimensional sum over the integers of a summand that depends on the angle structure equation matrices of $\mathcal{T}$; see Equation (17). The summand of $I_{\mathcal{T}}(\varpi)$ is a product of tetrahedron indices (one per tetrahedron of $\mathcal{T}$) of linear forms in $\boldsymbol{k} = (k_1, \dots, k_{n-1}) \in \mathbb{Z}^{n-1}$ and the turning number vectors $(a_\varpi \mid b_\varpi)$ of ϖ.

The building block of the summand is the tetrahedron index I_Δ, whose degree (ie minimum degree with respect to q) is a piecewise quadratic function on $\mathbb{R}^2$; see Section 4.2. By a *piecewise quadratic function* on $\mathbb{R}^m$, we mean that there exists a partition $\mathcal{F}$ of $\mathbb{R}^m$ into a finite number of chambers whose boundaries are rational polyhedral cones such that the restriction of the function to each chamber is given by a quadratic polynomial. It follows that for fixed ϖ, the degree $\delta(\varpi, \boldsymbol{k})$ of the summand in (17) is a piecewise quadratic function defined on a partition $\mathcal{F}_{\mathcal{T}}$ of $\mathbb{R}^{n-1}$. In a later publication, we will explain how to compute $\mathcal{F}_{\mathcal{T}}$ directly from $\mathcal{T}$. A priori, $\mathcal{F}_{\mathcal{T}}$ need not be a fan in $\mathbb{R}^{n-1}$ as the cones in the partition may not be convex.

Since $\mathcal{T}$ is 1–efficient, it follows that its index $I_{\mathcal{T}}(\varpi)(q)$ is a convergent series. In other words, the degree of the summand is a proper function on $\mathbb{Z}^{n-1}$. Thus, for fixed ϖ and every half-integer N, the set $\{\boldsymbol{k} \in \mathbb{Z}^{n-1} \mid \delta(\varpi, \boldsymbol{k}) \le N\}$ is finite. To compute the index of $\mathcal{T}$, we need to compute bounds on this finite set. Since δ is convex on rays and piecewise quadratic, it follows that to bound $\delta(\varpi, \boldsymbol{k})$, it suffices to bound the

restriction of $\delta(\varpi, \boldsymbol{k})$ to an arbitrary ray $\rho = \{k'\rho_0 \mid k' \in \mathbb{N}\}$ of $\mathcal{F}_{\mathcal{T}}$. Now $\delta(\varpi, k'\rho_0)$ is a quadratic function of $k' \in \mathbb{N}$, and we obtain sharp bounds for k_i typically of the form $k_i = O(\sqrt{N})$ and *exceptionally* of the form $k_i = O(N)$. The latter happens when δ has linear growth on some ray of $\mathcal{F}_{\mathcal{T}}$. These directions of linear growth (also observed in [18] in the context of stabilisation of the coloured Jones function) are computationally costly. For an example, see the case of the knot 6_1 discussed below.

The bounds for k_i discussed above are rigorous and sharp, and work well for $n = 2$ and $n = 3$ tetrahedra. However, they quickly become inefficient when n increases (eg $n = 9$). The better way to proceed for larger n, as was explained to us by D Zagier and is applied successfully in [19], is to use *iterated summation*. In the examples shown below for $n = 2$ and $n = 3$ iterated summation is not needed. For simplicity, we focus on 1–cusped manifolds and their index for $[\varpi] = 0 \in H_1(\partial M; \mathbb{Z})$. The data presented below are available from [15].

Remark 7.1 If two 1–cusped hyperbolic 3–manifolds M and M' have 1–efficient ideal triangulations $\mathcal{T}$ and $\mathcal{T}'$ with equal angle structure matrices, then $I_{\mathcal{T}}(0)(q) = I_{\mathcal{T}'}(0)(q)$. For example, M and $-M$ have such triangulations, where $-M$ denotes the orientation reversed cusped hyperbolic manifold. Also, M_ϕ and $M_{-\phi}$ have such triangulations for a pseudo-Anosov homeomorphism ϕ of a once punctured torus, where M_ϕ denotes the mapping torus of ϕ.

7.2 The index of the 4_1 knot complement

The default `SnapPy` triangulation $\mathcal{T}$ of the 4_1 knot complement uses 2 regular ideal tetrahedra and coincides with the Epstein–Penner decomposition, thus $\mathcal{X}^{\mathrm{EP}}_{4_1} = \{\mathcal{T}\}$. `SnapPy` gives the angle structure matrices of $\mathcal{T}$:

$$\overline{\mathbb{A}} = \begin{pmatrix} 2 & 2 \\ 0 & 0 \end{pmatrix}, \quad \overline{\mathbb{B}} = \begin{pmatrix} 1 & 1 \\ 1 & 1 \end{pmatrix}, \quad \overline{\mathbb{C}} = \begin{pmatrix} 0 & 0 \\ 2 & 2 \end{pmatrix}.$$

`SnapPy` also gives an additional two rows which correspond to the meridian and longitude equations; we will not use these in our examples so we omit them here. We eliminate $\overline{\mathbb{B}}$ to obtain $\mathbb{A}$ and $\mathbb{B}$. We choose our basic edge set $\mathcal{B} = \{e_1\}$ and excluded edge set $\mathcal{X} = \{e_2\}$. We can therefore ignore the rows of our matrices corresponding to e_2, and write

$$\mathbb{A}' = \begin{pmatrix} 1 & 1 \end{pmatrix}, \quad \mathbb{B}' = \begin{pmatrix} -1 & -1 \end{pmatrix}, \quad \nu' = \begin{pmatrix} 0 \end{pmatrix}.$$

Here $\mathbb{A}'$ is just $\mathbb{A}$ with the last row omitted, and similarly for the other primed symbols. We obtain the angle structure equations

$$\mathbb{A}'\alpha + \mathbb{B}'\gamma = \pi\nu'.$$

Equation (17) gives that

$$I_{4_1}(0)(q) = \sum_{k\in\mathbb{Z}} I_\Delta(k,k)(q)^2 \in \mathbb{Z}[\![q]\!].$$

Equation (12) implies that the degree $\delta(k)$ of the summand is given by the piecewise quadratic polynomial

$$\delta(k) = 2\delta(k,k) = 2k^2 + |k|.$$

Its corresponding fan $\mathcal{F}_\mathcal{T}$ in $\mathbb{R}$ consists of two rays, corresponding to the columns of the matrix

$$\begin{pmatrix} 1 & -1 \end{pmatrix}.$$

Here, a column vector v of a matrix, spans the ray $\mathbb{R}_+ v$. It follows that for every natural number N we have

$$I_{4_1}(0)(q) + O(q)^{N+1} = \sum_{k=\lfloor 1/4(-1-\sqrt{1+8N})\rfloor}^{\lceil 1/4(-1+\sqrt{1+8N})\rceil} I_\Delta(k,k)(q)^2 + O(q)^{N+1}.$$

To compute $I_\Delta(k,k)(q) + O(q)^{N+1}$, we use its definition (5) and truncate the $n-$ summation as follows

$$I_\Delta(k,k)(q) + O(q)^{N+1} = \sum_{n=\lfloor 1/2(-1+2k-\sqrt{1-4k+8k^2+8N})\rfloor}^{\lceil 1/4(-1+\sqrt{1+8N})\rceil} (-1)^n \frac{q^{n(n+1)/2-(n+k/2)k}}{(q)_n (q)_{n+k}} + O(q)^{N+1}. \tag{32}$$

Putting everything together, the first 100 coefficients of $I_{4_1}(0)(q)$ are given by

$$\begin{aligned}
&1 - 2q - 3q^2 + 2q^3 + 8q^4 + 18q^5 + 18q^6 + 14q^7 - 12q^8 - 52q^9 - 106q^{10} \\
&- 164q^{11} - 209q^{12} - 212q^{13} - 141q^{14} + 14q^{15} + 309q^{16} + 714q^{17} + 1249q^{18} \\
&+ 1824q^{19} + 2401q^{20} + 2794q^{21} + 2898q^{22} + 2434q^{23} + 1256q^{24} - 918q^{25} \\
&- 4186q^{26} - 8712q^{27} - 14394q^{28} - 21046q^{29} - 28184q^{30} - 35094q^{31} \\
&- 40740q^{32} - 43732q^{33} - 42508q^{34} - 35068q^{35} - 19524q^{36} + 6288q^{37} \\
&+ 43942q^{38} + 95026q^{39} + 159698q^{40} + 237774q^{41} + 326680q^{42} + 422880q^{43} \\
&+ 519595q^{44} + 608636q^{45} + 677761q^{46} + 713352q^{47} + 697625q^{48} + 611956q^{49} \\
&+ 434572q^{50} + 144616q^{51} - 279773q^{52} - 856288q^{53} - 1599627q^{54} \\
&- 2515906q^{55} - 3602521q^{56} - 4842516q^{57} - 6203552q^{58} - 7632646q^{59} \\
&- 9054429q^{60} - 10367858q^{61} - 11443874q^{62} - 12125534q^{63} - 12226286q^{64} \\
&- 11535062q^{65} - 9815935q^{66} - 6820480q^{67} - 2289703q^{68} + 4024698q^{69}
\end{aligned}$$

$$+12355340q^{70}+22887604q^{71}+35751602q^{72}+50979996q^{73}+68497913q^{74}$$
$$+88071340q^{75}+109297633q^{76}+131547294q^{77}+153959928q^{78}$$
$$+175385202q^{79}+194390216q^{80}+209208210q^{81}+217767013q^{82}$$
$$+217655122q^{83}+206182023q^{84}+180375446q^{85}+137083864q^{86}$$
$$+73018494q^{87}-15089960q^{88}-130393760q^{89}-275708923q^{90}$$
$$-453351590q^{91}-664856517q^{92}-910744842q^{93}-1190185170q^{94}$$
$$-1500703210q^{95}-1837805659q^{96}-2194650672q^{97}-2561673782q^{98}$$
$$-2926258326q^{99}-3272416148q^{100}.$$

The first 1000 coefficients are available from [15].

7.3 The index of the sister of the 4_1 knot complement

The 4_1 knot complement and its sister are the census manifolds `m004` and `m003` respectively, and are punctured torus bundles over a circle with monodromy $+RL$ and $-RL$ respectively [8]. The Epstein–Penner decompositions for `m004` and `m003` consist of two regular ideal tetrahedra. The edge gluing equations of $+RL$ and $-RL$ coincide. Thus, $I_{\texttt{m003}}(0) = I_{\texttt{m004}}(0)$.

7.4 The index of the 5_2 knot complement

The default `SnapPy` triangulation $\mathcal{T}$ of the 5_2 knot complement uses 3 ideal tetrahedra. The Epstein–Penner decomposition $\mathcal{T}^{\mathrm{EP}}$ uses 4 ideal tetrahedra. Both triangulations carry geometric shape structures and thus canonical strict angle structures. One can show that $\mathcal{T}$ and $\mathcal{T}^{\mathrm{EP}}$ are related by geometric 2–3 moves hence they have equal indices. For reasons of efficiency, we will work with the triangulation $\mathcal{T}$. Its angle structure matrices are given by

$$\overline{\mathbb{A}} = \begin{pmatrix} 1 & 1 & 1 \\ 0 & 0 & 0 \\ 1 & 1 & 1 \end{pmatrix}, \quad \overline{\mathbb{B}} = \begin{pmatrix} 0 & 2 & 0 \\ 1 & 0 & 1 \\ 1 & 0 & 1 \end{pmatrix}, \quad \overline{\mathbb{C}} = \begin{pmatrix} 1 & 0 & 1 \\ 1 & 2 & 1 \\ 0 & 0 & 0 \end{pmatrix}.$$

Eliminating $\overline{\mathbb{B}}$, and removing the third row (which corresponds to the third edge equation), we obtain the angle structure equations

$$\mathbb{A}'\alpha + \mathbb{B}'\gamma = \pi\nu',$$

where

$$\mathbb{A}' = \begin{pmatrix} 1 & -1 & 1 \\ -1 & 0 & -1 \end{pmatrix}, \quad \mathbb{B}' = \begin{pmatrix} 1 & -2 & 1 \\ 0 & 2 & 0 \end{pmatrix}, \quad \nu' = \begin{pmatrix} 0 \\ 0 \end{pmatrix}.$$

The index of $\mathcal{T}$ is given by

$$I_{5_2}(0)(q) = \sum_{(k_1,k_2)\in\mathbb{Z}^2} I_\Delta(-k_1, k_1-k_2)^2 I_\Delta(2k_1-2k_2, -k_1) \in \mathbb{Z}[\![q]\!]. \tag{33}$$

Equation (12) implies that the degree $\delta(k_1,k_2)$ of the summand is a piecewise quadratic polynomial with fan $\mathcal{F}_\mathcal{T}$ given by six rays, $\rho_1,\dots,\rho_6$, corresponding to the columns of the matrix

$$\begin{pmatrix} 2 & 1 & 0 & -1 & -1 & 0 \\ 1 & 1 & 1 & 0 & -1 & -1 \end{pmatrix}.$$

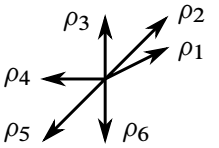

Figure 21: The fan of the summand of $I_{5_2}(0)$

Let C_{ij} denote the two-dimensional cone with rays ρ_i and ρ_j. Then we have

$$\delta(k_1,k_2) = \begin{cases} \frac{1}{2}k_1 + \frac{1}{2}k_1^2 & \text{if } (k_1,k_2)\in C_{12}, \\ -\frac{1}{2}k_1 - \frac{1}{2}k_1^2 + k_2 + k_2^2 & \text{if } (k_1,k_2)\in C_{23}, \\ -k_1 + k_1^2 + k_2 - 2k_1k_2 + k_2^2 & \text{if } (k_1,k_2)\in C_{34}, \\ -k_1 + k_1^2 & \text{if } (k_1,k_2)\in C_{45}, \\ k_1^2 - k_2 - 2k_1k_2 + 2k_2^2 & \text{if } (k_1,k_2)\in C_{56}, \\ k_1 + 2k_1^2 - k_2 - 4k_1k_2 + 2k_2^2 & \text{if } (k_1,k_2)\in C_{61}. \end{cases}$$

A plot of $\delta(k_1,k_2)$ for $k_1,k_2\in[-1,1]$ is given in Figure 22.

If $\delta(k_1,k_2)\le N$, then to bound k_1 from above and below we use the restriction to the rays ρ_1 and ρ_5 respectively. Likewise, to bound k_2 from above and below we use the restriction to the rays ρ_2 and ρ_5 respectively. The equations

$$\delta(k_1,k_1) = \begin{cases} (-1+k_1)k_1 & \text{if } k_1\le 0, \\ \frac{1}{2}k_1(1+k_1) & \text{if } k_1\ge 0, \end{cases}$$
$$\delta(2k_2,k_2) = \begin{cases} 2k_2(-1+2k_2)k_2 & \text{if } k_2\le 0, \\ k_2(1+2k_2) & \text{if } k_2\ge 0, \end{cases}$$

and the inequality $\delta(k_1,k_2)\le N$ give the bounds

$$\tfrac{1}{2}(1-\sqrt{1+4N}) \le k_1 \le \tfrac{1}{2}(1+\sqrt{1+8N}), \tag{34a}$$
$$\tfrac{1}{2}(1-\sqrt{1+4N}) \le k_2 \le \tfrac{1}{2}(1+\sqrt{1+8N}). \tag{34b}$$

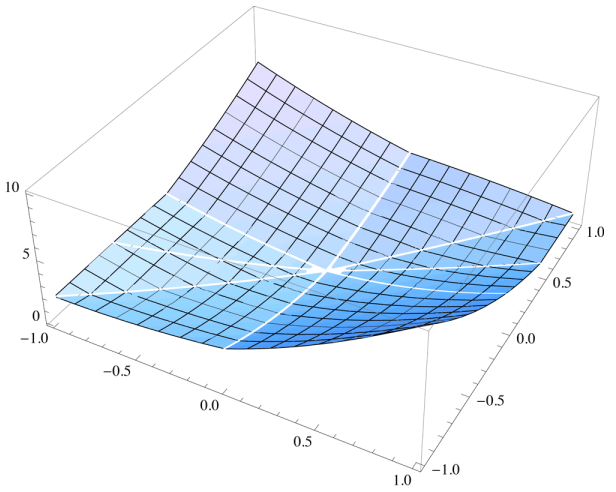

Figure 22: The plot of the degree of the summand of 5_2

With these bounds, we can compute the coefficients of $I_{5_2}(0)(q)$. The first 100 of them are given by

$$\begin{aligned}
&1-4q-q^2+16q^3+26q^4+23q^5-34q^6-122q^7-239q^8-312q^9-221q^{10}\\
&\quad+102q^{11}+778q^{12}+1757q^{13}+2930q^{14}+3825q^{15}+4003q^{16}+2560q^{17}\\
&\quad-1183q^{18}-8033q^{19}-18087q^{20}-30864q^{21}-44625q^{22}-56225q^{23}\\
&\quad-60913q^{24}-52342q^{25}-23373q^{26}+33675q^{27}+124356q^{28}+251997q^{29}\\
&\quad+412837q^{30}+596153q^{31}+778487q^{32}+925195q^{33}+984860q^{34}+895092q^{35}\\
&\quad+579789q^{36}-39418q^{37}-1039055q^{38}-2474979q^{39}-4370844q^{40}-6691737q^{41}\\
&\quad-9326308q^{42}-12059462q^{43}-14553043q^{44}-16329323q^{45}-16762776q^{46}\\
&\quad-15091256q^{47}-10436174q^{48}-1863234q^{49}+11551967q^{50}+30594044q^{51}\\
&\quad+55785006q^{52}+87178516q^{53}+124185931q^{54}+165312079q^{55}+207965719q^{56}\\
&\quad+248191454q^{57}+280543349q^{58}+297911617q^{59}+291580973q^{60}+251299184q^{61}\\
&\quad+165675668q^{62}+22662435q^{63}-189540512q^{64}-481437576q^{65}-860708203q^{66}\\
&\quad-1330509280q^{67}-1887333621q^{68}-2518748267q^{69}-3200856694q^{70}\\
&\quad-3895826567q^{71}-4549488766q^{72}-5089337005q^{73}-5423179738q^{74}\\
&\quad-5438686309q^{75}-5004368747q^{76}-3972096155q^{77}-2181963773q^{78}\\
&\quad+530655834q^{79}+4324768774q^{80}+9340768927q^{81}+15683465230q^{82}\\
&\quad+23402429365q^{83}+32468254286q^{84}+42746925974q^{85}+53970937518q^{86}\\
&\quad+65710530396q^{87}+77343886238q^{88}+88031000047q^{89}+96690414035q^{90}
\end{aligned}$$

$$+101984965333q^{91}+102316085357q^{92}+95834146866q^{93}+80464612248q^{94}$$
$$+53958404128q^{95}+13966121550q^{96}-41855327561q^{97}$$
$$-115704867879q^{98}-209460627592q^{99}-324467541887q^{100}.$$

The first 300 coefficients are available from [15].

7.5 The index of the $(-2,3,7)$ pretzel knot complement

The $(-2,3,7)$ pretzel knot is the 12 crossing knot `12n242` in the census. The default `SnapPy` triangulation $\mathcal{T}$ of the `12n242` complement uses 3 ideal tetrahedra, as does the Epstein–Penner decomposition $\mathcal{T}^{\mathrm{EP}}$. However, the two triangulations $\mathcal{T}$ and $\mathcal{T}^{\mathrm{EP}}$ are combinatorially different; for instance have edge-valencies $5,6,7$ and $5,5,8$ respectively. Nevertheless, both triangulations are geometric with canonical strict angle structure and are related by geometric 2–3 moves, which preserve the index. The angle structure equations of $\mathcal{T}$ are given by

$$\overline{\mathbb{A}}=\begin{pmatrix}1&0&0\\0&1&1\\1&1&1\end{pmatrix},\quad \overline{\mathbb{B}}=\begin{pmatrix}0&1&0\\1&1&0\\1&0&2\end{pmatrix},\quad \overline{\mathbb{C}}=\begin{pmatrix}1&1&2\\1&0&0\\0&1&0\end{pmatrix}.$$

Apply the following operations on $(\overline{\mathbb{A}}\mid\overline{\mathbb{B}}\mid\overline{\mathbb{C}})$:

- Permute the rows according to $(123)\mapsto(312)$.
- Permute the second and third columns of $\overline{\mathbb{A}}$ and simultaneously, of $\overline{\mathbb{B}}$ and $\overline{\mathbb{C}}$.
- If $\overline{\boldsymbol{a}}_1,\overline{\boldsymbol{b}}_1,\overline{\boldsymbol{c}}_1$ are the first columns of $\overline{\mathbb{A}}$, $\overline{\mathbb{B}}$ and $\overline{\mathbb{C}}$, then permute $(\overline{\boldsymbol{a}}_1\mid\overline{\boldsymbol{b}}_1\mid\overline{\boldsymbol{c}}_1)\mapsto(\overline{\boldsymbol{b}}_1\mid\overline{\boldsymbol{c}}_1\mid\overline{\boldsymbol{a}}_1)$.

After the above permutations, the matrix $(\overline{\mathbb{A}}\mid\overline{\mathbb{B}}\mid\overline{\mathbb{C}})$ of the $(-2,3,7)$ pretzel knot becomes the corresponding matrix of the 5_2 knot. Since the above permutations do not change the index, it follows that $I_{(-2,3,7)}(0)=I_{5_2}(0)$.

Exercise 7.2 Using the matrix $(\overline{\mathbb{A}}\mid\overline{\mathbb{B}}\mid\overline{\mathbb{C}})$ above, it follows that the index of $\mathcal{T}$ is given by

$$I_{(-2,3,7)}(0)(q)=\sum_{(k_1,k_2)\in\mathbb{Z}^2}(-1)^{k_2}q^{(k_1-2k_2)/2}I_\Delta(k_1,-k_2)\times I_\Delta(-k_1+k_2,k_1)I_\Delta(-2k_1+2k_2,k_1-2k_2). \tag{35}$$

On the other hand, the index of 5_2 is given by Equation (33). Using the identities of the tetrahedron index from Section 4, show that

$$\sum_{(k_1,k_2)\in\mathbb{Z}^2} I_\Delta(-k_1,k_1-k_2)^2 I_\Delta(2k_1-2k_2,-k_1) = \sum_{(k_1,k_2)\in\mathbb{Z}^2} (-1)^{k_2} q^{(k_1-2k_2)/2} I_\Delta(k_1,-k_2) I_\Delta(-k_1+k_2,k_1) \times I_\Delta(-2k_1+2k_2,k_1-2k_2).$$

7.6 The index of the 6_1 knot complement

In this section we discuss the index $I_{6_1}(0)$ as an example of the phenomenon of linear growth. The default `SnapPy` triangulation $\mathcal{T}$ of the 6_1 knot complement has 4 ideal tetrahedra, and the Epstein–Penner decomposition uses 6 ideal tetrahedra. The two triangulations are related by geometric 2–3 moves and so have equal indices. The angle structure equations of $\mathcal{T}$ are given by

$$\overline{\mathbb{A}} = \begin{pmatrix} 1 & 1 & 0 & 0 \\ 0 & 0 & 0 & 1 \\ 0 & 1 & 1 & 0 \\ 1 & 0 & 1 & 1 \end{pmatrix}, \quad \overline{\mathbb{B}} = \begin{pmatrix} 0 & 2 & 0 & 1 \\ 1 & 0 & 1 & 0 \\ 1 & 0 & 0 & 0 \\ 0 & 0 & 1 & 1 \end{pmatrix}, \quad \overline{\mathbb{C}} = \begin{pmatrix} 1 & 0 & 1 & 1 \\ 1 & 2 & 1 & 0 \\ 0 & 0 & 0 & 1 \\ 0 & 0 & 0 & 0 \end{pmatrix}.$$

Eliminating $\overline{\mathbb{B}}$, and removing the fourth row (which corresponds to the fourth edge equation), we obtain the angle structure equations

$$\mathbb{A}'\alpha + \mathbb{B}'\gamma = \pi\nu',$$

where

$$\mathbb{A}' = \begin{pmatrix} 1 & -1 & 0 & -1 \\ -1 & 0 & -1 & 1 \\ -1 & 1 & 1 & 0 \end{pmatrix}, \quad \mathbb{B}' = \begin{pmatrix} 1 & -2 & 1 & 0 \\ 0 & 2 & 0 & 0 \\ -1 & 0 & 0 & 1 \end{pmatrix}, \quad \nu' = \begin{pmatrix} -1 \\ 0 \\ 1 \end{pmatrix}.$$

The index of $\mathcal{T}$ is given by

$$I_{6_1}(0)(q) = \sum_{(k_1,k_2,k_3)\in\mathbb{Z}^3} q^{(-k_1+k_3)/2} I_\Delta(-k_1,-k_2+k_3) I_\Delta(2k_1-2k_2,-k_1+k_3) \times I_\Delta(-k_3,-k_1+k_2) I_\Delta(-k_1+k_3,k_1-k_2-k_3) \in \mathbb{Z}[\![q]\!].$$

$\mathcal{F}_\mathcal{T}$ in $\mathbb{R}^3$ has 18 rays, corresponding to the columns of the matrix

$$\begin{pmatrix} -1 & -1 & -1 & -1 & -1 & -1 & 0 & 0 & 0 & 0 & 0 & 0 & 1 & 1 & 1 & 1 & 2 & 3 \\ -2 & -2 & -1 & 0 & 0 & 1 & -1 & -1 & -1 & 0 & 1 & 1 & 0 & 0 & 1 & 1 & 1 & 2 \\ -3 & -1 & 0 & -1 & 0 & 0 & -2 & -1 & 0 & 1 & -1 & 0 & -1 & 1 & 0 & 1 & 1 & 1 \end{pmatrix}.$$

If $\delta(k_1,k_2,k_3)$ denotes the degree of the summand and $N\in\mathbb{N}$, then $\delta(k_1,k_2,k_3)\le N$ implies that (k_1,k_2,k_3) satisfy the bounds

$$\begin{aligned}
\tfrac{1}{2}(1-\sqrt{1+4N})\le k_1\le \tfrac{1}{2}(-1+\sqrt{1+12N}),\\
\tfrac{2}{3}(1-\sqrt{1+3N})\le k_2\le \tfrac{1}{2}(-1+\sqrt{1+8N}),\\
\tfrac{3}{7}(1-\sqrt{1+7N})\le k_3\le N.
\end{aligned}$$

Observe that the upper bound for k_3 is linear in N. For instance, when $N=3$, the following 17 terms (each a product of 4 truncated tetrahedron indices, as in Equation (32) for $N=3$) contribute to $I_{6_1}(0)+O(q)^4=1-4q+q^2+18q^3+O(q)^4$:

$$\begin{aligned}
&I_\Delta(-2,0)^2I_\Delta(0,-2)I_\Delta(0,0)-q^{-1/2}I_\Delta(-1,-1)I_\Delta(-1,0)I_\Delta(0,-1)I_\Delta(0,0)\\
&\quad+I_\Delta(-1,0)^2I_\Delta(0,-1)I_\Delta(0,0)+I_\Delta(0,0)^4+I_\Delta(-2,0)I_\Delta(0,-1)^2I_\Delta(0,1)\\
&\quad-q^{1/2}I_\Delta(-2,0)I_\Delta(-1,1)I_\Delta(0,1)I_\Delta(1,-2)-q^{1/2}I_\Delta(-1,0)I_\Delta(0,1)^2I_\Delta(1,-1)\\
&\quad-q^{-1/2}I_\Delta(-1,1)I_\Delta(0,-1)^2I_\Delta(1,0)-q^{1/2}I_\Delta(-2,1)I_\Delta(0,1)I_\Delta(1,-1)I_\Delta(1,0)\\
&\quad+I_\Delta(0,0)I_\Delta(0,1)I_\Delta(1,0)^2+I_\Delta(-2,0)I_\Delta(0,0)I_\Delta(1,-1)I_\Delta(1,1)\\
&\quad-q^{1/2}I_\Delta(0,0)I_\Delta(0,1)I_\Delta(1,0)I_\Delta(1,1)+qI_\Delta(-2,0)I_\Delta(0,2)^2I_\Delta(2,-2)\\
&\quad-q^{-1/2}I_\Delta(-2,0)I_\Delta(-1,-1)I_\Delta(-1,0)I_\Delta(2,-1)\\
&\quad-q^{-1/2}I_\Delta(-1,0)I_\Delta(-1,1)I_\Delta(0,-1)I_\Delta(2,-1)\\
&\quad-q^{-1/2}I_\Delta(-1,2)I_\Delta(0,0)I_\Delta(1,-1)I_\Delta(2,-1)\\
&\quad-q^{3/2}I_\Delta(-3,0)I_\Delta(0,3)^2I_\Delta(3,-3).
\end{aligned}$$

The first 50 coefficients of $I_{6_1}(0)$ are given by

$$\begin{aligned}
&1-4q+q^2+18q^3+22q^4+q^5-78q^6-178q^7-254q^8-188q^9+167q^{10}\\
&\quad+855q^{11}+1864q^{12}+2892q^{13}+3426q^{14}+2583q^{15}-488q^{16}-6698q^{17}\\
&\quad-16273q^{18}-28550q^{19}-41189q^{20}-49943q^{21}-48554q^{22}-28899q^{23}\\
&\quad+17621q^{24}+98726q^{25}+217819q^{26}+371551q^{27}+544496q^{28}+707360q^{29}\\
&\quad+811832q^{30}+792301q^{31}+565550q^{32}+40436q^{33}-872995q^{34}-2241496q^{35}\\
&\quad-4087180q^{36}-6354321q^{37}-8877834q^{38}-11348143q^{39}-13283739q^{40}\\
&\quad-14014789q^{41}-12685231q^{42}-8288627q^{43}+266720q^{44}+14032731q^{45}\\
&\quad+33862808q^{46}+60173861q^{47}+92687285q^{48}+130092845q^{49}+169735693q^{50}.
\end{aligned}$$

7.7 The index of the 7_2 knot complement

The index $I_{7_2}(0)$ is another example of linear growth. The default `SnapPy` triangulation $\mathcal{T}$ of the 7_2 knot complement has 4 ideal tetrahedra, and the Epstein–Penner

decomposition has 8 ideal tetrahedra. The two triangulations are related by geometric 2–3 moves and have equal indices. The angle structure equations of $\mathcal{T}$ are given by

$$\overline{\mathbb{A}} = \begin{pmatrix} 1 & 2 & 1 & 0 \\ 0 & 0 & 1 & 0 \\ 1 & 0 & 0 & 1 \\ 0 & 0 & 0 & 1 \end{pmatrix}, \quad \overline{\mathbb{B}} = \begin{pmatrix} 1 & 0 & 0 & 0 \\ 1 & 0 & 0 & 0 \\ 0 & 2 & 1 & 0 \\ 0 & 0 & 1 & 2 \end{pmatrix}, \quad \overline{\mathbb{C}} = \begin{pmatrix} 0 & 0 & 1 & 0 \\ 0 & 1 & 0 & 2 \\ 1 & 1 & 1 & 0 \\ 1 & 0 & 0 & 0 \end{pmatrix}.$$

Eliminating $\overline{\mathbb{B}}$, and removing the fourth row (which corresponds to the fourth edge equation), we obtain the angle structure equations

$$\mathbb{A}'\alpha + \mathbb{B}'\gamma = \pi\nu',$$

where

$$\mathbb{A}' = \begin{pmatrix} 0 & 2 & 1 & 0 \\ -1 & 0 & 1 & 0 \\ 1 & -2 & -1 & 1 \end{pmatrix} \qquad \mathbb{B}' = \begin{pmatrix} -1 & 0 & 1 & 0 \\ -1 & 1 & 0 & 2 \\ 1 & -1 & 0 & 0 \end{pmatrix} \qquad \nu' = \begin{pmatrix} 1 \\ 1 \\ -1 \end{pmatrix}.$$

The index of $\mathcal{T}$ is given by

$$I_{7_2}(0)(q) = \sum_{(k_1,k_2,k_3)\in\mathbb{Z}^3} (-1)^{k_1+k_2-k_3} q^{(k_1+k_2-k_3)/2} I_\Delta(-k_1, k_1+k_2-k_3) I_\Delta(-2k_2, k_3) \\ \times I_\Delta(k_1+k_2-k_3, -k_2+k_3) I_\Delta(-k_2+k_3, 2k_1-2k_3) \in \mathbb{Z}[\![q]\!].$$

$\mathcal{F}_\mathcal{T}$ in $\mathbb{R}^3$ has 14 rays, spanned by the columns of the matrix

$$\begin{pmatrix} -2 & -1 & -1 & 0 & 0 & 0 & 0 & 0 & 0 & 1 & 1 & 1 & 1 & 2 \\ -1 & -1 & 0 & -1 & -1 & -1 & 0 & 1 & 1 & 0 & 0 & 0 & 1 & 1 \\ -2 & -1 & 0 & -2 & -1 & 0 & 1 & -1 & 0 & 0 & 1 & 2 & 1 & 3 \end{pmatrix}.$$

If $\delta(k_1, k_2, k_3)$ denotes the degree of the summand and $N \in \mathbb{N}$, then $\delta(k_1, k_2, k_3) \le N$ implies that (k_1, k_2, k_3) satisfy the bounds

$$\begin{aligned} 1 - \sqrt{1+2N} \le k_1 &\le \tfrac{1}{2}(-1 + \sqrt{1+8N}), \\ \tfrac{1}{2}(1 - \sqrt{1+4N}) \le k_2 &\le N, \\ 1 - \sqrt{1+2N} \le k_3 &\le \tfrac{1}{2}(-1 + \sqrt{1+12N}). \end{aligned}$$

Observe that the upper bound for k_2 is linear in N. The first 50 coefficients of $I_{7_2}(0)$ are given by

$$\begin{aligned} 1 - 4q + q^2 + 16q^3 + 20q^4 + q^5 - 72q^6 - 156q^7 - 206q^8 - 98q^9 + 275q^{10} \\ + 924q^{11} + 1740q^{12} + 2370q^{13} + 2227q^{14} + 495q^{15} - 3485q^{16} - 10168q^{17} \\ - 19045q^{18} - 28467q^{19} - 34899q^{20} - 33157q^{21} - 16460q^{22} + 22305q^{23} \\ + 89035q^{24} + 185478q^{25} + 306146q^{26} + 434575q^{27} + 539981q^{28} + 575717q^{29} \end{aligned}$$

$$+479148q^{30}+176483q^{31}-408854q^{32}-1340316q^{33}-2648389q^{34}-4301970q^{35}$$
$$-6179555q^{36}-8036073q^{37}-9477453q^{38}-9942897q^{39}-8710346q^{40}-4925980q^{41}$$
$$+2323715q^{42}+13897628q^{43}+30430263q^{44}+52111135q^{45}+78414600q^{46}$$
$$+107796294q^{47}+137380650q^{48}+162674912q^{49}+177363801q^{50}.$$

7.8 Acknowledegments

S G wishes to thank Tudor Dimofte, Josephine Yu and especially Don Zagier for enlightening conversations. A preliminary report was delivered by S G during the Oberwolfach 8/2012 workshop on *Low-Dimensional Topology and Number Theory*; we thank the organizers, Paul E Gunnells, Walter Neumann, Adam S Sikora and Don Zagier, for their hospitality.

S G was supported in part by grant DMS 0805078 of the US National Science Foundation. C D H, J H R, H S were supported by the Australian Research Council grant DP1095760.

Appendix: The 2–3 move

For completeness, in this appendix we give a detailed proof of the invariance of the index under 2–3 moves, following [16, Section 6] and also [10]. Let M be a cusped 3–manifold and let ϖ be an oriented multicurve on ∂M. Consider two ideal triangulations $\mathcal{T}$ and $\widetilde{\mathcal{T}}$ of M with N and $N+1$ tetrahedra, respectively, related by a 2–3 move as shown in Figure 23, matching the conventions of [12, Section 3.6].

The main result of this section is the following.

Theorem A.1 *Suppose that $\mathcal{T}$ and $\widetilde{\mathcal{T}}$ are ideal triangulations related by a 2–3 move and both admit an index structure. Then, for any $[\varpi]\in H_1(\partial M;\mathbb{Z})$,*

$$I_{\mathcal{T}}([\varpi])=I_{\widetilde{\mathcal{T}}}([\varpi]).$$

Recall that the index is not changed by isotopies of ϖ and, from (25), can be written in the form

$$I_{\mathcal{T}}(\varpi)(q)=\sum_{\boldsymbol{k}\in\mathbb{Z}^{N-r}} q^{\sum_i k_i}\prod_j J(T_j;\boldsymbol{k},\varpi),$$

where the contribution from tetrahedron T_j is

$$J(T_j;\boldsymbol{k},\varpi)=J_\Delta(\overline{a}_j(\boldsymbol{k},\varpi),\overline{b}_j(\boldsymbol{k},\varpi),\overline{c}_j(\boldsymbol{k},\varpi)).$$

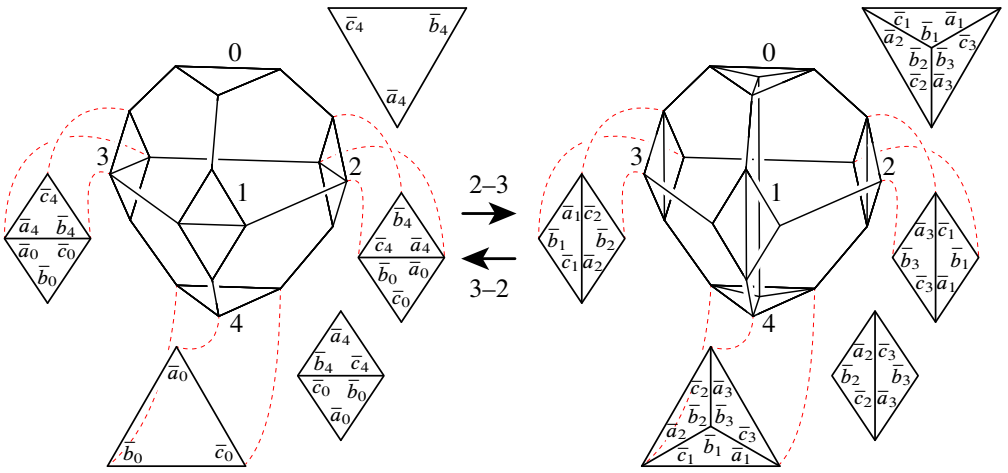

Figure 23: The 2–3 move shown with truncated tetrahedra and labelled vertices. The five triangulated ends of the tetrahedra before and after are shown in detail in the "zoomed in" pictures. The labels on the corners of the triangles are explained in Section 4.4. All truncated triangulation pictures are viewed from outside the tetrahedra.

Here we can think of $\boldsymbol{k}$ as a weight on the N edges of $\mathcal{T}$ and the summation is over $\mathbb{Z}^{N-r} \subset \mathbb{Z}^N$ corresponding to a set $\mathcal{B}$ of $N-r$ basic edges as in Theorem 4.3.

Definition A.2 Given ϖ as above and $\boldsymbol{k} \in \mathbb{Z}^N$, let $\varpi_{\boldsymbol{k}}$ denote a collection of disjoint oriented normal curves in ∂M obtained from ϖ by adding k_i small linking circles around the vertex at one end of the i^{th} edge in $\mathcal{T}$. (The circles are oriented anticlockwise if $k_i > 0$ and clockwise if $k_i < 0$.)

By Remark 4.1, we can think of the coefficient $\overline{a}_j(\boldsymbol{k}, \varpi)$ as the turning number $\overline{a}_{\varpi_{\boldsymbol{k}},j}$, as defined in Section 4.4, of $\varpi_{\boldsymbol{k}}$. Thus $\overline{a}_j(\boldsymbol{k}, \varpi)$ is a sum of 4 turning numbers of the multicurve $\varpi_{\boldsymbol{k}}$ as it turns around the $\overline{a}_j$ corners of the triangles of the j^{th} truncated tetrahedron, and similarly for $\overline{b}_j(\boldsymbol{k}, \varpi)$ and $\overline{c}_j(\boldsymbol{k}, \varpi)$. This point of view allows us to treat the contributions from edge weights in the index calculation in the same way as we treat the contributions from peripheral curves.

The triangulations $\mathcal{T}$ and $\widetilde{\mathcal{T}}$ only differ inside a bipyramid, and we label its vertices $0, 1, 2, 3, 4$ as in Figure 23, where 0 and 4 are the north and south poles, and $1, 2, 3$ are on the equator. This determines 5 tetrahedra $T_0, \dots, T_4$, where T_i is the tetrahedron "opposite" vertex i with vertex set obtained by omitting vertex i from the set $\{0, 1, 2, 3, 4\}$. The bipyramid can be decomposed into the two tetrahedra T_0, T_4 which contain the triangle 123, or into the three tetrahedra T_1, T_2, T_3 which contain the edge 04. Then it suffices to prove the following lemma.

Lemma A.3 (Pentagon equality for J) *Let ϖ be an oriented multicurve on ∂M as above. Let $\boldsymbol{k} = (k_1, \dots, k_N)$ be a weight function on the edges of $\mathcal{T}$, and let $\widetilde{\boldsymbol{k}} = (k_0, \boldsymbol{k})$ be an extension of $\boldsymbol{k}$ to a weight function on the edges of $\widetilde{\mathcal{T}}$, where k_0 is the weight on the new edge 04 introduced in the 2–3 move. Then, with the notation above,*

$$\sum_{k_0 \in \mathbb{Z}} q^{k_0} J(T_1; (k_0, \boldsymbol{k}), \varpi) J(T_2; (k_0, \boldsymbol{k}), \varpi) J(T_3; (k_0, \boldsymbol{k}), \varpi) = J(T_0; \boldsymbol{k}, \varpi) J(T_4; \boldsymbol{k}, \varpi). \tag{36}$$

Theorem A.1 now follows immediately: In the sum (25) for $I_{\mathcal{T}}$ we choose a set $\mathcal{X}$ of excluded edges from a maximal tree with 1– or 3–cycle for $\mathcal{T}$ as in Theorem 4.3. Then the *same* set of edges can be excluded from the summation for $I_{\widetilde{\mathcal{T}}}$, so the summation for $I_{\widetilde{\mathcal{T}}}$ is over the original set of basic edges $\mathcal{B}$ for $\mathcal{T}$ together with the new edge introduced in the 2–3 move.

Proof of Lemma A.3 The plan is as follows. First, we isotope ϖ if necessary, so that it intersects the truncated ends of the bipyramid involved in the 2–3 move in a standardised way. For a given $\boldsymbol{k}$, we consider $\varpi_{\boldsymbol{k}}$, and the $\varpi_{\widetilde{\boldsymbol{k}}}$, where $\widetilde{\boldsymbol{k}} = (k_0, \boldsymbol{k})$ and $k_0 \in \mathbb{Z}$. We calculate the left-hand side of (36) using the $\varpi_{\widetilde{\boldsymbol{k}}}$, and use the original version of the pentagon equality, (10), to show that it is equal to the right-hand side of (36), calculated using $\varpi_{\boldsymbol{k}}$

So, first we arrange ϖ appropriately. The induced triangulations of ∂M, $\mathcal{T}_\partial$ and $\widetilde{\mathcal{T}}_\partial$, determined by $\mathcal{T}$ and $\widetilde{\mathcal{T}}$ respectively are related by 1–3 and 2–2 moves as seen in Figure 23. We isotope ϖ if necessary, so that it is normal relative to both of the two induced triangulations of ∂M.

At each of the polar vertices of the bipyramid there is a 1–3 move on the boundary, and we can assume, after a further isotopy if necessary, that ϖ is represented by collections of oriented normal arcs as shown in Figure 24, with all turning numbers 0 at the new central vertex.

At each of the equatorial vertices there is a 2–2 move on the boundary, and we can represent ϖ by a collection of oriented normal arcs in a quadrilateral of the six types shown in the right-hand side of Figure 25. (Note that either $\overline{s} = 0$ or $\overline{t} = 0$ for an embedded normal curve ϖ.)

Then the corresponding turning numbers at the corners of the triangles in the left and centre of the figure are given by

$$\begin{aligned} &\overline{a} = \overline{y} + \overline{t}, \quad \overline{c} = \overline{y}' - \overline{s}, \quad \overline{a}' = \overline{y}' - \overline{t}, \quad \overline{c}' = \overline{y} + \overline{s}, \\ &\overline{x} = \overline{b}' - \overline{s}, \quad \overline{z} = \overline{b} - \overline{t}, \quad \overline{x}' = \overline{b} + \overline{s}, \quad \overline{z}' = \overline{b}' + \overline{t}. \end{aligned}$$

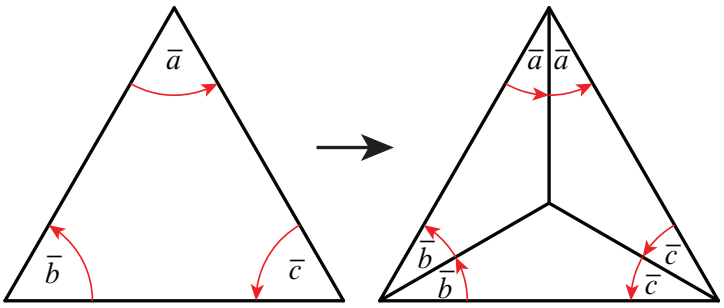

Figure 24: Change in turning numbers under a 1–3 move

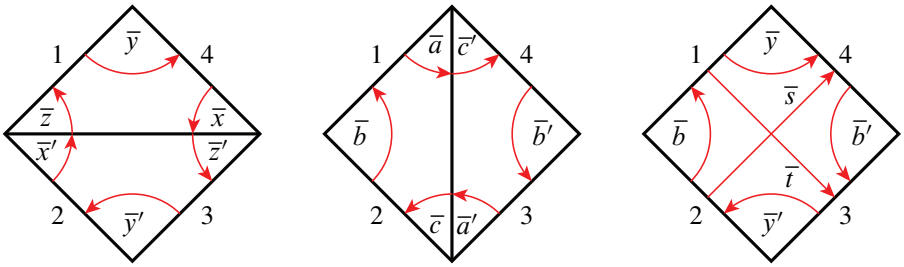

Figure 25: Change in turning numbers under a 2–2 move

For example, $\overline{a}$ is the signed number of (anticlockwise) normal arcs going from edge 1 to the vertical edge in the centre of the figure. But each such arc is a normal arc in the quadrilateral going from edge 1 to 3 or from edge 1 to edge 4, hence $\overline{a} = \overline{y} + \overline{t}$.

In particular, we have the following relations that will be used below:

$$\overline{a} + \overline{a}' = \overline{c} + \overline{c}' = \overline{y} + \overline{y}', \quad \overline{x} + \overline{x}' = \overline{z} + \overline{z}' = \overline{b} + \overline{b}', \tag{37}$$

$$2\overline{b} + \overline{c}' - \overline{a} = 2\overline{b} + \overline{a}' - \overline{c} = \overline{x}' + \overline{z}, \quad 2\overline{b}' + \overline{c} - \overline{a}' = 2\overline{b}' + \overline{a} - \overline{c}' = \overline{x} + \overline{z}'. \tag{38}$$

Now $\varpi_{\widetilde{\boldsymbol{k}}}$ is obtained from ϖ by adding small vertex linking circles around the vertices of $\widetilde{\mathcal{T}}_\partial$, and similarly $\varpi_{\boldsymbol{k}}$ is obtained from ϖ by adding small vertex linking circles around the vertices of $\mathcal{T}_\partial$. Note that we have a map from the turning numbers of ϖ relative to $\mathcal{T}$ to the turning numbers of ϖ relative to $\widetilde{\mathcal{T}}$. If we apply the same map to the turning numbers of $\varpi_{\boldsymbol{k}}$ relative to $\mathcal{T}$, we obtain the turning numbers of $\varpi_{(0,\boldsymbol{k})}$ relative to $\widetilde{\mathcal{T}}$.

In the following, we will abbreviate our notation as follows. Let

$$\begin{aligned} &\overline{a}_j = \overline{a}_j(\boldsymbol{k}, \varpi), && \overline{b}_j = \overline{b}_j(\boldsymbol{k}, \varpi), && \overline{c}_j = \overline{c}_j(\boldsymbol{k}, \varpi) && \text{for } j = 0, 4, \\ &\overline{a}_j = \overline{a}_j((0,\boldsymbol{k}), \varpi), && \overline{b}_j = \overline{b}_j((0,\boldsymbol{k}), \varpi), && \overline{c}_j = \overline{c}_j((0,\boldsymbol{k}), \varpi) && \text{for } j = 1, 2, 3. \end{aligned}$$

Recall that $\overline{a}_j(\boldsymbol{k},\varpi)$ is the sum of $\overline{a}_{\varpi,j}$ and the weights given by $\boldsymbol{k}$ on the two edges of tetrahedron j labelled $\overline{a}_j$, and similarly for $\overline{b}_j(\boldsymbol{k},\varpi)$, $\overline{c}_j(\boldsymbol{k},\varpi)$. Thus, replacing $\boldsymbol{k}$ by $\widetilde{\boldsymbol{k}}=(k_0,\boldsymbol{k})$ does not change $\overline{a}_j(\boldsymbol{k},\varpi)$ or $\overline{c}_j(\boldsymbol{k},\varpi)$ but we have $\overline{b}_j(\widetilde{\boldsymbol{k}},\varpi)=\overline{b}_j+k_0$ for $j=1,2,3$, since the new edge 04 is incident to angles labelled $\overline{b}_j$ in Figure 23.

We also let $\overline{A}_j=\overline{b}_j-\overline{c}_j$, $\overline{B}_j=\overline{c}_j-\overline{a}_j$, $\overline{C}_j=\overline{a}_j-\overline{b}_j$, and note that each of these is a sum of contributions from the 4 triangular corners of the (truncated) tetrahedron T_j. On each of these triangles, $\overline{A}_j,\overline{B}_j,\overline{C}_j$ represent inward intersection numbers of oriented normal arcs with the sides of the triangles as shown in Figure 26.

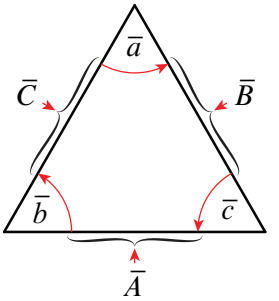

Figure 26: Intersection numbers and turning numbers in a triangle

Then we have

$$\overline{A}_j+\overline{B}_j+\overline{C}_j=0 \quad \text{for each } j, \tag{39}$$

$$\overline{B}_1+\overline{B}_2+\overline{B}_3=0. \tag{40}$$

To prove the last equation, we look at the contribution from each of the 5 corners of the bipyramid as shown in Figures 27 and 28. At the polar vertices $0,4$ the contribution to $\sum_i \overline{B}_i=\sum_{i=1}^3 \overline{a}_i-\sum_{i=1}^3 \overline{c}_i$ is zero from Figure 24, while at the equatorial vertices $1,2,3$ this follows from (37). Alternatively, one can look at the vertices $1,2,3$ as shown in Figures 27 and 28, and see that, for example, at vertex 1 the contribution to B_2 is cancelled by the contribution to B_3. Similar cancellations happen at vertices 2 and 3.

Now consider the left-hand side of (36). We have

$$\begin{aligned} J(T_1;(k_0,\boldsymbol{k}),\varpi) &= (-q^{1/2})^{-\overline{c}_1} I_\Delta(\overline{c}_1-\overline{a}_1,\overline{b}_1+k_0-\overline{c}_1) \\ &= (-q^{1/2})^{-\overline{c}_1} I_\Delta(\overline{B}_1,\overline{A}_1+k_0), \\ J(T_2;(k_0,\boldsymbol{k}),\varpi) &= (-q^{1/2})^{-\overline{c}_2} I_\Delta(\overline{c}_2-\overline{a}_2,\overline{b}_2+k_0-\overline{c}_2) \\ &= (-q^{1/2})^{-\overline{c}_2} I_\Delta(\overline{B}_2,\overline{A}_2+k_0), \end{aligned}$$

and

$$\begin{aligned} J(T_3;(k_0,\boldsymbol{k}),\varpi) &= (-q^{1/2})^{-\bar{a}_3} I_\Delta(\bar{a}_3-\bar{b}_3-k_0,\bar{c}_3-\bar{a}_3)\\ &= (-q^{1/2})^{-\bar{a}_3} I_\Delta(\bar{C}_3-k_0,\bar{B}_3)\\ &= (-q^{1/2})^{-\bar{a}_3} I_\Delta(-\bar{B}_3,-\bar{C}_3+k_0)\\ &= (-q^{1/2})^{-\bar{a}_3} I_\Delta(\bar{B}_1+\bar{B}_2,-\bar{C}_3+k_0) \end{aligned}$$

using the duality identity (8) and (40).

The pentagon identity (10) can be rewritten (by replacing e_3 by x_3+e_0) in the form

$$\begin{aligned} (41)\quad \sum_{e_0\in\mathbb{Z}} q^{e_0} I_\Delta(m_1,x_1+e_0) I_\Delta(m_2,x_2+e_0) I_\Delta(m_1+m_2,x_3+e_0)\\ = q^{-x_3} I_\Delta(m_1-x_2+x_3,x_1-x_3) I_\Delta(m_2-x_1+x_3,x_2-x_3). \end{aligned}$$

We apply this with $e_0=k_0, m_1=\bar{B}_1, m_2=\bar{B}_2, x_1=\bar{A}_1, x_2=\bar{A}_2$ and $x_3=-\bar{C}_3$. Then direct calculations, using the observations above, show that

(i) $m_1-x_2+x_3=\bar{B}_1-\bar{A}_2-\bar{C}_3=\bar{A}_0$,

(ii) $x_1-x_3=\bar{A}_1+\bar{C}_3=\bar{C}_0$,

(iii) $m_2-x_1+x_3=\bar{B}_2-\bar{A}_1-\bar{C}_3=\bar{B}_4$,

(iv) $x_2-x_3=\bar{A}_2+\bar{C}_3=\bar{A}_4$,

(v) $\bar{c}_1+\bar{c}_2+\bar{a}_3+2x_3=\bar{b}_0+\bar{c}_4$,

hence $(-q^{1/2})^{-\bar{c}_1-\bar{c}_2-\bar{a}_3} q^{-x_3} = (-q^{1/2})^{-\bar{b}_0-\bar{c}_4}$. Thus, multiplying equation (41) by $(-q^{1/2})^{-\bar{c}_1-\bar{c}_2-\bar{a}_3}$ gives

$$\begin{aligned} \sum_{k_0\in\mathbb{Z}} q^{k_0} J(T_1;(k_0,\boldsymbol{k}),\varpi) J(T_2;(k_0,\boldsymbol{k}),\varpi) J(T_3;(k_0,\boldsymbol{k}),\varpi)\\ = (-q^{1/2})^{-\bar{b}_0} I_\Delta(\bar{A}_0,\bar{C}_0)(-q^{1/2})^{-\bar{c}_4} I_\Delta(\bar{B}_4,\bar{A}_4)\\ = J(T_0;\boldsymbol{k},\varpi) J(T_4;\boldsymbol{k},\varpi), \end{aligned}$$

as desired.

The identities (i)–(v) are proved by looking separately at the contributions from the 5 corners of the bipyramid, and carefully studying Figures 27 and 28.

For example, to prove (i), we note that:

At vertex 1: $\bar{B}_1-\bar{A}_2-\bar{C}_3=0-\bar{A}_2-\bar{C}_3=-\bar{B}_0-\bar{C}_0=\bar{A}_0$.

At vertex 2: $\bar{B}_1-\bar{A}_2-\bar{C}_3=-\bar{B}_3-0-\bar{C}_3=\bar{A}_3=\bar{A}_0$.

At vertex 3: $\bar{B}_1-\bar{A}_2-\bar{C}_3=\bar{B}_1-\bar{A}_2-0=-\bar{B}_2-\bar{A}_2=\bar{C}_2=\bar{A}_0$.

At vertex 0: $\bar{B}_1-\bar{A}_2-\bar{C}_3=\bar{B}_1+\bar{C}_1+\bar{A}_1=0=\bar{A}_0$.

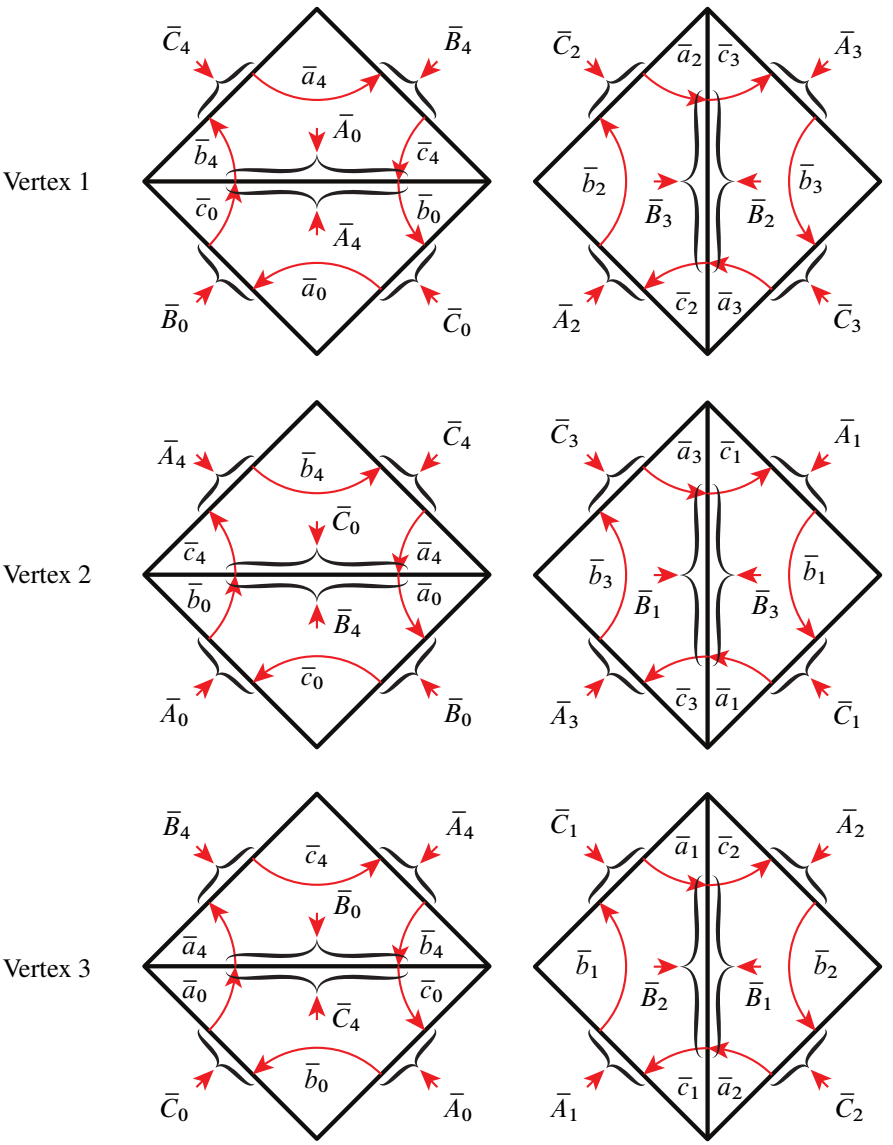

Figure 27: Turning numbers and intersection numbers at corners of the bipyramid

At vertex 4: $\bar{B}_1 - \bar{A}_2 - \bar{C}_3 = \bar{B}_1 + 0 = \bar{A}_0$.

For (ii), we note that:

At vertex 1: $\bar{A}_1 + \bar{C}_3 = 0 + \bar{C}_3 = \bar{C}_0$.

At vertex 2: $\bar{A}_1 + \bar{C}_3 = \bar{C}_4 + \bar{A}_4 = -\bar{B}_4 = \bar{C}_0$.

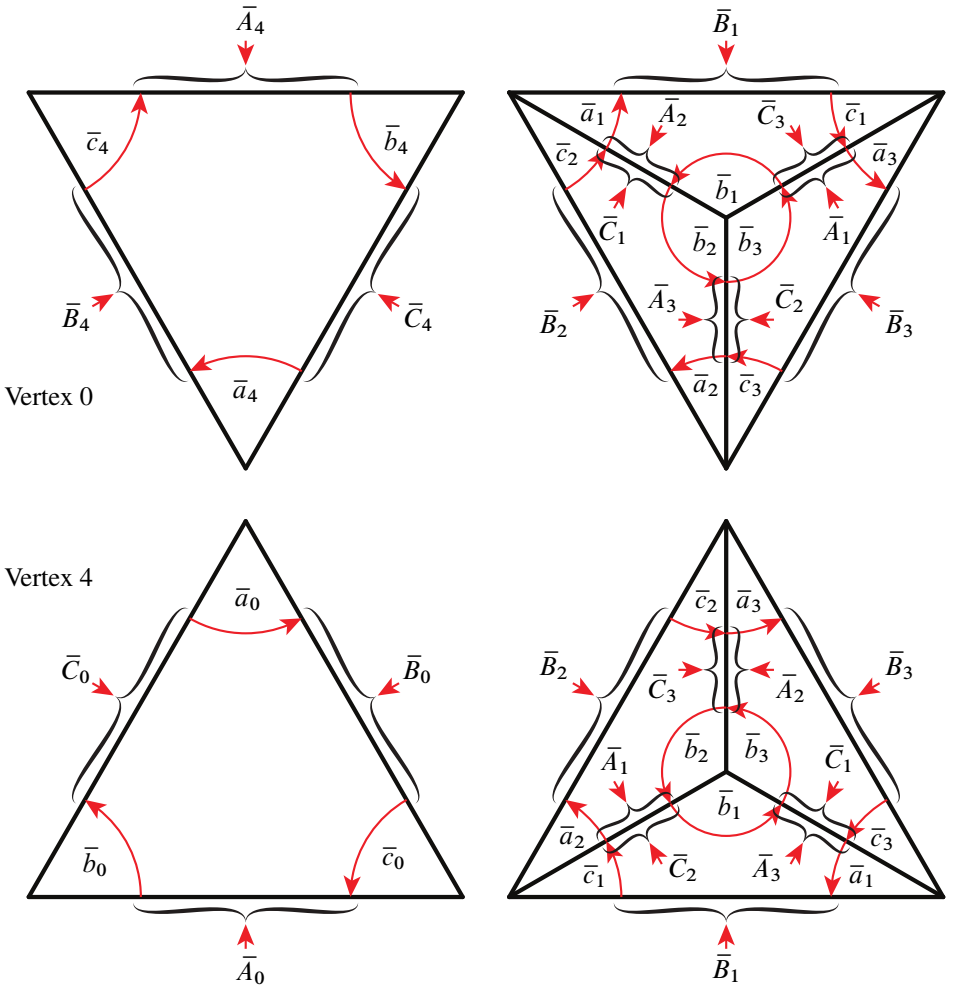

Figure 28: Turning numbers and intersection numbers at corners of the bipyramid

At vertex 3: $\bar{A}_1 + \bar{C}_3 = \bar{A}_1 = \bar{C}_0$.

At vertex 0: $\bar{A}_1 + \bar{C}_3 = 0 = \bar{C}_0$.

At vertex 4: $\bar{A}_1 + \bar{C}_3 = -\bar{C}_2 - \bar{A}_2 = \bar{B}_2 = \bar{C}_0$.

The equalities (iii), (iv) are verified similarly.

Finally, to prove (v), first note that since $x_3 = -\bar{C}_3 = \bar{b}_3 - \bar{a}_3$, we need to show that

$$\bar{c}_1 + \bar{c}_2 - \bar{a}_3 + 2\bar{b}_3 = \bar{b}_0 + \bar{c}_4.$$

Now at vertices 0 and 4, $\bar{b}_3 = \bar{b}_3(0, \boldsymbol{k}), \varpi) = 0$, since we can choose ϖ as in Figure 24. Further, $\bar{a}_j, \bar{b}_j, \bar{c}_j = 0$ at vertex j. Thus, from Figures 27 and 28:

At vertex 0: LHS $= \overline{c}_1 + \overline{c}_2 - \overline{a}_3 = \overline{b}_4 + \overline{c}_4 - \overline{b}_4 = \overline{c}_4 =$ RHS from Figure 24.

At vertex 4: LHS $= \overline{c}_1 + \overline{c}_2 - \overline{a}_3 = \overline{b}_0 + \overline{a}_0 - \overline{a}_0 = \overline{b}_0 =$ RHS from Figure 24.

At vertex 1: LHS $= \overline{c}_2 - \overline{a}_3 + 2\overline{b}_3 = \overline{b}_0 + \overline{c}_4$ by (38).

At vertex 2: LHS $= \overline{c}_1 - \overline{a}_3 + 2\overline{b}_3 = \overline{b}_0 + \overline{c}_4$ by (38).

At vertex 3: LHS $= \overline{c}_1 + \overline{c}_2 = \overline{b}_0 + \overline{c}_4$ by (37).

This completes the proof of Lemma A.3. □

References

[1] **H Akiyoshi**, *Finiteness of polyhedral decompositions of cusped hyperbolic manifolds obtained by the Epstein–Penner's method*, Proc. Amer. Math. Soc. 129 (2001) 2431–2439 MR1823928

[2] **J E Andersen**, **R Kashaev**, *A TQFT from Quantum Teichmüller theory*, Comm. Math. Phys. 330 (2014) 887–934 MR3227503

[3] **S Baseilhac**, **R Benedetti**, *Classical and quantum dilogarithmic invariants of flat* $\mathrm{PSL}(2,\mathbb{C})$*–bundles over* 3*–manifolds*, Geom. Topol. 9 (2005) 493–569 MR2140989

[4] **S Baseilhac**, **R Benedetti**, *Quantum hyperbolic geometry*, Algebr. Geom. Topol. 7 (2007) 845–917 MR2336244

[5] **C Beem**, **T Dimofte**, **S Pasquetti**, *Holomorphic blocks in three dimensions*, J. High Energy Phys. 2014 (2014) MR3303415

[6] **R Benedetti**, **C Petronio**, *Branched standard spines of* 3*–manifolds*, Lecture Notes in Mathematics 1653, Springer, Berlin (1997) MR1470454

[7] **D Cooper**, **M Culler**, **H Gillet**, **D D Long**, **P B Shalen**, *Plane curves associated to character varieties of* 3*–manifolds*, Invent. Math. 118 (1994) 47–84 MR1288467

[8] **M Culler**, **N M Dunfield**, **J R Weeks**, *SnapPy, a computer program for studying the topology of* 3*–manifolds* Available at `http://snappy.computop.org`

[9] **J A De Loera**, **J Rambau**, **F Santos**, *Triangulations: Structures for algorithms and applications*, Algorithms and Computation in Mathematics 25, Springer, Berlin (2010) MR2743368

[10] **T Dimofte**, **D Gaiotto**, **S Gukov**, 3*–manifolds and* 3*d indices*, Adv. Theor. Math. Phys. 17 (2013) 975–1076 MR3262519

[11] **T Dimofte**, **D Gaiotto**, **S Gukov**, *Gauge theories labelled by three-manifolds*, Comm. Math. Phys. 325 (2014) 367–419 MR3148093

[12] **T Dimofte**, **S Garoufalidis**, *The quantum content of the gluing equations*, Geom. Topol. 17 (2013) 1253–1315 MR3073925

[13] **D B A Epstein**, **R C Penner**, *Euclidean decompositions of noncompact hyperbolic manifolds*, J. Differential Geom. 27 (1988) 67–80 MR918457

[14] **C Frohman**, **J Kania-Bartoszynska**, *The quantum content of the normal surfaces in a three-manifold*, J. Knot Theory Ramifications 17 (2008) 1005–1033 MR2439773

[15] **S Garoufalidis**, *3D index data* Available at `http://www.math.gatech.edu/~stavros/publications/3Dindex.data`

[16] **S Garoufalidis**, *The 3D index of an ideal triangulation and angle structures* `arXiv:1208.1663` to appear in Ramanujan J.

[17] **S Garoufalidis**, **R Kashaev**, *From state-integrals to q–series* `arXiv:1304.2705` to be published in Math. Res. Letters

[18] **S Garoufalidis**, **T T Q Lê**, *Nahm sums, stability and the colored Jones polynomial*, Res. Math. Sci. 2 (2015) MR3375651

[19] **S Garoufalidis**, **T Vuong**, *Alternating knots, planar graphs, and q–series*, Ramanujan J. 36 (2015) 501–527 MR3317869

[20] **S Garoufalidis**, **D Zagier**, *Empirical relations between q–series and Kashaev's invariant of knots* (2013) preprint

[21] **I M Gel′fand**, **M M Kapranov**, **A V Zelevinsky**, *Discriminants, resultants, and multidimensional determinants*, Birkhäuser, Boston, MA (1994) MR1264417

[22] **F Guéritaud**, **S Schleimer**, *Canonical triangulations of Dehn fillings*, Geom. Topol. 14 (2010) 193–242 MR2578304

[23] **A Hatcher**, *Notes on basic* 3–*manifold topology* (2007) lecture notes Available at `http://www.math.cornell.edu/~hatcher/3M/3Mfds.pdf`

[24] **C D Hodgson**, **J H Rubinstein**, **H Segerman**, *Triangulations of hyperbolic* 3–*manifolds admitting strict angle structures*, J. Topol. 5 (2012) 887–908 MR3001314

[25] **W Jaco**, **J H Rubinstein**, 0–*efficient triangulations of* 3–*manifolds*, J. Differential Geom. 65 (2003) 61–168 MR2057531

[26] **V F R Jones**, *Hecke algebra representations of braid groups and link polynomials*, Ann. of Math. 126 (1987) 335–388 MR908150

[27] **E Kang**, **J H Rubinstein**, *Ideal triangulations of* 3–*manifolds, I: Spun normal surface theory*, from: "Proceedings of the Casson Fest", (C Gordon, Y Rieck, editors), Geom. Topol. Monogr. 7 (2004) 235–265 MR2172486

[28] **E Kang**, **J H Rubinstein**, *Ideal triangulations of* 3–*manifolds, II: Taut and angle structures*, Algebr. Geom. Topol. 5 (2005) 1505–1533 MR2186107

[29] **R M Kashaev**, *The hyperbolic volume of knots from the quantum dilogarithm*, Lett. Math. Phys. 39 (1997) 269–275 MR1434238

[30] **R Kashaev**, **F Luo**, **G Vartanov**, *A TQFT of Turaev–Viro type on shaped triangulations* `arXiv:1210.8393`

[31] **M Lackenby**, *Taut ideal triangulations of 3–manifolds*, Geom. Topol. 4 (2000) 369–395 MR1790190

[32] **M Lackenby**, *Word hyperbolic Dehn surgery*, Invent. Math. 140 (2000) 243–282 MR1756996

[33] **M Lackenby**, *An algorithm to determine the Heegaard genus of simple 3–manifolds with nonempty boundary*, Alg. Geom. Topol. 8 (2008) 911–934

[34] **J-L Loday**, *Realization of the Stasheff polytope*, Arch. Math. (Basel) 83 (2004) 267–278 MR2108555

[35] **F Luo**, **S Tillmann**, *Angle structures and normal surfaces*, Trans. Amer. Math. Soc. 360 (2008) 2849–2866 MR2379778

[36] **S MacLane**, *Categories for the working mathematician*, Graduate Texts in Mathematics 5, Springer, New York (1971) MR0354798

[37] **S V Matveev**, *Transformations of special spines, and the Zeeman conjecture*, Izv. Akad. Nauk SSSR Ser. Mat. 51 (1987) 1104–1116, 1119 MR925096 In Russian; translated in Math. USSR-Izv. 31 (1988) 423–434

[38] **S Matveev**, *Algorithmic topology and classification of 3–manifolds*, 2nd edition, Algorithms and Computation in Mathematics 9, Springer, Berlin (2007) MR2341532

[39] **W D Neumann**, *Combinatorics of triangulations and the Chern–Simons invariant for hyperbolic 3–manifolds*, from: "Topology '90", (B Apanasov, W D Neumann, A W Reid, L Siebenmann, editors), Ohio State Univ. Math. Res. Inst. Publ. 1, de Gruyter, Berlin (1992) 243–271 MR1184397

[40] **W D Neumann**, **D Zagier**, *Volumes of hyperbolic three-manifolds*, Topology 24 (1985) 307–332 MR815482

[41] **C Petronio**, *Standard spines and 3–manifolds*, PhD thesis, Scuola Normale Superiore, Pisa (1995)

[42] **R Piergallini**, *Standard moves for standard polyhedra and spines*, Rend. Circ. Mat. Palermo Suppl. (1988) 391–414 MR958750

[43] **J H Rubinstein**, *Polyhedral minimal surfaces, Heegaard splittings and decision problems for 3–dimensional manifolds*, from: "Geometric topology", (W H Kazez, editor), AMS/IP Stud. Adv. Math. 2, Amer. Math. Soc. (1997) 1–20 MR1470718

[44] **F Santos**, *Geometric bistellar flips: The setting, the context and a construction*, from: "International Congress of Mathematicians, Vol. III", (M Sanz-Solé, J Soria, J L Varona, J Verdera, editors), Eur. Math. Soc., Zürich (2006) 931–962 MR2275713

[45] **J D Stasheff**, *Homotopy associativity of H –spaces, I, II*, Trans. Amer. Math. Soc. 108, 275-292; ibid. 108 (1963) 293–312 MR0158400

[46] **J Stasheff**, *From operads to "physically" inspired theories*, from: "Operads: Proceedings of Renaissance Conferences", (J-L Loday, J D Stasheff, A A Voronov, editors), Contemp. Math. 202, Amer. Math. Soc. (1997) 53–81 MR1436917

[47] **M Stocking**, *Almost normal surfaces in 3–manifolds*, Trans. Amer. Math. Soc. 352 (2000) 171–207 MR1491877

[48] **W P Thurston**, *The geometry and topology of three-manifolds*, lecture notes, Princeton University (1979) Available at `http://msri.org/publications/books/gt3m`

[49] **J Weeks**, *Hyperbolic structures on three-manifolds*, PhD thesis, Princeton Univ. (1985)

SG: *School of Mathematics, Georgia Institute of Technology*
686 Cherry Street, Atlanta, GA 30332-0160, USA

CDH, JHR, HS: *Department of Mathematics and Statistics, The University of Melbourne*
Melbourne, Parkville VIC 3010, Australia

HS: *Department of Mathematics, Oklahoma State University*
Stillwater, VIC 74078, USA

`stavros@math.gatech.edu, craigdh@unimelb.edu.au, H.Rubinstein@ms.unimelb.edu.au, rubin@ms.unimelb.edu.au, segerman@math.okstate.edu`

`http://www.math.gatech.edu/~stavros, http://www.ms.unimelb.edu.au/~cdh/, http://www.ms.unimelb.edu.au/~rubin, http://math.okstate.edu/people/segerman/`

Proposed: Cameron Gordon Received: 30 October 2013
Seconded: Peter Teichner, Robion Kirby Accepted: 9 January 2015